

ROBUST MUSCLE SYNERGIES FOR POSTURAL CONTROL

A Dissertation
Presented to
The Academic Faculty

by

Gelsy Torres-Oviedo

In Partial Fulfillment
of the Requirements for the Degree
Doctorate of Philosophy in the
School of The Wallace H. Coulter Department of Biomedical Engineering

Georgia Institute of Technology
May 2007

COPYRIGHT 2007 BY GELSY TORRES-OVIEDO

ROBUST MUSCLE SYNERGIES FOR POSTURAL CONTROL

Approved by:

Dr. Lena H. Ting, Advisor
School of Biomedical Engineering
*Georgia Institute of Technology/Emory
University*

Dr. T. Richard Nichols
School of Biomedical Engineering
*Georgia Institute of Technology/Emory
University*

Dr. Young-Hui Chang
School of Applied Physiology
Georgia Institute of Technology

Dr. Steve L. Wolf
School of Medicine
Emory University

Dr. Robert H. Lee
School of Biomedical Engineering
*Georgia Institute of Technology/Emory
University*

Date Approved: April 9th, 2007

To my family

ACKNOWLEDGEMENTS

The work presented here is the result of perseverance and hard work that I would have never been able to endure in the absence of my family's cheerful thoughts and love. In particular, I would like to thank my brother Esteban Torres Oviedo for teaching me the amazing accomplishments that can be achieved with hard work and enthusiasm. Esteban's motivation and love for life has served me, among multiple people, as an inspiration. Similarly, I would like to thank my parents Gloria Oviedo Galdeano and Esteban F. Torres Briones for helping me appreciate my brother's triumphs and efforts in the everyday life. They have been extraordinary parents who have played a very important role in the success of their three children. Their constant words of affirmation have engraved in me tremendous self-confidence that has allowed me to follow and realize all my dreams. I also would like to thank my lovely sister Gloria Gysel Torres Oviedo ("Tay") for giving me the opportunity to closely share with a loved one, my personal experiences. Tay's understanding has been unconditional and her support has giving me sunshine even in the darkest moments. I would like to thank all of them for making me feel their company every single day of my life, regardless of time and distance.

I would like to thank my advisor, Prof. Lena H. Ting, for her guidance, patience, and hard work. Lena facilitated my understanding of concepts that are the basis of my research. Most importantly, she helped me develop skills that I never expected to gain during my doctoral work. For example, thanks to her I learned to criticize, synthesize, and communicate knowledge, which make up the essential skills for becoming an independent thinker. Gaining these skills and modifying my thinking process was very challenging; Lena's trust and perseverance, however, encouraged me to accomplish it. I am thankful I was able to share this learning experience with her. I will try to follow her example as an outstanding researcher and exceptional educator.

I would like to thank the people in the Ting Group for their insightful comments about my work throughout the duration of my doctorate. In particular, I would like to thank J. Lucas McKay for the enriching discussions we had. He helped me comprehend the motor control field better. I also would like to thank Nathan E. Bunderson, Stacie A. Chavatal, Kartik Sundar, Keith Van Antwerp, and Torrence D. J. Welch for their thoughtful comments and editorial help during the preparation of this manuscript. I would like to thank J. Robert Warren and Timothy Otchy for their excellent technical support developing the experimental apparatus. Finally I am very thankful to everyone in the Ting Group for their friendship; they made my stay in the lab very enjoyable.

I would like to thank my PhD committee for their interest in this work and for providing thoughtful comments about my research during the process of my doctorate. I also would like to thank them for reading preliminary versions of this manuscript and providing very thoughtful comments.

I would like to thank Jane M. Macpherson for providing the postural cat data and for her insightful comments during the first stage of my research work.

I also would like to thank Josef Käs and Anna L. Lin for their marvelous support during my application process to various PhD programs in the United States. As well as, giving me the opportunity to experience research in an actual laboratory. The research I did under their supervision during my undergraduate studies solidified my passion for scientific work.

Being far away from my family, my friends played a very important role during my doctorate. They all helped me go through the personal journey I experienced during the realization of this work. I would like to thank especially Gianluca Piazza for being an exceptional example and for helping me improve as a person. I would like to thank Mercedes Leboeiro (“Meche”) and Onyinechi Irrechuku (“Onyi”) for their warm support and company when I needed it the most. I also would like to thank Andreas Muller for always listening and giving me hope.

Last but not least I would like to thank God. Since only Devine influence can explain the series of extraordinary events that lead me to accomplish this dissertation. Starting from the superb family who has always encouraged me to the wonderful opportunities I have encountered and seized along the way. Thank you.

TABLE OF CONTENTS

	Page
ACKNOWLEDGEMENTS	iv
LIST OF TABLES	xii
LIST OF FIGURES	xiii
LIST OF SYMBOLS AND ABBREVIATIONS	xxii
SUMMARY	xxv
<u>CHAPTER</u>	
1 INTRODUCTION	26
1.1 Bernstein's degrees of freedom problem	26
1.2 Muscle synergies simplify muscle coordination	26
1.3 Why study standing postural control	28
1.4 Muscle synergies for postural control	29
1.4.1 Early models of postural synergies	29
1.4.2 Problems with <i>fixed</i> muscle synergies	30
1.4.3 Alternate muscle synergy model	31
1.5 Thesis overview	32
1.5.1 Study 1: Muscle synergies for human standing postural control	32
1.5.2 Study 2: Robustness of muscle synergies for human standing postural control	32
1.5.3 Study 3: Robust muscle synergies in cat control high-level biomechanical variables	33
2 MUSCLE SYNERGIES CHARACTERIZE HUMAN POSTURAL RESPONSES	34
2.1 Introduction	35
2.2 Methods	37

2.2.1	Experimental setup	37
2.2.2	Data processing	38
2.2.3	Extraction of muscle synergies	40
2.3	Results	42
2.3.1	A few muscle synergies can reproduce EMG patterns that vary with time and perturbation direction	43
2.3.2	Inter-trial variations in EMG patterns are accounted for by modulating muscle synergy activations	46
2.3.3	Similarities in muscle synergies across subjects	48
2.4	Discussion	51
2.4.1	Spatial variability	52
2.4.2	Temporal variability	52
2.4.3	Inter-trial variability	54
2.4.4	Muscle synergy robustness across subjects	55
2.4.5	Muscle synergy generality	56
3	ROBUSTNESS OF MUSCLE SYNERGIES ACROSS A VARIETY OF HUMAN POSTURAL CONFIGURATIONS	58
3.1	Introduction	59
3.2	Methods	62
3.2.1	Experimental setup	62
3.2.2	Data processing	65
3.2.3	Extraction of muscle synergies	65
3.2.3.1	Extraction of training muscle synergies	66
3.2.3.2	Extraction of task-specific muscle synergies	67
3.2.4	Data analysis	68
3.3	Results	69

3.3.1	Changing the initial stance configuration alters the postural responses	70
3.3.2	Identification of training and task-specific muscle synergies	73
3.3.2.1	Muscle synergies extracted from the training condition reproduce responses in all stance width conditions	75
3.3.2.2	Task-specific muscle synergies represent spatial activation patterns particular to the test condition	75
3.3.3	Magnitude and directionality of muscle synergy tuning curves change with stance	78
3.3.3.1	Training muscle synergy activations increase when stance width decreases	78
3.3.3.2	Training muscle synergy activations vary in a complex fashion in the one-leg and crouched condition	79
3.3.4	Temporal features of synergy activations only change in drastically distinct stances	81
3.3.4.1	Onset latencies of training muscle synergies are maintained with stance width	81
3.3.4.2	Temporal profiles and onset latencies of muscle synergies change in one-leg and crouched stance	81
3.3.5	Similarities between task-specific muscle synergies and some training muscle synergies	83
3.3.6	Averaged EMG responses in all stance conditions were reproduced by training and task-specific muscle synergies Muscle synergy generality	83
3.3.7	Inter-trial variations in EMG patterns in all stance conditions are accounted for by modulating muscle synergy activations	86
3.3.8	Similarities in muscle synergies across subjects	88
3.4	Discussion	94
3.4.1	Generality of muscle synergies in stance width conditions	94
3.4.2	Addition of task-specific muscle synergies in drastically distinct stances	96
3.4.3	Mechanisms underlying muscle synergy activations	99
3.4.4	Generality across tasks vs robustness across subjects	100

3.4.5 Clinical implications	101
4 ROBUSTNESS OF FUNCTIONAL MUSCLE SYNERGIES IN CATS	103
4.1 Introduction	103
4.2 Methods	106
4.2.1 Experimental setup	106
4.2.2 Data processing	109
4.2.3 Extraction of functional muscle synergies	113
4.2.4 Data analysis	116
4.3 Results	117
4.3.1 Five functional muscle synergies extracted from preferred stance reproduce responses at all stance distances	118
4.3.2 Activation of functional muscle synergies changes with stance distances	121
4.3.3 Synergy force vectors are consistent with respect to the limb axis	124
4.3.4 Functional muscle synergies extracted from translation data reproduce rotation data	127
4.3.5 Muscle synergies and synergy force vectors are similar across cats	130
4.4 Discussion	133
4.4.1 Methodological considerations	133
4.4.2 Functional significance of muscle synergies	135
4.4.3 Functional consequences of limb-referenced synergy force vectors	137
4.4.4 How are muscles synergies encoded in the nervous system?	139
5 DISCUSSION	142
5.1 Conclusions	142
5.1.1 Functional muscle synergies simplify motor control	142
5.1.2 Sensorimotor transformations for postural control	143

5.1.3	What factors determine the characteristics of <i>preferred</i> muscle activation patterns specified by muscle synergies?	144
5.1.4	Development of muscle synergies	145
5.2	Study limitations	147
5.2.1	A two-dimensional paradigm	147
5.2.2	Robustness of muscle synergies over time	147
5.2.3	Methodological improvements	148
5.3	Future directions	148
5.3.1	Functions of muscle synergies	148
5.3.2	Muscle synergies reflect biomechanical or neural constraints?	149
5.3.3	Optimality of muscle synergies	149
5.3.4	Changes in muscle synergies with motor learning	150
5.3.5	Clinical applications	150
APPENDIX A: ROBUSTNESS OF MUSCLE SYNERGIES OVER ENTIRE TIME COURSE OF POSUTRAL RESPONSES		152
A.1	Introduction	152
A.2	Methods	152
A.3	Results	153
A.4	Conclusions	154
REFERENCES		155
VITA		169

LIST OF TABLES

	Page
Table 2.1: List of the muscles recorded from the right leg and trunk across subjects	39
Table 4.1: Inclusive list of the muscles recorded from the left hindlimb across cats	120
Table 4.2: r^2 values of EMG and force tuning curve reconstructions in the stance distance group	125
Table 4.3: Mean angle of GRF rotation, θ , for all cats at all stance distances	125
Table 4.4: r^2 or VAF% values of EMG and force tuning curve reconstructions in translation-rotation group	129

LIST OF FIGURES

- | | Page |
|--|------|
| Figure 2.1: Example of postural responses to backwards perturbation of the support surface. <i>A.</i> Balance perturbations were induced by a ramp-and-hold motion of the support surface. EMG responses are directionally specific and typically occur with a 100-ms onset latency following platform motion (vertical dashed line). Mean EMG activity in 3 time bins of 75ms (EMG_{APR1} , EMG_{APR2} , EMG_{APR3}) during the APR period were computed for each perturbation (shaded areas). <i>B.</i> Coordinate system for support surface translations in 12 evenly spaced directions in the horizontal plane. Muscle tuning curves represent changes in APR activation in a single time bin over all perturbation directions. | 40 |
| Figure 2.2: Muscle activations during background and during responses evoked by all perturbation directions during all time bins in an example subject. Directional tuning is observed in the activation of all the muscles. Inter-trial variations of muscle activations are observed by the vertical spread of data points (black dots). Gray traces indicate the mean responses. | 44 |
| Figure 2.3: Muscle synergy vectors and synergy activation coefficients for a representative subject. <i>A.</i> Muscle synergy vectors, W_i , extracted from EMG data during quiet stance and three APR time bins. Each bar represents the relative level of activation of each muscle within the synergy (see Methods section for muscle abbreviations). <i>B.</i> Activation coefficients, C_i , for each of the 6 synergies during each time bin in multiple perturbation directions. Each dot represents the activity of the muscle synergy in a single trial. Directional tuning of muscle synergies over the three time bins can be observed. For example W_1 is mainly active during the initial period of the APR in backward directions (180° to 270°) whereas W_4 is active during the later time bin of the APR in forward directions (0° to 90°). | 46 |
| Figure 2.4: Tuning curves in a sample subject during two time bins. The original data are shown by the dashed black line and the reconstructed data by the solid black line. The contribution from each synergy to the reconstruction is shown by the corresponding colored line. This is computed by multiplying each training muscle synergy vector W by their corresponding averaged synergy activation coefficients across all trials (\bar{C}_i). | 47 |

Figure 2.5: Inter-trial variations in the postural responses of two muscles. *A.* PERO responses in APR2 to 10 randomly interspersed trials in the medial-forward (120°) direction. The magnitude of the colored bars represents the contribution of each synergy to the activation of PERO in these 10 trials. The recorded data are indicated by black stars and the reconstructed data by solid black dots. Percentage values indicate the variability accounted for by the muscle synergies (VAF%) *B.* Muscle activation patterns across all muscles in APR2 (EMG_{APR2}) are shown. Trial-to-trial variations in PERO result from the variations in muscle synergies that activate multiple muscles. All muscles belonging to synergy 6 (green) increase in trial 7 and decrease in trial 8, as does PERO activity. *C.* GMED activation to lateral perturbations (0°). *D.* Muscle activation patterns across all muscles in trial 7 and 9. 49

Figure 2.6: Muscle synergies and mean synergy activation coefficients for all subjects. *A.* 4 to 6 synergies were identified in each subject. Muscle composition of most of the synergies was similar across subjects ($0.55 < r^2 < 0.94$); muscle synergies W_{1-5} are the most consistent across subjects. Not all the subjects used the same synergies; in particular synergy W_6 (dark green synergy) was only found in four subjects. We identified “goal equivalent” muscle synergies (muscle synergies on gray background), which were activated for the same range of perturbations but had different muscle composition. Also we identified muscle synergies that were very similar in muscle composition but were activated for different range of perturbation directions when compared to other subjects (muscle synergies in gray outline). *B.* The directional tuning of muscle synergy coefficients is similar across subjects, especially for “ankle” strategy synergy 1 (red traces) active during background and backwards perturbation directions (180° to 360°). Gray traces are the tuning curves of muscle synergies with gray outline in 2.6A. These muscle synergies were similar in muscle composition across subjects but different in spatiotemporal activations. 50

Figure 3.1: Example of postural responses to a leftward-forward perturbation of the support surface. *A.* Balance perturbations were induced by a ramp-and-hold motion of the support surface. Same parameters of platform motion were used for perturbations in all stance conditions except for the one-leg stance, in which a smaller platform motion was used. *B.* EMG responses to same balance perturbations in the same direction under different stance conditions. Muscle responses typically occur with a 100-ms onset latency following platform motion (vertical dashed line). Mean EMG activity in 3 time bins of 75ms (EMG_{APR1} , EMG_{APR2} , EMG_{APR3}) during the APR period were computed for each perturbation (shaded areas). 63

Figure 3.2: Tuning curves of multiple muscles in all stance conditions during one time bin. Magnitude and spatial variations in postural responses were observed when subjects stood in different stance configurations. Magnitude of responses increased when stance width decreased. Spatial changes in postural responses are observed in the one-leg, crouched, and widest stance conditions. Black traces indicate the mean response and gray dots represent responses in each trial. Inter-trial variations in postural responses were also observed in all stance conditions. 71

Figure 3.3: Muscle activations of a sample subject during background and during responses evoked by all perturbation directions in all stance conditions. Directional tuning in the activation of all the muscles is observed in all stance conditions. Differences in muscle onset latencies and changes in directional tuning over time can be observed by comparing responses over the three time bins (APR1, APR2, and APR3). Muscle onset latencies in all stance conditions are similar except for the crouched stance condition (red trace), in which proximal muscles are active during early time bins of the APR when they are normally inactive. 73

Figure 3.4: *A.* overall VAF for each stance condition by increasing numbers of synergies in a sample subject 3. Six muscle synergies extracted from the training condition accounted for 93% (narrow), 93% (normal), 92% (wide), 92% (widest), 84% (one-leg), and 73% (crouched), of total variability in each stance condition. *B.* VAF for each muscle's responses (left) and VAF as a function of perturbation direction during background and during the three time bins characterizing the APR (right) in all stance conditions. Colored lines indicate the VAF values when different number of training muscle synergies are used to reproduce each muscle responses. Dots indicate the VAF values characterizing the reconstruction of each trial. VAF >75% for all perturbation directions when six training muscle synergies are used for the data reconstruction in all stance width conditions (red traces). However additional muscle synergies are needed for the reconstruction of crouched and one-leg conditions. *C.* VAF when task-specific muscle synergies are included for the data reconstruction. One additional muscle synergy is needed to improve the directional profile of VAF in the crouched and one-leg stance conditions (dark green traces). 76

Figure 3.5: Muscle synergy vectors and synergy activation coefficients for a representative subject. *A.* Training muscle synergy vectors, W_i^{Tr} , extracted from EMG training data (normal stance condition data in this subject) during quiet stance and three APR time bins. Each bar represents the relative level of activation of each muscle within the synergy (see Methods section for muscle abbreviations). *B.* Activation coefficients, C_i^{Tr} , for each of the 6 synergies in all stance width conditions during two time bins in multiple perturbation directions. Each dot represents the activity of the muscle synergy in a single trial. Directional tuning of muscle synergies over the three time bins can be observed. Changes in magnitudes and spatial tuning of synergy activation coefficients were observed with stance width. For example, the activation of W_5^{Tr} increased when stance width decreased and its tuning curve changed in the widest stance condition. Inter-trial variation of muscle synergy activations are observed by the vertical spread of activation coefficients. 77

Figure 3.6: Training and task-specific muscle synergies with their correspondent averaged synergy activation coefficients across trials *A.* Training muscle synergy vectors, W_i^{Tr} , extracted from training EMG data during quiet stance and three APR time bins. Each bar represents the relative level of activation of each muscle within the synergy (see Methods section for muscle abbreviations). *B.* Averaged activation coefficients, \bar{C}_i , for each of the 6 synergies in normal, crouched, and one-leg stance condition during one time bins in multiple perturbation directions. Directional tuning of training muscle synergies can be observed. *C.* Task-specific muscle synergies for crouched and one-leg stance condition. Task-specific muscle synergies are mainly formed by one single muscle highly activated. *D.* Averaged activation coefficients for each task-specific muscle synergy, \bar{C}_i^{test} . Task-specific muscle synergies were relevant to the specific test condition only. Each task-specific muscle synergy has a directional tuning maintained with time. Notice their activation coefficients are zero for the normal stance and other test condition. 80

Figure 3.7: *A.* Training muscle synergy vectors, W_i^{Tr} *B.* Averaged activation coefficients, \bar{C}_i , for each stance width condition during three time in multiple perturbation directions. Directional tuning of training muscle synergies can be observed. Magnitude changes in muscle synergy activations are observed. In general muscle synergies are activated more in narrow than wide and widest stance conditions. 82

Figure 3.8: Tuning curves in a sample subject in all stance width conditions during two time bins. The original data are shown by the dashed black line and the reconstructed data by the solid black line. The contribution from each synergy to the reconstruction is shown by the corresponding colored line. This is computed by multiplying each training muscle synergy vector W by their corresponding averaged synergy activation coefficients across all trials (\bar{C}_i).84

Figure 3.9: Tuning curves in a sample subject during in one-leg and crouched stance configuration during one time bin. The original data are shown by the dashed black line and the reconstructed data by the solid black line. The contribution from each synergy to the reconstruction is shown by the corresponding colored line. This is computed by multiplying each training muscle synergy vector W by their corresponding averaged synergy activation coefficients across all trials (\bar{C}_i). 85

Figure 3.10: Inter-trial variations in the postural responses of one muscle in three sample stance conditions. *A.* TFL responses in APR2 to 5 randomly interspersed trials in the rightward-forwards (60°) direction in normal, widest, and crouched stance condition. The magnitude of the colored bars represents the contribution of each muscle synergy to the activation of TFL in these 5 trials. The recorded data are indicated by black stars and the reconstructed data by solid black dots. Percentage values indicate the variability accounted for by the muscle synergies (VAF) *B.* Muscle activation patterns across all muscles in APR2 (EMG_{APR2}) are shown. Trial-to-trial variations in TFL result from the variations in muscle synergies that activate multiple muscles. For example in normal stance (left column), all muscles belonging to W_2^{Tr} (green) and TFL activity increase in trial 1 and decrease in trial 5. Similar observations can be made in the other two sample stance conditions. 87

Figure 3.11: Training muscle synergies and task-specific muscle synergies for all subjects. *A.* 5 to 7 training muscle synergies were identified in each subject. Muscle composition of most of W_n^{Tr} was similar across subjects ($0.6 > r^2 > 0.96$); muscle synergies W_{1-5}^{Tr} are the most consistent across subjects. However, differences in muscle composition and synergy activation coefficients across subjects were also identified. Muscle synergies with a gray outline differ in their muscle composition from the other muscle synergies in the cluster but have very similar activation coefficients in all stance conditions. On the other hand muscle synergies on shaded background differ in their activations but have very similar muscle composition to the rest of the muscle synergies in the cluster. Not all the subjects used the same synergies; in particular muscle synergy W_6^{Tr} and W_7^{Tr} were only found in 5 and 2 subjects, respectively. Differences in muscle synergies across subjects indicate that subjects use different muscle activation patterns for maintaining balance in response to the same balance perturbations. 88

Figure 3.12: Averaged synergy activations coefficients for training muscle synergies of all subjects. The directional tuning of muscle synergy coefficients is similar across subjects, especially for “ankle” strategy synergy 1 (red traces) active during background and backwards perturbation directions (180° to 360°). Gray traces correspond are the averaged synergy activation coefficients of subjects having muscle synergies with very similar muscle composition but different activation coefficients from the other subjects. Differences in synergy activations of muscle synergies with similar muscle composition might indicate that subjects choose to activate their muscle synergies differently. 89

Figure 3.13: Averaged synergy activation coefficients of task-specific muscle synergies across subjects. The directional tuning of muscle synergy coefficients is similar across subjects for all time bins. W_2^{1L} , only identified in subject 8, was highly activated in response to medial balance perturbations as indicated by its spatial tuning curve W_2^{1L} . In addition W_3^{1L} was highly activated during background period when subject 8 was standing on one leg before the balance perturbation. 91

Figure 3.14: EMG activation patterns of sample subject 4 in response to one single perturbation direction in all stance conditions. Muscle activation pattern represented by W_6 is consistently observed in EMG responses of this subject in all stance conditions. 93

Figure 4.1: Coordinate system for support surface translations and rotations in 16 evenly spaced directions around the horizontal plane. The coordinate systems used to describe rotation and translation directions were defined such that the horizontal displacement of the cat’s CoM relative to the feet was in the same direction at the end of each translation or rotation. For example, a backwards platform translation and a head down rotation are defined as perturbations in same 0° direction because both displace the cat’s CoM forward, relative to the feet. The coordinate system of force plate recordings is also shown. 108

Figure 4.2: Left hindlimb EMG and force responses of two cats during different experimental conditions. *A*: Responses of cat Bi to 210° platform translation at shortest (13cm) and long (34cm) stance distances. Overall, the EMG activity of most of the recorded muscles was higher at short stance compared to long. *B*: Responses of cat Kn to 225° translation and rotation. Note the overall smaller amplitude of response for rotation compared with translation. Vertical dashed lines mark onset of platform motion. In all cats, the EMG_{BK} and GRF_{BK} responses during background, were quantified by the mean activity over the shaded area before platform onset. Similarly, EMG_{APR} and GRF_{APR} were quantified by the mean activity over the time window indicated by the shaded areas following platform onset. Note the time offset between the EMG_{APR} period and the GRF_{APR} period. Passive changes in force due to platform motion are observed between the dashed line and the gray area indicating the GRF_{APR} window. In the case of platform rotation, note that passive changes in force are relatively large and in the opposite direction to changes in force during the GRF_{APR} window. 110

Figure 4.3: Schematic diagram of EMG and force analysis procedure. *A*: Example of background EMG from 2 muscles, EMG_{BK} , and vertical force, GRF_{zBK} during quiet stance prior to each perturbation direction. *B*: Example tuning curves for the postural response, EMG_{APR} , of the two muscles, and force tuning curve for the vertical component during the postural response, GRF_{zAPR} . In this example, the two muscles are co-activated at each direction while GRF_{zAPR} decreases below background levels for directions 0-180° and increases for 180-360°. *C*: W_1 and W_2 represent functional muscle synergies extracted from the example data. Both muscles (mus_1 and mus_2) are active in each synergy, but with different relative levels of activation (dark and light shaded areas under the EMG tuning curves in B correspond to the activation of synergies 1 and 2, respectively). Before synergy extraction, the active force is decomposed into the absolute values of positive and negative changes from background levels (bottom two plots). Synergy 1 is associated with a change in the positive z-force (F_{APRz+}) and synergy 2, with the negative z-force (F_{APRz-}). 112

Figure 4.4: *A*. Variability accounted for by increasing numbers of synergies for entire datasets at each stance distance for cat Bi. 5 synergies accounted for 96% of total variability in translation at the preferred stance (red line). These same 5 synergies accounted for 84%, 88%, and 87% of the total data variability at shortest, short, and long stance, respectively. *B*. Variability accounted for at each stance distance as a function of perturbation direction for cat Bi. The synergies used to obtain these VAF values were extracted from EMG and force responses during background and APR periods. *C*. Variability accounted for at each stance distance of cat Bi when synergies were extracted from EMG data only. The dimensionality of the synergy set used to characterize muscle postural responses was the same whether or not forces were included in the synergy extraction analysis. 119

Figure 4.5: *A.* Muscle synergy vectors, W_{EMG} , extracted from translation at the preferred stance distance for cat Bi. Each bar represents the relative level of activation for each muscle within the synergy (see Table 4.1 for muscle abbreviations). *B.* Activation coefficients, C_i , for each of the 5 synergies at 4 stance distances. Upper traces show background, quiet stance activation levels across direction. Lower traces show the response to translation across direction. *C.* Synergy force vectors, W_F , associated with each muscle synergy (same color coding), drawn in the sagittal, frontal, and horizontal planes. Vectors are expressed as forces applied by the limb against the support. Note that the scale for the horizontal plane has been magnified for easier viewing. 122

Figure 4.6: EMG tuning curves of the automatic postural response in cat Bi for translations at 4 stance distances. The original data are shown by the dashed black line and the reconstructed data by the solid black line. The contribution from each synergy to the reconstruction is shown by the corresponding colored line. This is computed by multiplying each functional synergy vector W by its activation coefficient C . 123

Figure 4.7: *A,B.* Synergy force vectors extracted from translation data at the preferred stance distance, for cat Bi. Vectors are expressed as forces applied by the limb against the support, and are rotated in the sagittal plane such that the z-axis is collinear with the mean GRF vector observed during quiet standing, which itself rotates with stance distance. Coordinate axes of the F-frame are shown at each stance distance. *C.* Applied force tuning curves for translation at 4 stance distances for cat Bi, expressed in the F-frame coordinate system. Black dashed lines indicate the original experimental data, black solid lines the reconstructed data and colored lines the contributions from each synergy force vector. *D.* Tuning curves of the recorded force amplitude data from cat Bi for 4 stance distances. The forces have been separated into components as described in the text. The same data are drawn in two different coordinate reference frames, Earth-based (solid gray lines) and F-frame based (dashed black lines). Note that the phase of the F_y force tuning curves remains constant when expressed in limb coordinates, but changes in Earth coordinates. 126

Figure 4.8: Translation synergies applied to platform rotation data. Left panel: synergy vectors, W , extracted from translation data of cat Wo. Center panel: activation coefficients, C , of each synergy for background activity during quiet stance and for the response to translation (solid lines) and rotation (dashed lines). Right panel: synergy force vectors associated with each of the 5 muscle synergies, drawn in 3 planes. 128

Figure 4.9: Muscle (*A*) and force (*B*) tuning curves of the automatic postural response to translations (left column) and rotations (right column). Details as in Figure 7. Force tuning curves are expressed in the Earth reference frame because cats stood at their preferred stance distance during both types of perturbation. 130

Figure 4.10: Functional muscle synergies, synergy activation coefficients, and synergy force vectors across subjects. In all cats, 5 synergies accounted for >96% of the variability in response to translation at the preferred stance. The directional tuning of muscle synergy coefficients is similar across the 6 cats ($r^2 > 0.6$ except for C_5 of cat Ni and An). Muscle synergies are similar across cats ($r^2 > 0.6$) except for W_{EMG3} of the 6 cats and W_{EMG1} of cat Ni and cat Kn ($r^2 < 0.47$). The direction of three synergy force vectors, W_{F1} (red), W_{F2} (yellow), and W_{F4} (blue) is similar across cats ($r^2 > 0.74$) with the exception of W_{F4} of cat Ru and Kn (when compared to Ni). W_{F3} (green) and W_{F5} (purple) are only similar in some cases. Only those muscles recorded in common (indicated by colored bars) were used for calculating r^2 in the comparison of muscle synergies across cats. Gray bars indicate the remainder of muscles recorded in each subject.132

Figure A.1: Percent EMG variability accounted for by 5 synergies over time and perturbations in cat Ru. 154

Figure A.2: Muscle synergies and synergy activation levels versus perturbation direction and time. 154

LIST OF SYMBOLS AND ABBREVIATIONS

An	cat Anakn
APR	Automatic postural response
BFEM	Biceps femoris
BFMA	Anterior biceps femoris
BFMM	Medial biceps femoris
BFMP	Posterior biceps femoris
Bi	cat Bidry
C_i	i^{th} synergy activation coefficients
\bar{C}_i	i^{th} averaged synergy activation coefficients across all trials
C_i^{L}	i^{th} synergy coefficients of task-specific synergy in one-leg condition
C_i^{Cr}	i^{th} synergy coefficients of task-specific synergy in crouched condition
C_i^{Tr}	i^{th} synergy activation coefficients of training muscle synergies
CoM	Center of Mass
CP	cerebral palsy
EDL	Extensor digitorum longus
EMG	Electromyographic
ERSP	Erector spinae
EXOB	External oblique
FDL	Flexor digitorum longus
Fx	Endpoint force in x direction
Fy	Endpoint force in y direction
Fz	Endpoint force in z direction

GMED	Gluteus medius
GLUA	Anterior gluteus medius
GLUP	Posterior gluteus medius
GLUT	Gluteus medius
GRAA	Anterior gracilis
GRAP	Posterior gracilis
GRF	Ground reaction force
ILPS	Iliopsoas
Kn	cat Knobi
LGAS	Lateral gastrocnemius
M1	motor cortex
MCP	Metacarpophalangeal
MGAS	Medial gastrocnemius
MTP	Metatarsophalangeal
Ni	cat Nikey
NMF	non-negative matrix factorization
PERO	Peroneus Longus
PLAN	Plantaris
r^2	coefficient of determination
REAB	Rectus abdominalis
REFM	Rectus femoris
Ru	cat Russl
SEMA	Anterior semimembranosus
SEMB	Semimembranosus

SEMP	Posterior semimembranosus
SEMT	Semitendinosus
SOL	Soleus
SRTA	Anterior sartorius
SRTM	Medial sartorius
STEN	Semitendinosus
TA	Tibialis anterior
TFL	Tensor fasciae latae
TIBA	Tibialis anterior
VAF	% variability accounted for
VMED	Vastus medialis
VLAT	Vastus lateralis
W_{EMGi}	i^{th} functional muscle synergy
W_{Fi}	i^{th} synergy force vector
W_i	i^{th} muscle synergy
W_i^{Tr}	i^{th} training muscle synergy
W_i^{Cr}	i^{th} task-specific synergy in crouched condition
W_i^{1L}	i^{th} task-specific synergy in one-leg condition
Wo	cat Wooky

SUMMARY

The musculoskeletal structure of the human and animal body provides multiple solutions for performing any single motor behavior. The *long-term goal* of the work presented here is to determine the neuromechanical strategies used by the nervous system to appropriately coordinate muscles in order to achieve the performance of daily motor tasks. The *overall hypothesis* is that the nervous system simplifies muscle coordination by the flexible activation of muscle synergies, defined as a group of muscles activated as a unit, that perform task-level biomechanical functions. To test this hypothesis we investigated whether muscle synergies can be robustly used as building blocks for constructing the spatiotemporal muscle coordination patterns in human and feline postural control under a variety of biomechanical contexts.

We demonstrated the generality and robustness of muscle synergies as a simplification strategy for both human and animal postural control. A few robust muscle synergies were able to reproduce the spatial and temporal variability in human and cat postural responses, regardless of stance configuration and perturbation type. In addition inter-trial variability in human postural responses was also accounted for by these muscle synergies. Finally, the activation of each muscle synergy in cat produced a specific stabilizing force vector, suggesting that muscle synergies control task-level variables. The identified muscle synergies may represent general modules of motor output underlying muscle coordination in posture that can be activated in different sensory contexts to achieve different postural goals. Therefore muscle synergies represents a simplifying mechanism for muscle coordination in natural behaviors not only because it is a strategy for reducing the number of variables to be controlled, but because it represents a mechanism for simply controlling multi-segmental task-level variables.

CHAPTER 1

INTRODUCTION

1.1 Bernstein's degrees of freedom problem

Most natural behaviors can be accomplished by a variety of joint motion combinations. Further, a combination of joint motions can be produced by an unlimited number of different muscle activation patterns. Thus the musculoskeletal structure of the body provides multiple solutions for performing any single motor behavior. How does the central nervous system decide what muscles to activate among all the possible solutions? This unconstrained problem, first stated by Bernstein, is known as the degrees of freedom problem (Bernstein 1967). Bernstein proposed that the nervous system solves this problem by reducing the number of variables to be controlled through the simultaneous coordination of multiple joints by the activation of multiple muscles as a unit. Bernstein's work initiated a long line of research that investigates whether the nervous system independently controls each muscle or simplifies muscle coordination by the simultaneous control of multiple muscles.

1.2 Muscle synergies simplifying muscle coordination

In this work, a muscle synergy is defined as a group of muscles activated as a unit by a single neural command. Muscle synergies simplify muscle coordination because the activation of multiple muscles in synchrony by a single neural command reduces the number of variables controlled during natural behaviors. It has been proposed that muscles forming a muscle synergy might be activated with specific relative gains such that each muscle synergy represents a *fixed* muscle activation pattern (Tresch et al. 1999). Thus muscle synergies can be used as building blocks for constructing the muscle coordination required to perform natural behaviors such as walking, swimming, jumping, finger spelling, and postural balance in vertebrates and invertebrates (for review see Flash

and Hochner 2005). Alternatively, the nervous system would have to specify the activation of each muscle and coordinate it with the activation of all other muscles across the body during every single motor task.

Muscle synergies may represent functional modules since muscles forming a synergy might generate torques at multiple joints across the body, thus the activation of a muscle synergy might perform a multi-segmental tasks such as producing an end-point force or displacing the body center of mass (CoM) in a particular direction. Several studies have correlated the activation of muscle synergies to biomechanical outputs such as endpoint forces during postural control (Ting and Macpherson 2005), hand posture during finger spelling (Weiss and Flanders 2004), foot and limb kinematics in walking (Ivanenko et al. 2003; Ivanenko et al. 2004), kick direction in frogs (Saltiel 2001), center of pressure movement in standing (Krishnamoorthy et al. 2003), and foot acceleration in pedaling (Ting et al. 1999). We present in Chapter 4 results demonstrating muscle synergies are associated with the generation of end-point forces that produce stabilizing forces in cat during multiple postures.

Therefore, muscle synergies could reflect a mechanism used by the nervous system to simply control mechanical variables relevant to the task at hand. Several studies have demonstrated that in order to successfully achieve a motor behavior the nervous system performs a tight control of variables relevant to the task (task-level variables), such as endpoint trajectory during reaching (Hogan et al. 1987), and a loose control of local variables, such as individual joint angles or muscle activation patterns (Macpherson 1991; Scholz and Schoner 1999). Since the activation of muscle synergies might results in generating biomechanical functions relevant to the task, the nervous system could simply control task-level variables by modulating muscle synergies producing biomechanical functions. Therefore, under the assumption that it would require a lot of effort from the nervous system to determine the individual joint torques needed to control a task-level variable and specify the muscle activations that would

generate those joint torques, it can be hypothesized that the nervous system simplifies muscle coordination by activating muscle synergies representing functional motor modules that control task-level variables.

1.3 Why study standing postural control?

Postural control in standing balance is essential for performing any voluntary motor behavior. From a child taking their first step to a ballerina performing a complicated leap; balance is actively controlled by the nervous system to achieve the task at hand. Therefore we are interested in investigating the underlying mechanisms for muscle coordination during postural control.

Additionally, falling is the leading cause of health problems in the elderly (Minino et al. 2002), thus a better understanding of muscle coordination required for balance might give insight into strategies required for fall prevention. Current theoretical and experimental work in postural control investigates separately the biomechanical and neural characteristics of postural control (Allum et al. 2002; Diener et al. 1988; Dimitrova et al. 2004a; Kuo 1995). Few studies integrating both neuromuscular activity and biomechanical behavior have been completed (Jacobs and Macpherson 1996; Jo and Massaquoi 2004; Ting and Macpherson 2005). The approach proposed in this study could be used to understand how the nervous system coordinates muscle activity to generate the biomechanical outputs needed for maintaining balance. Therefore, results from our research might enable us to better assess the functional consequences of abnormal muscle activation patterns in patients with poor balance such as stroke or Parkinsonian patients (Dimitrova et al. 2004a; Dimitrova et al. 2004b; Horak et al. 2005; Rocchi et al. 2004).

We chose to investigate muscle coordination in the context of postural control not only because of its volitional and clinical relevance but also because of its quasi-static characteristics (Horak and Macpherson 1996). Linear models have been shown to predict muscle activation patterns in isometric conditions (cf. van Bolhuis and Gielen 1999) such

as the quasi-isometric postural task. Therefore, linear models can be used to investigate the underlying mechanisms of muscle coordination in postural tasks because the nonlinearities in muscle activation due to large movements are minimized.

Although standing postural control can be considered a quasi-static behavior, the muscle coordination required for performing this task has the complex features of many other motor behaviors. Therefore, because of its quasi-static characteristics yet complex muscle activation patterns, postural control represents a tractable and useful motor behavior model for investigating the underlying muscle coordination strategies. The pertinent features of postural responses are described in the following section.

1.4 Muscle synergies in postural control

Standing postural control is a multi-segmental task that requires the activation of multiple muscles to maintain the body CoM within the base of support area, which is the area under and between the feet. In response to a balance disturbance, end-point forces are required to move the CoM back to the region of stability bounded by the base of support area. The transformation from muscle activations to forces and then to movement of CoM is complex because the contraction of a single muscle can lead to the acceleration of all remote joints (Zajac and Gordon 1989). Therefore, predicting the muscle coordination required for maintaining balance is a complex problem.

1.4.1 Early models of postural synergies

Two distinct and stereotypical muscle activation patterns evoked in response to anterior and posterior support surface displacements were the first muscle synergies identified during postural control (Nashner 1977). These two muscle synergies implemented each one of the two postural strategies called “ankle” and “hip” strategy. These muscle synergies had very consistent temporal and spatial features, supporting the

hypothesis of existing modular motor output patterns as high level organizing principles for movement.

1.4.2 Problems with *fixed* muscle synergies

Different muscle activation patterns from the *fixed* postural synergies described by Nashner were observed under experimental conditions evoking more naturalistic responses. A large variety of muscle activation patterns different from those described by Nashner were observed in response to different perturbation directions (Henry et al. 1998; Macpherson 1988b), changes in stance configuration (Henry et al. 2001; Macpherson and Fung 1999; Torres-Oviedo et al. 2006), and changes prior subject experience (Horak and Nashner 1986).

High degree of variability is observed in postural responses evoked during different paradigms challenged the hypothesis of simultaneous activation of muscles in synergies. Spatial variability in cat (Macpherson 1988b) and human (Henry et al. 1998) postural responses is characterized by the different muscle activation patterns evoked in response to multidirectional support surface motions. In addition, temporal variability in human postural responses is evident by the non-strict coactivation and non-consistent temporal sequence of muscle activations elicited in response to multi-directional balance perturbations in the normal stance (Gruneberg et al. 2005; Henry et al. 1998) and under different stance configurations (Burtner et al. 1998; Woollacott et al. 1998). Moreover, variability in postural strategy selection resulting in different mixtures of the “ankle” and “hip” strategies is characterized by the inter-trial variations of postural responses to identical balance perturbations (Horak and Nashner 1986). Finally, additional magnitude, spatial, and temporal changes occur when postural responses are evoked under different stance configurations in cat (Macpherson and Fung 1999; Torres-Oviedo et al. 2006) and human (Henry et al. 2001).

Therefore, spatial and temporal variability in cat and human postural responses, the postural strategy selection variability in human standing postural control, as well as additional spatial and temporal variability induced by changes in posture suggests independent muscle control of every muscle is needed in order to produce the adequate postural responses to the context of the task at hand.

1.4.3 Alternate muscle synergy model

Horak and Macpherson proposed the flexible activation of muscle synergies may execute multiple postural strategies (Horak et al. 1997; Macpherson 1991). While high degree of variability is observed in postural responses evoked during different paradigms, the strategies performed to maintain balance are limited. Moreover, despite of muscle redundancy we do not observe an unlimited combination of muscle activation patterns during postural responses. Therefore, it has been suggested that the flexible activation of muscle synergies may be used to execute the various postural strategies selected based on multiple factors such as environmental context, mental state, and behavioral goal (Horak et al. 1997). In this work we demonstrate quantitatively that the flexible activation of muscle synergies can reproduce the complexity of individual muscle activation patterns in response to support surface balance perturbations.

Finally if muscle synergies reflect an actual neural control strategy, then one should expect a certain robustness, or generality, of the synergy structure across a variety of behavioral tasks as well as across individuals. A few studies have demonstrated the generality of muscle synergies across behaviors (d'Avella and Bizzi 2005) and across variations of a motor behaviors (Krishnamoorthy et al. 2004). In the current study we further investigate the generality and robustness of muscle synergies for postural control by examining whether the muscle synergies reproducing cat and human postural responses are specific to a single postural task and time period of the postural response or generalize across tasks (cf. Chapter 3 and Chapter 4) and time course of the response.

1.5 Thesis Overview

The three studies presented in this work aim to address the issue of generality and robustness of functional muscle synergies as a simplification strategy for postural control. In the first study we identified muscle synergies that could robustly reproduce spatial, temporal, and inter-trial variations in muscle postural responses during a postural task. In the second study we investigated the robustness of muscle synergies across a variety of postural tasks. Finally, we investigated whether the activation of each muscle synergy in cats was associated with a biomechanical function such as produced a specific stabilizing force vector.

1.5.1 Study 1: Muscle synergies for human standing postural control.

We *hypothesize* that a few muscle synergies can reproduce the spatial, temporal, and inter-trial variability in postural responses to multidirectional support surface translations. Volunteers underwent multidirectional support surface translations. We extracted functional muscle synergies from electromyographic (EMG) postural responses in a few trials (training trials) and used them to reconstruct EMG postural responses in the remaining trials. Our results show that spatial, temporal, and inter-trial variability in postural responses are reproduced by variations in the activation of a general set of muscle synergies. Therefore, the identified muscle synergies may be used by the nervous system to implement postural strategies for standing postural control.

1.5.2 Study 2: Robustness of muscle synergies for human standing postural control

We *hypothesize* that a few functional muscle synergies can reproduce the postural responses to multidirectional support surface translations even if the postural responses are altered by changing the stance configuration. Volunteers underwent multidirectional support surface translations at different postural configurations, with the natural stance as the control condition. We extracted functional muscle synergies from the postural

responses in the control condition and used them to reconstruct the postural responses to all other experimental conditions. Our results show that magnitude, spatial, and temporal changes in postural responses caused by changes in biomechanical task are reproduced by variations in the activation of a general set of muscle synergies. Therefore, muscle synergies represent general motor output patterns used as a simplification mechanism for producing postural responses in different biomechanical contexts, suggesting that muscle synergies in standing postural control represent a neural and not biomechanical constraint.

1.5.3 Study 3: Robust muscle synergies in cat control high-level biomechanical variables

We *hypothesize* that muscle synergies are associated with biomechanical output such as end-point forces. Furthermore, we *hypothesize* these *functional* muscle synergies can reproduce the EMG and force patterns produced in response to multidirectional support surface translations even if these postural responses are altered by changing the postural configuration. Three cats were perturbed by multidirectional support surface translations at different postural configurations, with the natural stance being the control condition. We extracted functional muscle synergies from the postural responses in the control condition and used these functional muscle synergies to reconstruct the postural responses in all other experimental conditions. Our results show that a few functional muscle synergies have a consistent biomechanical output across different postures, and variations in their activation robustly reproduce muscle and force patterns in different stance configurations. Therefore, muscle synergies not only are a general simplification strategy for postural control but also are a mechanism that simplifies the sensorimotor transformations required to generate the appropriate stabilizing forces to counteract balance perturbations.

CHAPTER 2

MUSCLE SYNERGIES CHARACTERIZE

HUMAN POSTURAL RESPONSES

Postural control is a natural behavior that requires the spatial and temporal coordination of multiple muscles. Complex muscle activation patterns characterizing postural responses suggest the need for independent muscle control. However, our previous work shows that postural responses in cats can be robustly reproduced by the activation of a few muscle synergies (Ting and Macpherson 2005; Torres-Oviedo et al. 2006). We now investigate whether a similar simplification structure is used for human postural control. We hypothesized that a few muscle synergies could account for the inter-trial variability in automatic postural responses from different perturbation directions, as well as different postural strategies. Postural responses to multidirectional support-surface translations in 16 muscles of the lower back and leg were analyzed in nine healthy subjects. Six or fewer muscle synergies were required to reproduce the postural responses of each subject. The composition and temporal activation of several muscle synergies identified across all subjects were consistent with the previously identified “ankle” and “hip” strategies in human postural responses. Moreover, inter-trial variability in muscle activation patterns was successfully reproduced by modulating the activity of the various muscle synergies. This suggests that trial-to-trial variations in the activation of individual muscles are correlated, and moreover, represent variations in the amplitude of descending neural commands that activate individual muscle synergies. Finally, composition and temporal activation of most of the muscle synergies were similar across subjects. These results suggest that muscles synergies represent a general simplification strategy underlying muscle coordination in postural tasks.

2.1 Introduction

Several studies have demonstrated that muscle synergies, or M-modes (Krishnamoorthy et al. 2004; 2003), defined as low-dimensional modules formed by muscles activated in synchrony (Cappellini et al. 2006; Cheung et al. 2005; Ivanenko et al. 2005; Ivanenko et al. 2003; Ivanenko et al. 2004; Ting and Macpherson 2005; Torres-Oviedo et al. 2006) or with fixed time delays (d'Avella et al. 2006; d'Avella et al. 2003) may be used by the nervous system as building blocks for constructing motor output patterns during both locomotor and postural tasks. In this study we define a muscle synergy as a group of muscles activated in synchrony with fixed relative gains, thus, a synergy represents a muscle activation pattern with consistent spatial characteristics. We investigated whether a few muscle synergies could reproduce the coordinated spatiotemporal muscle activation patterns observed during human postural responses.

In both humans and cats, muscle activation patterns in response to multidirectional balance perturbations vary as a function of perturbation direction, suggesting independent muscle activation (Allum et al. 2003; Carpenter et al. 1999; Henry et al. 2001; Henry et al. 1998; Macpherson 1988b). However, in cats, this directional tuning of responses can be reproduced by the activation of a general set of muscle synergies across a wide range of postural tasks (Ting and Macpherson 2005; Torres-Oviedo et al. 2006). Principles of sensorimotor integration during postural control are quite similar in humans and cats, despite differences in stance configuration and biomechanics (Dunbar et al. 1986; Horak and Macpherson 1996). Therefore, we investigated whether human postural responses to multidirectional perturbations can also be explained by the activation of a limited set of muscle synergies.

In contrast to cats, humans can use several postural strategies to maintain balance resulting in considerable inter-trial variations of electromyographic (EMG) responses to identical balance perturbations (Horak and Nashner 1986). Factors that affect the choice of strategy include prior experience, habituation, expectation, and fear (Carpenter et al.

2006; Keshner et al. 1987; Woollacott and Shumway-Cook 2002). The two most extreme human postural responses are the “ankle” and “hip” strategies, in which muscle activation patterns have very different spatiotemporal characteristics (Horak et al. 1997; Horak and Macpherson 1996). These strategies have recently been shown to be independent modes of movement (Alexandrov et al. 1998; Alexandrov et al. 2005; Alexandrov et al. 2001a; b; Creath et al. 2005; Massion et al. 2004), suggesting that they could result from the activation of independent muscle synergies. The “ankle” and “hip” strategies can also be concurrently activated, creating a continuum of possible postural responses representing different mixtures of the two strategies (Creath et al. 2005; Horak and Macpherson 1996). In this study, we tested whether muscle synergy analysis could be used to quantify the variable contribution of each strategy to each given postural response.

These postural strategies also induce considerable variations in muscle onset latency in human postural responses. For example, “ankle strategy” responses are characterized by shorter onset latencies than “hip strategy” responses (Horak and Macpherson 1996). Previous studies have overcome this issue by averaging over large time windows (Henry et al. 2001; Henry et al. 1998) or time windows that vary with individual muscle onset (Carpenter et al. 1999). In the current study, we analyzed multiple time windows during the automatic postural response (APR) to explicitly examine whether the temporal variation in muscle onset latencies could be accounted for by differential temporal activation of muscle synergies.

The spatiotemporal features of EMG patterns representing different postural strategies have been traditionally characterized by analyzing the average across multiple trials that exhibit consistent postural responses (Carpenter et al. 1999; Gruneberg et al. 2005; Henry et al. 1998; Horak and Macpherson 1996; Horak and Nashner 1986; Nashner 1977). This approach, however, has the disadvantage of relying on the repeatability of postural responses. In such studies, inter-trial variations must be

minimized in order to avoid confounded averaged responses. This might present a problem especially in clinical research where fewer trials, and less consistent postural responses might be collected, inducing large inter-trial variations in EMG patterns. Recent factorization algorithms have been able to identify consistent muscle activation patterns in non-averaged trials during frog scratching, swimming, and jumping (Cheung et al. 2005; Tresch et al. 1999). We investigated whether a similar factorization analysis could enable us to identify spatiotemporal characteristics of human postural strategies in a dataset containing high inter-trial variability. This would provide a powerful diagnostic tool since the analysis would not require repeatability in postural responses to characterize muscle coordination of the motor behavior in question.

We demonstrated that a small set of muscle synergies can robustly account for a wide range of muscle activation patterns during human postural responses. We were able to reproduce directional tuning of EMG patterns, temporal differences in muscle onset latencies, and variations in postural strategy using a few muscle synergies. Muscle synergy analysis effectively decomposed “mixed” responses in individual trials into contributions from different postural strategies, demonstrating that consistency in postural responses is not required to identify robust muscle synergies. We further demonstrated similarities in muscle synergy patterns across subjects. Taken together, our findings suggest that the identified muscle synergies represent modules of motor output that can be recruited in variable proportions during postural responses.

2.2 Methods

2.2.1 Experimental setup

Nine healthy subjects, 4 females and 5 males (ages 19-27), were tested following an experimental protocol approved by the Georgia Tech and Emory University Institutional Review Boards. Subjects stood on a platform that was made to translate in a

set of twelve directions evenly distributed in the horizontal plane (Fig. 1B). Ramp-and-hold perturbations of 12.4-cm total displacement, 35-cm/s peak velocity, and 490-cm/s² (0.5 g) peak accelerations were presented.

Because we were interested in examining the richest possible dataset (see Discussion), we used an experimental paradigm that has been shown to elicit a wide range of postural strategies (Horak 1996; Horak and Nashner 1986). In this paradigm, the “normal stance” (medial-lateral stance width of 19 cm) trials were randomly presented among trials of different stance configurations. Over the course of experimental sessions held on two consecutive days, subjects received ten replicates of each perturbation direction in normal stance and five replicates of other direction/stance combinations. The electrode positions on the subject’s body were marked to ensure similar electrode placement in both experimental sessions. As an initial study in the current paper we will present the analysis of the normal stance responses.

EMG activity was recorded from sixteen leg and lower-back muscles of the subject’s right side. Table 2.1 contains an inclusive list of all the recorded muscles. EMG data were filtered and processed offline using a set of custom MATLAB routines. EMG data were high-pass filtered at 35 Hz, de-meaned, rectified, and low-pass filtered at 40 Hz.

2.2.2 Data processing

To account for temporal variation in EMG activity, four time periods (“bins”) were analyzed: quiet standing during a 280-ms background period (BK) that ended 170 ms before the perturbation, and three 75-ms time bins beginning 100 ms (APR1), 175 ms (APR2), and 250 ms (APR3) after perturbation onset (Fig. 2.1).

These time bins were chosen based on previous studies characterizing the different temporal features of muscle activity during the time course of the postural response (Diener et al. 1988). Mean muscle activity during these four time bins was

computed for each of the 16 muscles in each trial. From these, we generated a vector of data for each of the 16 muscles that included 4 time bins x 12 directions x 10 trials = 480 data points. EMGs were normalized to their respective maximum response amplitude during background and APR period across all perturbation directions so that all values of each muscle were between 0 and 1. Then, each muscle data vector, which consisted of EMG_{BK} , EMG_{APR1} , EMG_{APR2} , and EMG_{APR3} across all perturbation directions, was normalized to have unit variance to ensure the activity in all muscles was equally weighted.

Table 2.1 List of the muscles recorded from the right leg and trunk across subjects.

Label	Muscle name	Label	Muscle name
GMED	Gluteus medius	REAB	Rectus abdominalis
VLAT	Vastus lateralis	SEMT	Semitendinosus
VMED	Vastus medialis	BFEM	Biceps femoris
SOL	Soleus	REFM	Rectus femoris
PERO	Peroneus Longus	SEMB	Semimembranosus
TFL	Tensor fasciae latae	MGAS	Medial gastrocnemius
TIBA	Tibialis anterior	LGAS	Lateral gastrocnemius
ERSP	Erector spinae	EXOB	External oblique

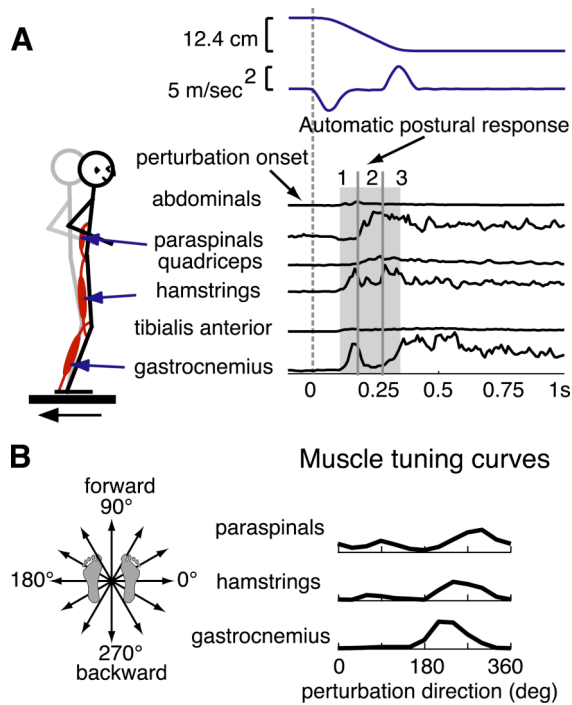


Figure 2.1 Example of postural responses to backwards perturbation of the support surface. *A*. Balance perturbations were induced by a ramp-and-hold motion of the support surface. EMG responses are directionally specific and typically occur with a 100-ms onset latency following platform motion (vertical dashed line). Mean EMG activity in 3 time bins of 75ms (EMG_{APR1} , EMG_{APR2} , EMG_{APR3}) during the APR period were computed for each perturbation (shaded areas). *B*. Coordinate system for support surface translations in 12 evenly spaced directions in the horizontal plane. Muscle tuning curves represent changes in APR activation in a single time bin over all perturbation directions.

2.2.3 Extraction of Muscle Synergies

Using nonnegative matrix factorization (Cheung et al. 2005; Lee and Seung 2001; Torres-Oviedo et al. 2006; Tresch et al. 2006), we extracted muscle synergies from the EMG data matrix. This linear decomposition technique assumes that each muscle activation pattern, \mathbf{M} , evoked by a perturbation at a given time period (e.g. EMG_{APR2} , and EMG_{APR3} shown in Fig. 2.5) is composed of a linear combination of a few (N_{syn}) muscle synergies \mathbf{W}_i , each activated by synergy activation coefficient c_i . Thus, the net muscle activation pattern vector \mathbf{M} takes the form:

$$\mathbf{M} = c_1 \mathbf{W}_1 + c_2 \mathbf{W}_2 + \dots + c_n \mathbf{W}_n$$

\mathbf{W}_i is a vector that specifies the spatial pattern of muscle activity defined by muscle synergy i . Each element of \mathbf{W}_i represents a muscle, whose relative contribution to the muscle synergy takes a value between 0 and 1. These values forming a muscle synergy are constant over all trials and the entire muscle synergy is modulated by a single, scalar, non-negative, activation coefficient c_i . The activation coefficient c_i represents the purported neural command to the muscle synergy that determines the relative contribution of the muscle synergy \mathbf{W}_i to the overall muscle activation pattern, \mathbf{M} . For each synergy i , the set of activations c_i across all perturbation directions during quiet stance and during the three APR periods is the vector \mathbf{C}_i . The \mathbf{C}_i components during the three APR periods represent the tuning curves that describe how the activation of the muscle synergy \mathbf{W}_i changes as a function of perturbation direction and time.

In all our subjects we iterated the analysis by varying N_{syn} between 1 and 10 and then selected the least number of synergies that could adequately reconstruct background and APR responses of each muscle in all the trials, as determined by greater than 75% variability accounted for (VAF) in each muscle data vector. VAF is defined as $100 \times$ uncentered Pearson correlation coefficient (Torres-Oviedo et al. 2006; Zar 1999). This criterion ensured that each muscle tuning curve would be well-reconstructed, so that the critical spatiotemporal features of each muscle activation pattern were well-accounted for by the muscle synergies. In general, by satisfying this local criterion, the total VAF in the dataset was well over 90%.

For cross-validation purposes we also extracted N_{syn} synergies from 60% of the trials at each perturbation direction (training trials) and used them to reconstruct the muscle responses in the remaining trials (testing trials). For each subject, we also extracted a set of N_{syn} muscle synergies from the averaged response for each direction as in previous studies (Ting and Macpherson 2005; Torres-Oviedo et al. 2006) to determine whether the predictive power of muscle synergies increased when inter-trial variability was considered.

Muscle synergies extracted from all trials of each subject were ranked based on muscle composition and synergy activation profiles rather than on percentage of contribution to the total data variability (as in other factorization methods such as principal component analysis). We performed a *functional sorting* because subjects might use muscle synergies differently, causing comparable muscle synergies to have large differences in contribution to the total data variability. Thus, muscle synergies across individuals were classified based on their similarity, as determined by the coefficient of determination ($r^2 > 0.55$) between all training and task-specific muscle synergies and their corresponding averaged synergy activation coefficients across all trials (\bar{C}).

An initial sorting was performed by comparing muscle synergies and their \bar{C} s of all subjects to a reference subject and an initial averaged set of W s and \bar{C} s vectors across subjects was computed. Then using an iterative process, muscle synergies with similar muscle composition ($r^2 > 0.55$) or similar activation coefficients \bar{C} s ($r^2 > 0.55$) to the averaged W and C vectors were grouped. The averaged set of W s and \bar{C} s vectors across subjects used as a reference were updated every time a muscle synergy was discriminated from a group. We monitored when muscle synergies were part of a group because of their similar muscle composition, activation coefficients, or both. The r^2 values obtained not only served as a sorting parameter, but also as a measure to evaluate the generality of muscle synergies across subjects.

2.3 Results

For each subject, a few muscle synergies were found to reproduce spatiotemporal muscle activation patterns recorded during quiet stance and during responses to multidirectional balance perturbations. Trial-to-trial variations in muscle activations were accounted for by trial-to-trial variations in synergy activation coefficients that represent neural commands to the various muscle synergies. Finally, all subjects

exhibited muscle synergies that were similar in terms of muscle composition and spatiotemporal activation pattern.

2.3.1 A few muscle synergies can reproduce EMG patterns that vary with time and perturbation direction

Differences in postural responses elicited across all muscles were observed in the spatial, temporal, and inter-trial variability of the data. Each muscle was activated in response to a range of perturbation directions. This directional sensitivity is represented by muscle tuning curves (Fig. 2.2; gray traces), which were unique to each muscle even if similarities in muscle tuning curves were observed. However, the onset latency in the EMG responses varied across muscles. For example, all proximal muscles except for erector spinae, external oblique, and gluteus medius were inactive during APR1 and were highly activated during later time bins. In addition, the directional sensitivity of the responses of more proximal muscles, such as vastus lateralis, tensor fascia latae, and rectus abdominalis, changed during the three time bins of the APR (Fig. 2.2). Finally, inter-trial variations of muscle activations were also observed in muscle responses to each perturbation direction (Fig. 2.2; black dots). These characteristics of postural responses were consistent with results from previous studies using similar paradigms (Carpenter et al. 1999; Gruneberg et al. 2005; Henry et al. 1998; Horak and Nashner 1986)

An adequate reconstruction of muscle activation patterns measured over all trials, including all perturbation directions and all time bins was obtained by the linear combination of a few muscle synergies. Six or fewer muscle synergies accounted for $92 \pm 2\%$ of the total data variability in the 9 subjects. The mean total VAF in the training datasets was $92 \pm 2\%$ and in the test data set was $90 \pm 2\%$. Background and APR responses of every muscle in all trials were well reconstructed, as determined by VAF% $>75\%$ in all muscles. In all subjects, the number of muscle synergies that could reproduce the postural responses varied between 4 and 6 (Fig. 2.5). The number of synergies chosen

for each subject was corroborated by the fact that adding more synergies contributed evenly to the VAF of all muscles, suggesting that the extra synergies reconstructed only random variations in the data.

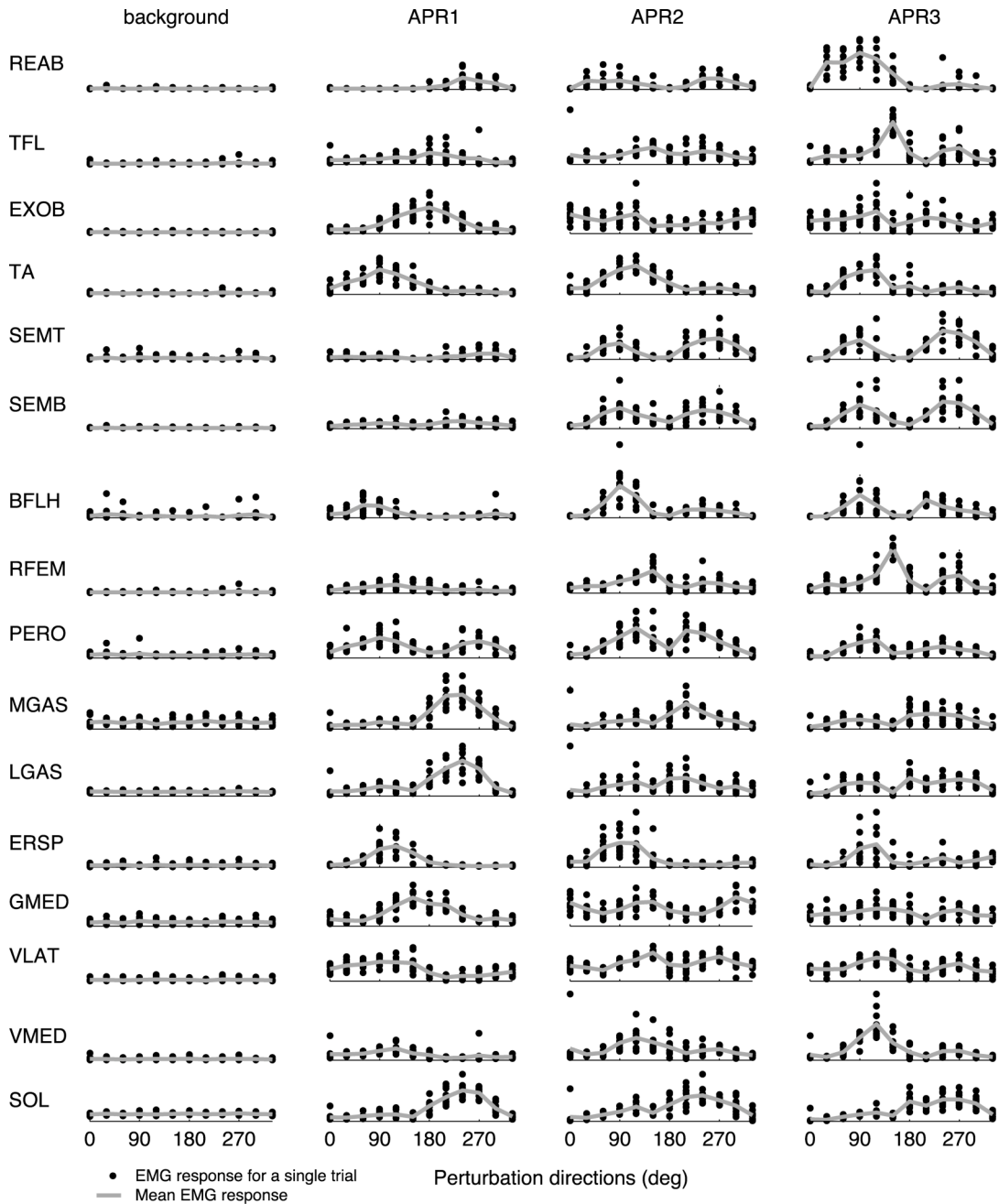


Figure 2.2 Muscle activations during background and during responses evoked by all perturbation directions during all time bins in an example subject. Directional tuning is observed in the activation of all the muscles. Inter-trial variations of muscle activations are observed by the vertical spread of data points (black dots). Gray traces indicate the mean responses.

Each muscle synergy, W_i , specifies the activation of several muscles across the body (Fig. 2.3 left column), and each muscle synergy was activated during specific perturbation directions and time bins, as specified by C_i (Fig. 2.3 right columns). Muscle synergies were not strictly grouped by anatomical classification but appear to be grouped by function. For example, in muscle synergies of a representative subject (Fig. 2.3), W_1 activated the gastrocnemii, peroneus and soleus, and was active in backward (270°) perturbations, consistent with the “ankle” strategy. W_2 was active in forward perturbations and activated the tibialis anterior, but also includes a number of extensors that were presumably activated to prevent knee and hip joint flexion during the “ankle” strategy to forward perturbations. These two muscle synergies were highly activated during the early time bins of the APR. Synergies $W_{3,4}$ involved trunk and proximal muscles and were active in later time bins (APR_2 and APR_3). W_5 was formed by abductor gluteus medius and lateral trunk muscle external oblique and it was primarily active in medial-lateral (180° and 0°) perturbations. W_6 is composed of biceps femoris, a knee flexor and hip extensor, ankle dorsiflexor tibialis anterior and ankle evertor peroneus, as well as anti-gravity muscles erector spinae and soleus. The activation and muscle composition of this muscle synergy might be explained by the particular behavior of these subject who bent their knees in response to perturbations. Only one muscle synergy, W_1 , which included soleus, was active during the background period to provide antigravity support (Fig. 2.3, red muscle synergy). This muscle synergy was observed in all of the subjects (Fig. 2.5). The independent activation of muscle synergies enabled them to reproduce changes in EMGs with both time and perturbation direction.

These muscle synergies can reproduce postural responses of individual muscles. Changes in directional tuning with time bins of individual muscles are reproduced by changes in the contribution of entire muscles synergies to the activation of each muscle (Fig. 2.4). The net activation of some muscles such as RFEM is accounted for by one

single synergy on all time periods while the activation of some other muscles like PERO is accounted for by the activation of two different synergies.

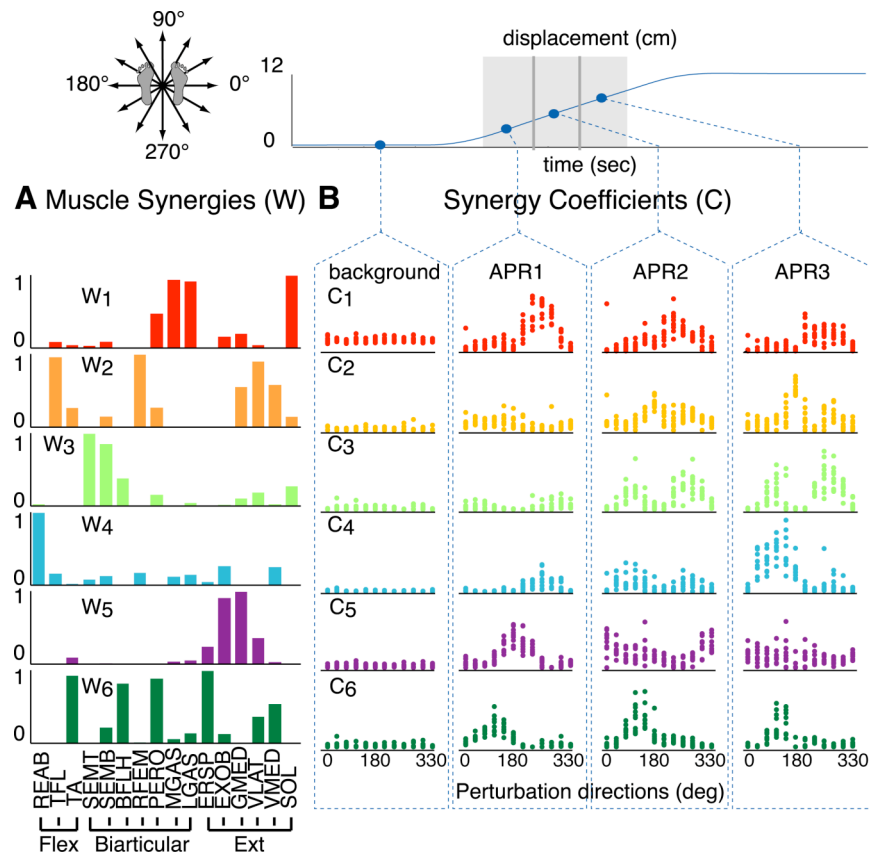


Figure 2.3 Muscle synergy vectors and synergy activation coefficients for a representative subject. *A.* Muscle synergy vectors, W_i , extracted from EMG data during quiet stance and three APR time bins. Each bar represents the relative level of activation of each muscle within the synergy (see Methods section for muscle abbreviations). *B.* Activation coefficients, C_i , for each of the 6 synergies during each time bin in multiple perturbation directions. Each dot represents the activity of the muscle synergy in a single trial. Directional tuning of muscle synergies over the three time bins can be observed. For example W_1 is mainly active during the initial period of the APR in backward directions (180° to 270°) whereas W_4 is active during the later time bin of the APR in forward directions (0° to 90°).

2.3.2 Inter-trial variations in EMG patterns are accounted for by modulating muscle synergy activations

EMG activity varied from trial-to-trial in each muscle, however the patterns of variation were not random or independent across muscles and could be explained by

inter-trial differences in muscle synergy activations. Overall muscle synergies were directionally tuned, being activated for a specific range of perturbation directions.

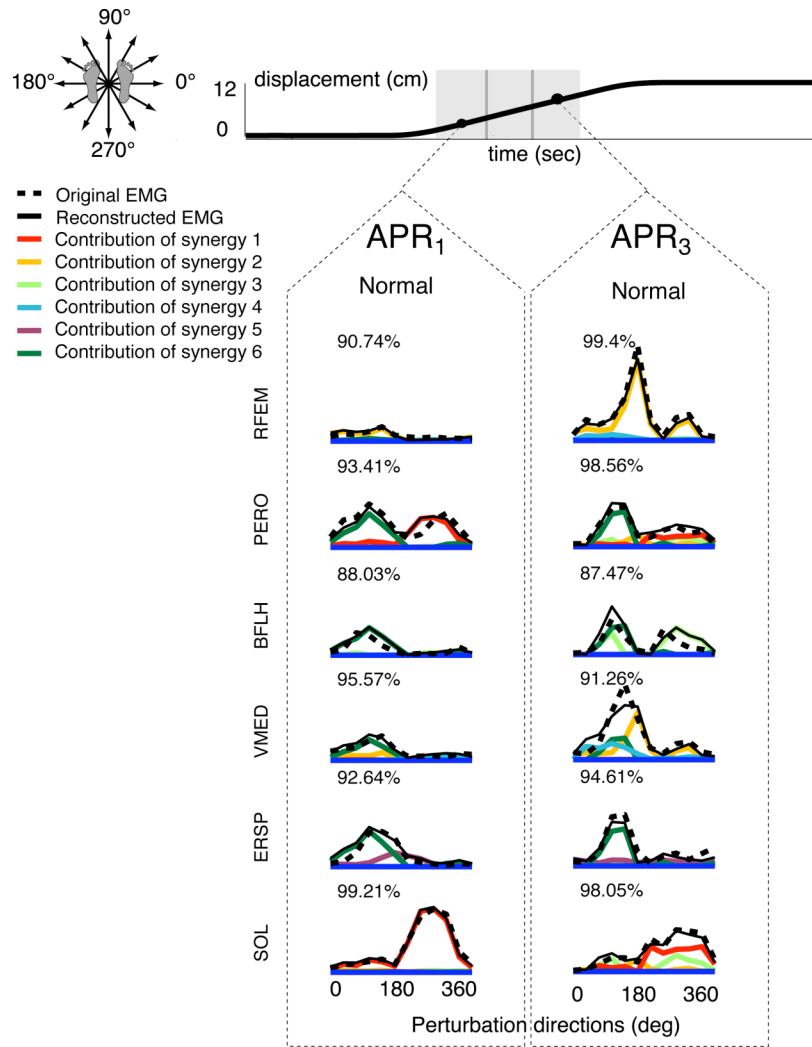


Figure 2.4 Mean tuning curves in a sample subject during two time bins. The original data are shown by the dashed black line and the reconstructed data by the solid black line. The contribution from each synergy to the reconstruction is shown by the corresponding colored line. This is computed by multiplying each training muscle synergy vector W by their corresponding averaged synergy activation coefficients across all trials (\bar{C}_i).

However, the exact level of muscle synergy activation varied from trial-to-trial (Fig. 2.3), which affected the level of activity in all muscles within the muscle synergy. For example responses of peroneus to a forward-lateral (120°) perturbation varied trial-by-trial (Fig. 2.2 and 2.5A). In trial 7, peroneus was highly activated whereas in trial 8 peroneus activity was reduced. This difference was not simply a random variation in

muscle activity, because all the other muscles belonging to W_6 also showed increased activity (Fig. 2.4B, dark green bars). Similarly, the level of activation in gluteus medius varied in response to lateral balance perturbations (0°) (Fig. 2.1 and 2.5C). The level of activation in the gluteus medius could be attributed to the activation of two different muscle synergies (Fig. 2.5C; bottom panel, W_2 , yellow, and W_5 , purple), which affected the overall pattern of activation across all muscles involved in those muscle synergies.

Prior balance perturbation conditions may have affected the responses evoked in subsequent trials. Immediately prior to trial 7, the subject underwent the same lateral perturbation (0°). In contrast, immediately prior to trial 9, the subject responded to a perturbation direction in the opposite direction (180°). The contribution of W_5 might have been reduced in trial 7 due to habituation and increased in trial 9 due to the difference between the prior and subsequent perturbation.

In contrast, muscle synergies extracted from averaged data in each direction had diminished predictive power in reconstructing inter-trial variations in EMGs. When muscle synergies from averaged data were used for the reconstruction of muscle activation patterns the mean VAF decreased by $16 \pm 5\%$ in the training dataset and $17 \pm 6\%$ in the testing dataset. Increasing the number of muscle synergies extracted from averaged data did not improve the reconstruction of inter-trial variations in EMG patterns. If the variations in EMG patterns were due to random variability, then we would expect a comparable VAF whether averaged data or individual trials were analyzed. However, the analysis of individual trials increased the predictive power of muscle synergies, further suggesting that inter-trial variations in EMG patterns were due to variations in the contributions of the muscles synergies to each individual trial.

2.3.3 Similarities in muscle synergies across subjects

Muscle synergy composition and recruitment was similar across subjects (Fig. 2.6A; $0.50 > r^2 > 0.94$). W_1 through W_4 were found in 6 subjects. These appear to

quantify the classic muscle synergies observed during “ankle” and “hip” strategy as indicated by their muscle composition and the temporal characteristics of their activations (Fig. 2.6B; \bar{C}_1 through \bar{C}_4 traces). Muscle synergy activation coefficients were consistent across all subjects (Fig. 2.6B; $0.40 > r^2 > 0.96$), especially \bar{C}_1 ($R^2 > 0.84$) indicating the regions of activation of the extensor ankle W_1 .

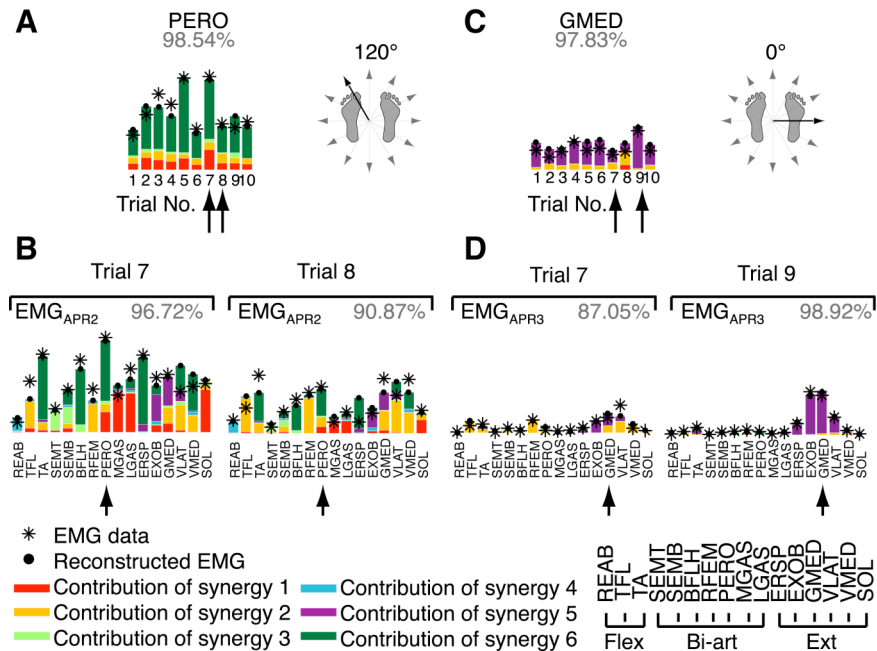


Figure 2.5 Inter-trial variations in the postural responses of two muscles. *A.* PERO responses in APR2 to 10 randomly interspersed trials in the medial-forward (120°) direction. The magnitude of the colored bars represents the contribution of each synergy to the activation of PERO in these 10 trials. The recorded data are indicated by black stars and the reconstructed data by solid black dots. Percentage values indicate the variability accounted for by the muscle synergies (VAF%) *B.* Muscle activation patterns across all muscles in APR2 (EMG_{APR2}) are shown. Trial-to-trial variations in PERO result from the variations in muscle synergies that activate multiple muscles. All muscles belonging to synergy 6 (green) increase in trial 7 and decrease in trial 8, as does PERO activity. *C.* GMED activation to lateral perturbations (0°). *D.* Muscle activation patterns across all muscles in trial 7 and 9.

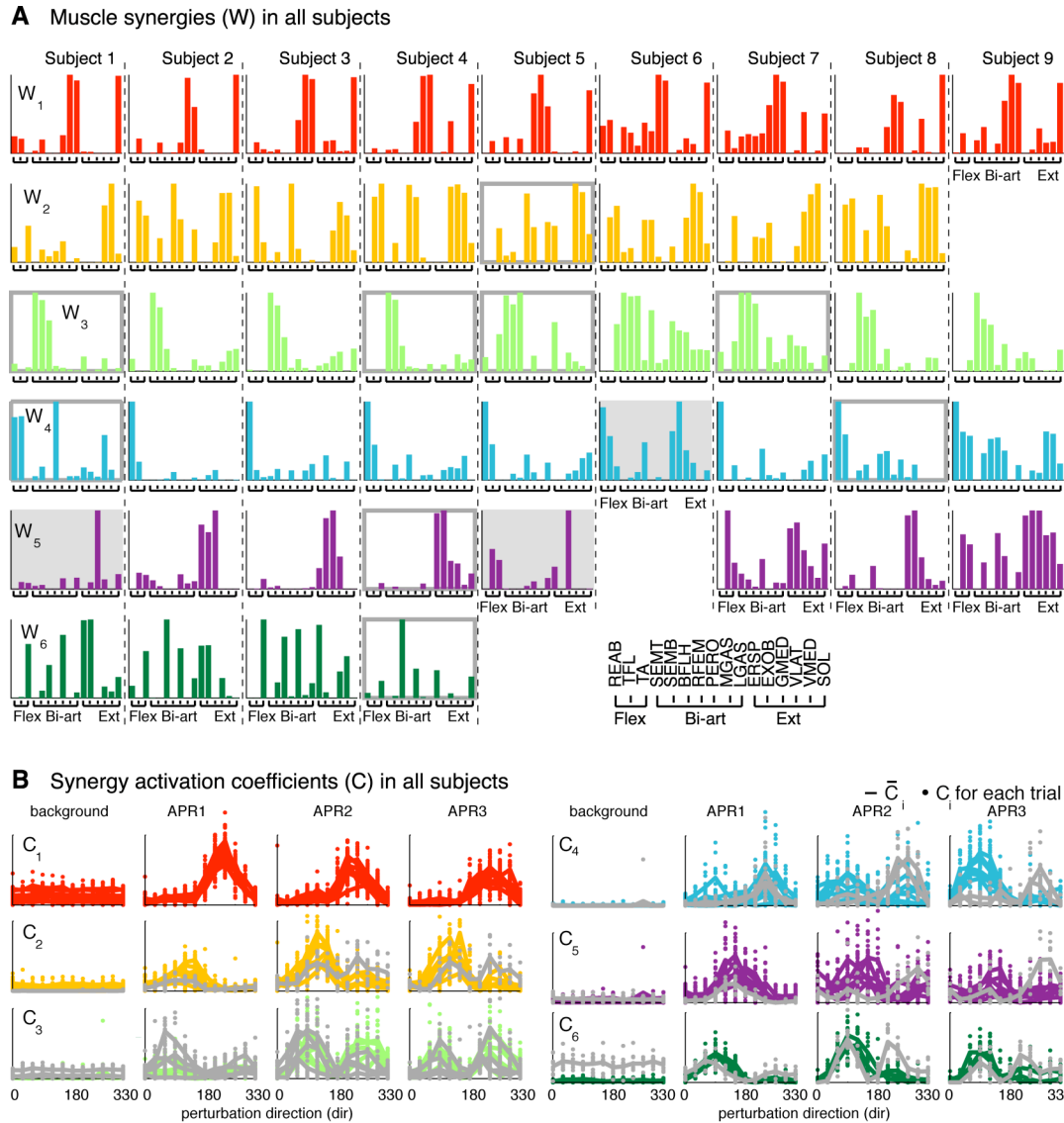


Figure 2.6. Muscle synergies and mean synergy activation coefficients for all subjects. A. 4 to 6 synergies were identified in each subject. Muscle composition of most of the synergies was similar across subjects ($0.55 > r^2 > 0.94$); muscle synergies W_{1-5} are the most consistent across subjects. Not all the subjects used the same synergies; in particular synergy W_6 (dark green synergy) was only found in four subjects. We identified “goal equivalent” muscle synergies (muscle synergies on gray background), which were activated for the same range of perturbations but had different muscle composition. Also we identified muscle synergies that were very similar in muscle composition but were activated for different range of perturbation directions when compared to other subjects (muscle synergies in gray outline). B. The directional tuning of muscle synergy coefficients is similar across subjects, especially for “ankle” strategy synergy 1 (red traces) active during background and backwards perturbation directions (180° to 360°). Gray traces are the tuning curves of muscle synergies with gray outline in 2.6A. These muscle synergies were similar in muscle composition across subjects but different in spatiotemporal activations.

Our analysis also revealed certain subject-specific muscle synergies, such as W_6 in subjects 1 through 4. This muscle synergy was mainly activated in response to forward perturbations, except for subject 4 in which this same synergy was active during background period, when subject is standing before perturbation, and in response to forward (90°) and backward-lateral (240°) support surface motions (Fig. 2.6B; gray trace in W_6 row).

Across subjects, W_5 had different muscle composition, yet appeared to have the same function of maintaining hip medial-lateral stability. Most of the subjects used W_5 , these muscle synergies had similar tuning curves despite the differences in muscle composition (Fig. 2.6A; dark backgrounds). The fact that they were activated with similar directional tuning, suggests that W_5 in all subjects can stabilize the body to the same range of forward perturbations. Therefore, these muscle synergies may represent different muscle activation strategies for achieving the same task.

2.4 Discussion

In summary, a few muscle synergies account for the spatial, temporal, and postural strategy variability in human postural responses. In each subject, spatiotemporal characteristics of muscle activation patterns were reproduced by the independent modulation of a few muscle synergies. We were able to quantify the contributions of different postural strategies to “mixed” responses from individual trials. Moreover, repeatability in postural responses was not needed to identify robust muscle synergies. Thus, the factorization analysis performed here represents a powerful diagnostic tool that assesses relevant EMG spatiotemporal features in datasets containing high inter-trial variations. Further, the consistency of muscle synergy composition across subjects and the similarity in muscle synergy activation patterns across subjects suggest a robust muscle synergy organization underlying neural control of human balance.

2.4.1 Spatial variability

Our analysis quantitatively identified muscle synergies that produce muscle activation patterns associated with the “ankle” and “hip” strategies previously described in human balance control (Horak et al. 1997; Horak and Macpherson 1996). For example, the motor patterns represented by W_1 is consistent with the spatial muscle activation patterns characteristic of the “ankle” strategy. Similarly, W_{2-4} represent motor patterns consistent with the “hip” strategy, where proximal muscles have larger activations than ankle muscles causing a fast movement of the CoM (Henry et al. 1998; Horak and Macpherson 1996). The superposition of muscle synergies can generate the more complex motor patterns that have been described as the combination of these two strategies in both the sagittal (Horak and Nashner 1986) and frontal planes (Carpenter et al. 1999; Gruneberg et al. 2005).

Maintaining balance is a multisegmental task that requires interjoint coordination. In multiple studies Alexandrov and colleagues have shown that ankle and hip strategies each define patterns of torque that are coupled across the body to produce coordinated postural responses (Alexandrov et al. 1998; Alexandrov et al. 2005; Alexandrov et al. 2001a; b). In our “ankle” muscle synergies, several proximal muscles are also activated, probably to prevent motion in the hip and knee joints caused by interaction torques (Zajac 2002; Zajac and Gordon 1989). This is particularly true in response to forward perturbations where no mechanical limits of joint range can be utilized (cf. backward perturbations which tend to extend the knee)(Horak and Macpherson 1996; Horak and Nashner 1986). Further testing using musculoskeletal models is needed to determine the influence of biomechanics in muscle synergy organization.

2.4.2 Temporal variability

The variations in onset latencies in muscle activity could be accounted for by the differential activation of muscle synergies over time. Namely, in response to anterior-

posterior perturbations, muscle synergies formed by distal ankle muscles were activated first and muscle synergies formed by proximal leg and trunk muscles were activated later. These results are consistent with previous studies reporting distal to proximal muscle responses to anterior-posterior balance perturbations (Horak and Macpherson 1996). Moreover, during medial-lateral perturbations W_2 and W_5 , mainly formed by proximal muscles and few distal muscles, were the only synergies activated. Therefore in medial-lateral balance perturbations proximal muscles responded with the same latency as the distal ankle muscles, temporal organization that is consistent with previous studies (Carpenter et al. 1999; Gruneberg et al. 2005; Henry et al. 1998). Using just three time bins, we were able to characterize basic temporal features in synergy activations that were consistent with previous studies describing temporal features of individual muscle activations. These time bins characterized the primary temporal phases of the postural response. If we were to use a finer temporal resolution, we anticipate a more accurate timing profile of synergy activations showing the transitions between postural strategies would be observed, but the basic synergy organization and conclusion of the study would remain unchanged.

Our results suggest that the neural commands activating the various muscle synergies have different and independent time-courses. Other studies have addressed temporal differences in muscle activation during locomotor behaviors or fast reaching movements by identifying fixed time delays associated with each muscle synergy (d'Avella et al. 2006; d'Avella et al. 2003), suggesting feedforward muscle synergy activation. While this may be appropriate for rhythmic locomotor behaviors or ballistic movements, muscle activation in postural responses to balance perturbations is modulated by sensory feedback due to the perturbation (Kuo 1995; 2005; Park et al. 2004; Peterka 2002). Thus, in our analysis we assumed that each muscle synergy was a time-invariant muscle activation pattern and the entire muscle synergy could be modulated by time-dependent feedback signals. This is consistent with the effect of

sensory feedback on synergy activation coefficients revealed during locomotion behaviors of intact and deafferented frogs (Cheung et al. 2005).

2.4.3 Inter-trial variability

Inter-trial variations in muscle activation patterns reflect differences in postural strategies used in each trial. Variations in muscle activation patterns during postural responses are highly influenced by prior trial conditions. Adaptation studies show that postural responses to support surface translations on a stable surface are affected by prior experience consisting of the same task on an unstable surface (Horak 1996; Horak and Nashner 1986). Other factors that affect the choice of strategy include prior experience, habituation, expectation, and fear (Carpenter et al. 2006; Keshner et al. 1987; Woollacott and Shumway-Cook 2002). Prior studies have had difficulty dealing with this inter-trial variability because most response represent compound “ankle” and “hip” strategies, defined as “mixed” strategies (Horak and Macpherson 1996; Horak and Nashner 1986). In our experiments we induced high inter-trial variability by randomly interspersing trials with different perturbation directions and stance configurations. We were able to decompose muscle activation patterns in each individual trial or response into explicit contributions of each postural strategy, as represented by a specific muscle synergy. Thus, our analysis represents a powerful method that could be used for clinical research to assess important spatiotemporal features of the muscle coordination needed to perform the task in a dataset containing high inter-trial variations. The robustness of muscle synergies across multiple trials suggests muscle synergies encode goal-directed patterns of motor output that are modulated by higher centers to produce the appropriate postural response based on the particular postural strategy and postural task (Dietz 1992; Horak 1996).

2.4.4 Muscle synergy robustness across subjects

Similarity in muscle synergies may reflect consistency in neural circuitry or biomechanical constraints across subjects. All subjects used a consistent low-dimensional set of muscle synergies over two consecutive days and a few muscle synergy patterns were similar across subjects. These results suggest muscle synergies might be programmed in the nervous system as indicated by studies in kicks and frog locomotive behaviors revealing muscle synergies encoded in the frog spinal cord (Hart and Giszter 2004; Saltiel et al. 2005; Saltiel et al. 2001). In addition, the biomechanics of the body might also influence the consistency of muscle synergies. For example, the biomechanics of the human hand has been shown to constrain the variability in muscle activation patterns when producing voluntary finger end-point forces (Valero-Cuevas 2000; Valero-Cuevas et al. 1998).

Differences in muscle synergy composition may reflect subject-specific movement patterns and demonstrate the musculoskeletal redundancy in achieving the task of keeping the center of mass over the base of support during a postural perturbation. W_5 in all subjects were activated for the same directions of balance perturbation but their muscle composition varies across subjects (Fig. 2.6; muscle synergies on gray background). Similarly, subject 1 through 4 used a “knee” strategy synergy, W_6 , which was not found in other subjects. Similar inter-subject differences in muscle synergies have been shown in upper-arm movements where two different strategies are used to produce the same movement (Sabatini 2002).

While differences in anatomy may contribute to differences in muscle synergies, it is likely that prior training and motor skill influenced subject-specific movement patterns. Learning a motor skill may influence the performance of another motor skill (Schmidt and Lee 2005) and this generalization depends on the context in which our limbs are normally used (Krakauer et al. 2006). Also, new synergies and new contributions of each synergy to net motor output can be formed when individuals are

trained to perform different motor behaviors (Mussa-Ivaldi and Bizzi 2000). Our analysis might be useful for quantifying changes in muscle synergy organization with rehabilitation, or to compare and contrast strategies used by different subjects.

2.4.5 Muscle synergy generality

In the current study, we demonstrate that more than one synergy can be used to stabilize the center of mass for a given perturbation direction. Similarly, multiple synergies have been identified in the frog for performing leg extension (Saltiel et al. 1998). Therefore, while constraining the possible motor output patterns for a particular movement, the use of muscle synergies does not uniquely specify the response pattern used for a given postural perturbation.

That the muscle synergies identified could account for variations within a single postural task demonstrates that muscle synergies may indeed be modules used for controlling task-level variables, such as center of mass motion. Several studies have shown that the activation of muscle synergies correlates to the control of task-level variable such as endpoint force (Ting and Macpherson 2005), or center of pressure displacement (Krishnamoorthy et al. 2003) in postural tasks, and endpoint foot kinematics during locomotion (Ivanenko et al. 2003). It remains to be seen whether the muscle synergies identified here are general across a wide range of stance configurations (Henry et al. 2001), or for different types of postural responses such as taking a compensatory step (McIlroy and Maki 1993; 1999). However, prior work demonstrating the generality of muscle synergies across different postural and locomotor tasks in animals (d'Avella and Bizzi 2005; Torres-Oviedo et al. 2006) suggests that the muscles synergies identified probably represent some general motor output patterns for movement. The existence of such modules of motor output are consistent with the fact that neural firing in the motor cortex (Georgopoulos et al. 1982) and spinal cord (Poppele and Bosco 2003) appear to encode task-level variables. This is further supported by the

modular behaviors evoked by stimulation of the premotor cortex (Graziano 2006) and the spinal cord (Lemay and Grill 2004; Saltiel et al. 2001). Our results provide evidence for the hypothesis that muscle coordination can be simplified by the activation of muscle synergies that represent tailored modules controlling specific task-level variables. Moreover, the contributions of each muscle synergy can be modulated by descending influences on postural strategy such as prior experience or anticipation, as well as regulated through sensory feedback to perform motor behaviors.

CHAPTER 3

ROBUSTNESS OF MUSCLE SYNERGIES CHARACTERIZING HUMAN POSTURAL RESPONSES

In Chapter 2 we demonstrated that a few muscle synergies were able to reproduce postural responses to multidirectional balance perturbations in human subjects. In this study we investigated whether these muscle synergies are part of a general postural strategy or whether they are specific to the standing postural task presented in Chapter 2. To address this question of generality we tested whether muscle synergies identified in EMG responses when standing in a “typical” stance configuration could robustly account for the altered postural responses observed in other stance configurations. Support surface translations in multiple directions in the horizontal plane were used to perturb nine healthy subjects standing in 6 different stance conditions: 1) one-leg, 2) narrow, 3) wide, 4) very wide, 5) crouched, and 6) normal stance (control condition). We analyzed spatial, temporal, and inter-trial variations in the activation patterns of 16 leg and lower back muscles during quiet stance and during automatic postural responses in all stance conditions. Non-negative matrix factorization was used to extract muscle synergies from the “training condition,” which was either narrow or normal stance depending on the subject. In all subjects the number of muscle synergies required to reproduce the postural responses in the training condition varied between four and six. These muscle synergies extracted from the training condition were subsequently able to reconstruct $93 \pm 0.8\%$ (narrow), $93 \pm 1.4\%$ (normal), $93 \pm 1\%$ (wide), $92 \pm 1\%$ (widest), $84 \pm 9.9\%$ (crouched), and $84 \pm 4.7\%$ (one-leg) of the total data variability in all other stance conditions. In order to fully reproduce all muscle activation patterns in the one-leg and crouched stance conditions two or fewer additional muscle synergies were required in most subjects. Most of the muscle synergies were therefore *general* across stance conditions, although they were recruited differently in each stance condition. Finally, muscle synergies were

robust across subjects ($0.6 < r^2 < 0.98$). The robustness of synergy organization across postures and subjects suggests that muscle synergies represent a *general* simplification strategy underlying muscle coordination in postural control.

3.1 Introduction

Recent studies provide evidence that the nervous system does not control muscles independently during complex, natural behaviors, but uses a few neural commands that activate preferred patterns of muscle activation, called muscle synergies (Cheung et al. 2005; d'Avella and Bizzi 2005; d'Avella et al. 2006; d'Avella et al. 2003; Sabatini 2002; Ting and Macpherson 2005; Torres-Oviedo et al. 2006; Tresch et al. 2006; Tresch et al. 1999) or M-modes (Krishnamoorthy et al. 2004; 2003; Latash et al. 2002). Several studies have demonstrated the generality in activation of modular motor outputs during different locomotor behaviors (Cappellini et al. 2006; Ivanenko et al. 2005; Ivanenko et al. 2004). However, only a few studies have addressed the question of generality in muscle synergies across different motor behaviors (d'Avella and Bizzi 2005; Jing et al. 2004; Poggio and Bizzi 2004) or across varieties of a single motor behavior (Krishnamoorthy et al. 2004; Raasch and Zajac 1999; Torres-Oviedo et al. 2006). Therefore, in this study we further investigate the generality of muscle synergies previously identified in a standing postural control task (cf. Chapter 2) across multiple postural tasks.

It remains to be determined whether new postural strategies are needed to recover balance when the biomechanical context changes. Our recent work has shown that the spectrum of possible human postural responses are reproduced by variations in contributions of muscle synergies representing the “ankle” and “hip” strategies (Chapter 2), which are the most distinct postural strategies characterized by muscle activation patterns with very different spatial and temporal features (Horak et al. 1997; Horak and Macpherson 1996; Horak and Nashner 1986). In this study we intersperse balance

disturbance directions and biomechanical contexts to induce a range of different postural strategies (Horak 1996; Horak and Nashner 1986). We hypothesize that variation in the relative contribution of muscle synergies used in the normal stance suffices to produce appropriate postural responses in different biomechanical contexts, as was observed in feline postural control (Torres-Oviedo et al. 2006). To test this hypothesis we studied muscle activation patterns during balance perturbations under specific biomechanical contexts that altered magnitude, temporal, and spatial features of postural responses.

Changes in stance width alter the magnitude of postural responses due to biomechanical constraints such as body biomechanics and gravity. The stiffness of the musculoskeletal system, which influences the magnitude of muscle activations, is modulated with stance width (Day et al. 1993; Winter et al. 1998). Also based on physics, to counteract the effect of gravity and maintain static equilibrium the whole-body center of mass has to be maintained within the base of support, defined as the area delimited by the body segments in contact with the environment (e.g., the area under and between the feet, Horak and Macpherson 1996). Consequently, more active postural control is required when the base of support is small, as demonstrated by the increase in EMG stabilizing responses when base of support decreases in cats (Macpherson and Fung 1998; Torres-Oviedo et al. 2006) and in humans (Henry et al. 2001; Horak and Macpherson 1996). Overall changes in stance width alter magnitude of postural responses but activation onset latencies and spatial tuning across muscles are maintained with stance width in humans (Henry et al. 2001). This suggests the same muscle synergies are consistently used across these different postures. We used a quantitative approach to determine whether the muscle synergies used for multidirectional postural control previously identified by us (Chapter 2) and others (Henry et al. 2001; Henry et al. 1998; Horak et al. 1997; Horak and Nashner 1986) are generally used as a simplification strategy for postural control under several biomechanically distinct conditions.

Changes in temporal characteristics of postural responses are induced by balance perturbations in more extreme changes in posture. Typically, muscles across the human body respond following a distal-to-proximal temporal sequence to support-surface balance perturbations in anterior-posterior directions (Henry et al. 1998; Horak et al. 1997; Horak and Macpherson 1996; Horak and Nashner 1986) but not in medial-lateral directions (Gruneberg et al. 2004; Gruneberg et al. 2005). This temporal organization is not maintained in all perturbation directions when subjects stand in a crouched posture, in which proximal and distal muscles are activated simultaneously (Burtner et al. 1998; Woollacott et al. 1998). In the current study, we analyzed multiple time windows during the automatic postural response (APR) to explicitly examine whether the temporal variation in muscle onset latencies due to stance biomechanical changes could be accounted for by differential temporal activation of muscle synergies. We hypothesize that altering the activation of a general set of muscle synergies can reproduce the characteristic changes in onset latency accompanying drastic changes in posture.

Postural responses to multidirectional support-surface translations in one-leg stance have not been previously investigated but this stance configuration should induce changes in spatial tuning of postural responses. Studies in one-leg quiet stance reveal differences in ground reaction forces and EMG activations between one-leg and bipedal stances, suggesting differences in spatial activation patterns and possibly in postural strategies between these two stance conditions. Contrary to bipedal stance, in which end-point force directions in horizontal plane are only directed laterally (Henry et al. 2001), end-point force directions in one-leg quiet stance are multidirectional (Jonsson et al. 2004). Consequently, high EMG activations of lateral muscles observed in one-leg quiet stance (Kumagai et al. 1997; Tropp and Odenrick 1988; Van Deun et al. 2007) might be due to the need for medial stabilizing end-point forces required for the postural task. We hypothesize similar changes in spatial activation patterns will be required to maintain balance during multidirectional support-surface translations in one-leg stance. We will

test whether muscle synergies form normal (bipedal) stance are also used in one-leg stance and whether different muscle synergies are required to maintain one-leg standing balance.

Here we demonstrate that a small set of *general* muscle synergies can robustly reproduce human postural responses to multidirectional support-surface perturbations at a variety of initial stance configurations. A single set of muscle synergies reproduce magnitude, temporal, and spatial changes of individual EMG responses induced by changes in the initial stance configuration. However, task-specific muscle synergies are required to reproduce large spatial and magnitude changes in postural responses observed in the one-leg and crouched conditions, respectively. Thus, task-specific muscle synergies in one-leg stance represent muscle activation patterns particular to this task, but task-specific muscle synergies identified in crouched configuration might represent the non-linear activation of muscles forming one of the *general* muscle synergies. We further demonstrate similarities in muscle synergy patterns across subjects. Taken together, our findings suggest that the identified muscle synergies represent *general* modules of motor output for standing postural control recruited in variable proportions depending on the biomechanics of the task at hand.

3.2 Methods

3.2.1 Experimental setup

We tested whether a general set of muscle synergies could reproduce postural responses elicited in biomechanically distinct stance configurations. All experimental protocols were approved by the Georgia Tech and Emory University Institutional Review Boards. Nine healthy subjects (5 females and 4 males, aged 18-31) stood on a platform that translated in twelve directions evenly distributed in the horizontal plane (Fig. 3.1).

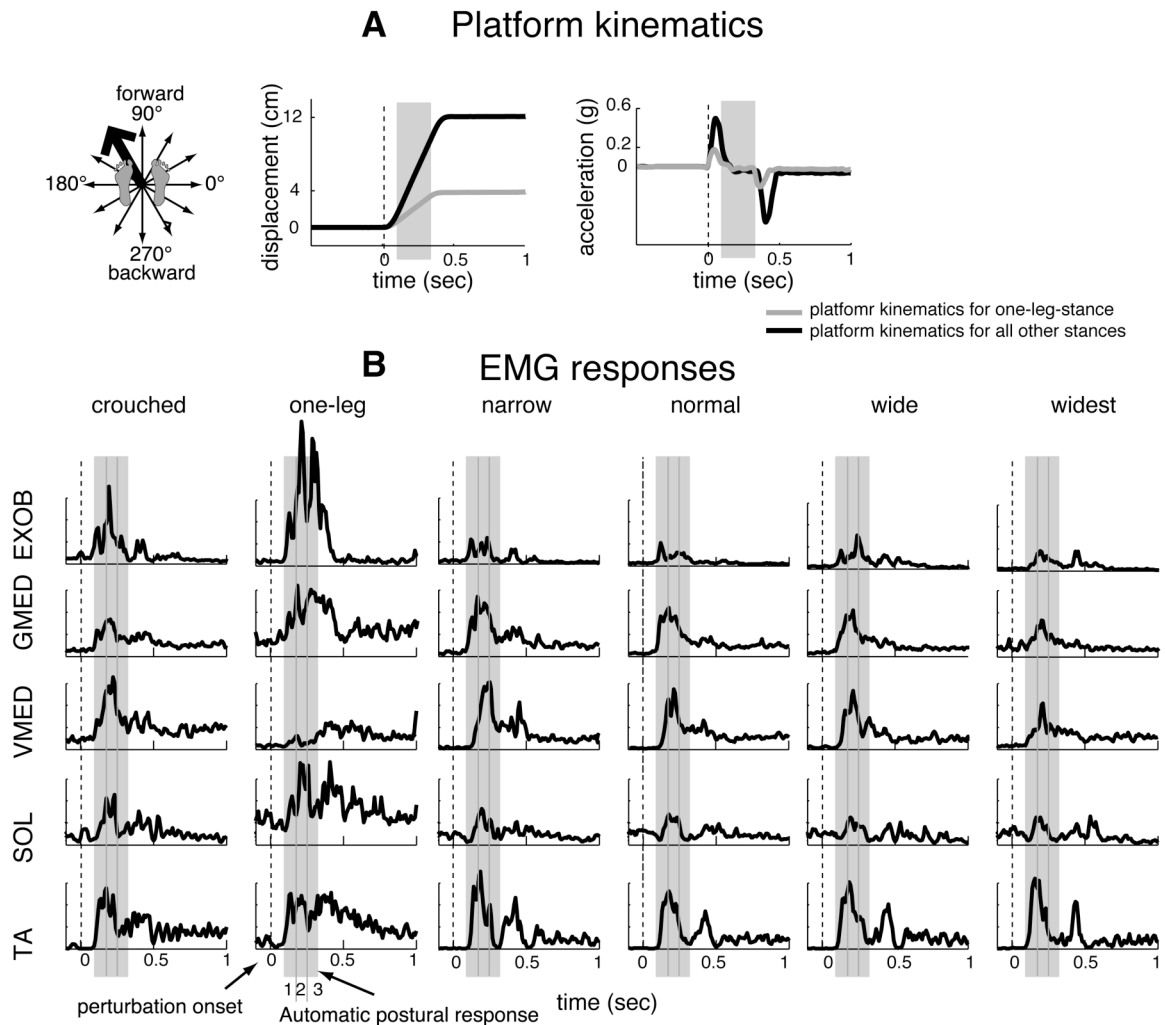


Figure 3.1 Example of postural responses to a leftward-forward perturbation of the support surface. *A.* Balance perturbations were induced by a ramp-and-hold motion of the support surface. Same parameters of platform motion were used for perturbations in all stance conditions except for the one-leg stance, in which a smaller platform motion was used. *B.* EMG responses to same balance perturbations in the same direction under different stance conditions. Muscle responses typically occur with a 100-ms onset latency following platform motion (vertical dashed line). Mean EMG activity in 3 time bins of 75ms (EMG_{APR1} , EMG_{APR2} , EMG_{APR3}) during the APR period were computed for each perturbation (shaded areas).

Subjects stood at six biomechanically distinct stance conditions – narrow, normal, wide, very wide, one-leg and crouched stance – yielding a total of 72 different perturbation direction and stance combinations. Ramp-and-hold support surface translations of 12.4-cm total displacement, 35-cm/s peak velocity, and 0.5g ($\sim 490\text{-cm/s}^2$)

peak acceleration were used for all experimental conditions except for the one-leg stance, for which a smaller perturbation of 4-cm total displacement, 12-cm/s peak velocity, and 0.2g (~196-cm/s²) peak acceleration were used. EMG activity was recorded from sixteen leg and lower-back muscles of the subject's right side. We recorded the activity of the same muscles as in Chapter 2 (Table 2.1). EMG data were processed offline using a set of custom MATLAB routines. EMG data were high-pass filtered at 35 Hz, de-meaned, rectified, and low-pass filtered at 40 Hz.

Because we were interested in examining the richest possible dataset (Torres-Oviedo et al. 2006) we presented the stance/direction combinations in random order. This paradigm induces high inter-trial variability in the postural response by cueing several postural strategies (Horak 1996; Horak and Nashner 1986). We did not explicitly monitor the initial joint angles and center of pressure location prior to each trial to allow some variation in the initial posture across trials of the same stance condition. In the narrow, normal, wide, and widest stances subjects were instructed to stand on the translating platform placing their heels on marks located 9-cm, 19-cm, 30-cm, and 60-cm apart, respectively. These medial-lateral stance widths were chosen based on previous studies using a similar paradigm (Henry et al. 2001; Henry et al. 1998). In the one-leg stance, subjects maintained their balance on their right leg (dominant leg for all subjects) throughout the entire platform motion, without using the non-standing leg to brace their ankle, as instructed by the experimenter. Finally in the crouched stance, subjects bent their knees without squatting (approximately 20° knee flexion) and maintained their torso relatively upright.

Over the course of experimental sessions held on two consecutive days, subjects received ten replicates of each perturbation direction in the normal stance and five replicates of each of the other direction/stance combinations. Narrow, wide, and widest stances were tested during the first session; one-leg and crouched stances were tested during the second session. Normal stance was tested during both sessions as a control.

EMGs were normalized to their mean peak activation in the control condition. Normalizing the data in this way reduced sensitivity to outliers. Electrode positions on the subject's body were marked to ensure similar electrode placement in both experimental sessions.

3.2.2 Data processing

To account for temporal variation in EMG activity, four time periods (“bins”) were analyzed: a 280-ms background period (BK) that ended 170 ms before the perturbation, and each of three 75-ms time bins beginning 100 ms (APR1), 175 ms (APR2), and 250 ms (APR3) after perturbation onset (Fig. 3.1). Identical time bins were used in the study presented in Chapter 2; they were chosen based on previous studies (Diener et al. 1988). For each of the 16 muscles, we averaged the activity over these four time bins to create a vector of data composed of 4 time bins x 12 directions x 10 trials = 480 data points for each stance condition.

3.2.3 Extraction of Muscle Synergies

The main purpose of this study was to investigate the robustness of muscle synergies for postural control across stance configurations. We tested whether muscle synergies identified in postural responses in one stance condition, defined as training condition, could reproduce the postural responses in the other stance conditions, defined as test conditions. In general, we selected the stance condition with the largest postural response magnitudes across all muscles as the training condition. In subjects 8 and 10, this was narrow stance; in all other subjects the training condition was normal stance. Thus, the normal or narrow stance data were the richest data sets, allowing the extraction of the most comprehensive muscle synergies (Torres-Oviedo et al. 2006). To ensure the activity in all muscles was equally weighted in the muscle synergy extraction algorithms, muscle data vectors consisting of EMGBK, EMGAPR1, EMGAPR2, and EMGAPR3 across

all perturbation directions from the training condition were normalized to have unit variance. Then, muscle data vectors from the test conditions were normalized with the same factors as the training condition to maintain consistent units across conditions.

3.2.3.1 Extraction of training muscle synergies

Using the same linear decomposition technique presented in Chapter 2, non-negative matrix factorization (Cheung et al. 2005; Lee and Seung 2001; Torres-Oviedo et al. 2006; Tresch et al. 2006), we extracted muscle synergies from the training condition EMG data. We refer to these muscle synergies as training muscle synergies. This linear decomposition technique assumes that each muscle activation pattern, M^{Tr} , evoked by a perturbation at a given time period (e.g. EMGAPR2, and EMGAPR3 shown in Fig. 2.5) is composed of a linear combination of a few (N_{syn}) training muscle synergies W_i^{Tr} , each activated by synergy activation coefficient c_{Tri} . Thus, the predicted muscle activation pattern \hat{M}^{Tr} takes the form:

$$\hat{M}^{Tr}(t) = \sum_{i=1}^{i=N_{syn}} c_{Tri}(t) W_i^{Tr};$$

$$c_{Tri} \geq 0 \quad \text{and} \quad W_i^{Tr} \geq 0$$

The i^{th} training muscle synergy, W_i^{Tr} , is represented as a vector that specifies a spatial pattern of muscle activity identified in the training condition dataset. Each element of W_i^{Tr} represents a muscle, whose relative contribution to the training muscle synergy is time-invariant and takes a value between 0 and 1. The non-negative activation coefficient c_{Tri} represents the purported neural command to the training muscle synergy that determines the relative contribution of W_i^{Tr} to the overall predicted muscle activation pattern, \hat{M}^{Tr} . The set of activations c_{Tri} of W_i^{Tr} across all perturbation directions during quiet stance and during the three APR periods is the vector $C_{training i}$. The components of

$C_{training\ i}$ are tuning curves that describe how the activation of W_i^{Tr} changes as a function of perturbation direction and time.

3.2.3.2 Extraction of task-specific muscle synergies

To identify muscle synergies specific to a given stance configuration, we applied the same principles used in the reformulation of the NMF algorithm by Cheung et al. (Cheung et al. 2005) for extracting muscle synergies relevant to the test condition only. These were called here task-specific muscle synergies W^{test} . We provided the algorithm with the test condition data and the muscle synergies extracted from the training condition, W^{Tr} . The algorithm first performs a least square fit to determine the non-negative coefficients C_{test} that would best reconstruct the test condition data only using W^{Tr} . Subsequently, the algorithm determines W^{test} that reconstruct the test condition data not accounted for by W^{Tr} . Thus, similar to a multiple regression, the net muscle activation pattern in the test condition \hat{M}^{test} was obtained by the projection of the test data onto W^{Tr} and W^{test} extracted from the residual data. Stated formally:

$$\hat{M}^{test}(t) = \sum_{i=1}^{i=N_{syn}} c_{test\ i}(t) W_i^{Tr} + \sum_{i=1}^{i=N_{test}} c_i^{test}(t) W_i^{test}$$

$$c_{test\ i}, c_i^{test} \geq 0 \quad \text{and} \quad W_i^{Tr}, W_i^{test} \geq 0$$

The i^{th} task-specific muscle synergy, W_i^{test} , is a time-invariant non-negative vector that specifies a spatial pattern of muscle activity featured in the test data only. The magnitude of its contribution to \hat{M}^{test} is determined by c_i^{test} , representing the neural command to W_i^{test} . C_i^{test} is the set of activations c_i^{test} of W_i^{test} across all perturbation directions and time periods. Thus, C^{test} describes how the activation of the task-specific muscle synergies W^{test} change as a function of perturbation direction and time.

To validate whether this reformulation of the NMF algorithm was able to isolate muscle activation patterns specific to the test condition, W^{test} and C^{test} were compared to muscle synergies and their corresponding activation coefficients that were directly extracted from test condition data using the traditional NMF algorithm.

3.2.4 Data Analysis

In all our subjects we extracted training muscle synergies using an iterative process where N_{syn} varied between 1 and 16, the number of muscles. Muscle synergies extracted from the training condition data were used to reconstruct data from the test conditions. We then determined the coefficients C_{wide} , C_{widest} , $C_{crouched}$, $C_{one-legged}$, and C_{narrow} or C_{normal} (whichever was not used as training condition) that would best reconstruct the postural responses at each stance configuration using the training muscle synergies. Simultaneously, we extracted task-specific synergies when the training synergies could not reproduce the test condition responses, as determined by greater than 75% variability accounted for (VAF) in each muscle data vector. VAF is defined as $100 \times$ uncentered Pearson correlation coefficient (Torres-Oviedo et al. 2006; Zar 1999). Thus, we selected the least number of training and task-specific muscle synergies that could adequately reconstruct background and APR responses of each muscle in all the trials of all direction/stance combinations. This criterion ensured that each muscle tuning curve at all stance configurations would be well-reconstructed, so that the critical spatiotemporal features of each muscle activation pattern were well-accounted for by the muscle synergies. In general, by satisfying this local criterion, the total VAF in the dataset was well over 90%.

Similar to the study presented in Chapter 2, training and task-specific muscle synergies of all subjects were ranked based on muscle composition and synergy activation profiles rather than on percentage of contribution to the total data variability

(as in other factorization methods such as principal component analysis). We performed a *functional sorting* because subjects might use muscle synergies differently, causing comparable muscle synergies to have large differences in contribution to the total data variability. We assumed muscle synergies activated for the same range of perturbations would have the same function. Thus, muscle synergies across individuals were classified based on their similarity, as determined by the coefficient of determination ($r^2 > 0.6$) between all training and task-specific muscle synergies and their corresponding averaged synergy activation coefficients across all trials (\bar{C}).

To evaluate the robustness of muscle synergies across subjects, an initial sorting was performed by comparing muscle synergies and their \bar{C} s of all subjects to a reference subject. Then an initial averaged set of W s and \bar{C} s vectors across subjects was computed. Using an iterative process, muscle synergies with similar muscle composition ($r^2 > 0.6$) or similar activation coefficients \bar{C} s ($r^2 > 0.6$) to the averaged W and C vectors were separated into clusters. The averaged set of W s and \bar{C} s vectors across subjects used as a reference were updated every time a muscle synergy was discriminated from a group. We monitored when muscle synergies were part of a group because of their similar muscle composition, activation coefficients, or both. The r^2 values obtained not only served as a sorting parameter, but also as a measure to evaluate the generality of muscle synergies across subjects.

3.3 Results

In all subjects, muscle synergies identified in postural responses in the training condition were adequate to reproduce postural responses in all stance width conditions. However, in drastically distinct stance conditions, such as one-leg and crouched stance, task-specific muscle synergies were also required to reproduce postural responses. Changes in stance configuration introduced spatial and temporal variation in the postural

responses, which were accounted for by variation in the activation of the identified muscle synergies. Common muscle synergies that were similar in terms of muscle composition and spatiotemporal activation pattern were identified in all subjects.

3.3.1 Changing the initial stance configuration alters the postural responses

Stance condition variation introduced large spatial and temporal variations in the postural responses. These changes were similar to the ones reported in previous studies investigating the effect of stance width (Henry et al. 2001) and crouched posture (Burtner et al. 1998; Woollacott et al. 1998) on the postural response.

The magnitude of muscle activity in postural responses was modulated by stance configuration. In all stances each muscle was activated in response to a range of perturbation directions, represented by muscle tuning curves (Fig. 3.2; black traces), whose amplitudes were modulated by stance configuration. The representative data of subject 3 is presented in Fig. 3.2. The postural response magnitude of several muscles (primarily proximal rather than distal muscles) decreased as stance width increased, resulting in systematic changes in tuning curve amplitude (Fig. 3.2). Similarly, all muscles exhibited altered postural response magnitude in the one-leg and crouched stance compared to normal stance; however, these changes were non-monotonic. For example, in the one-leg stance, postural responses of ankle and hip abductors increased (Fig. 3.3) but those of other proximal muscles, such as hip flexors and hamstrings, decreased compared to normal stance (Fig. 3.2). Responses of agonist/antagonist ankle muscles, such as TA and SOL, and all thigh and trunk muscles (Fig. 3.2), except for hip flexor REAB and BFLH (Fig. 3.3), increased in the crouched stance condition compared to normal stance.

Changes directional tuning of postural responses were observed in all subjects when their balance was perturbed in widest, crouched, and one-leg stance but not under narrow, normal, and wide stance (Fig. 3.2).

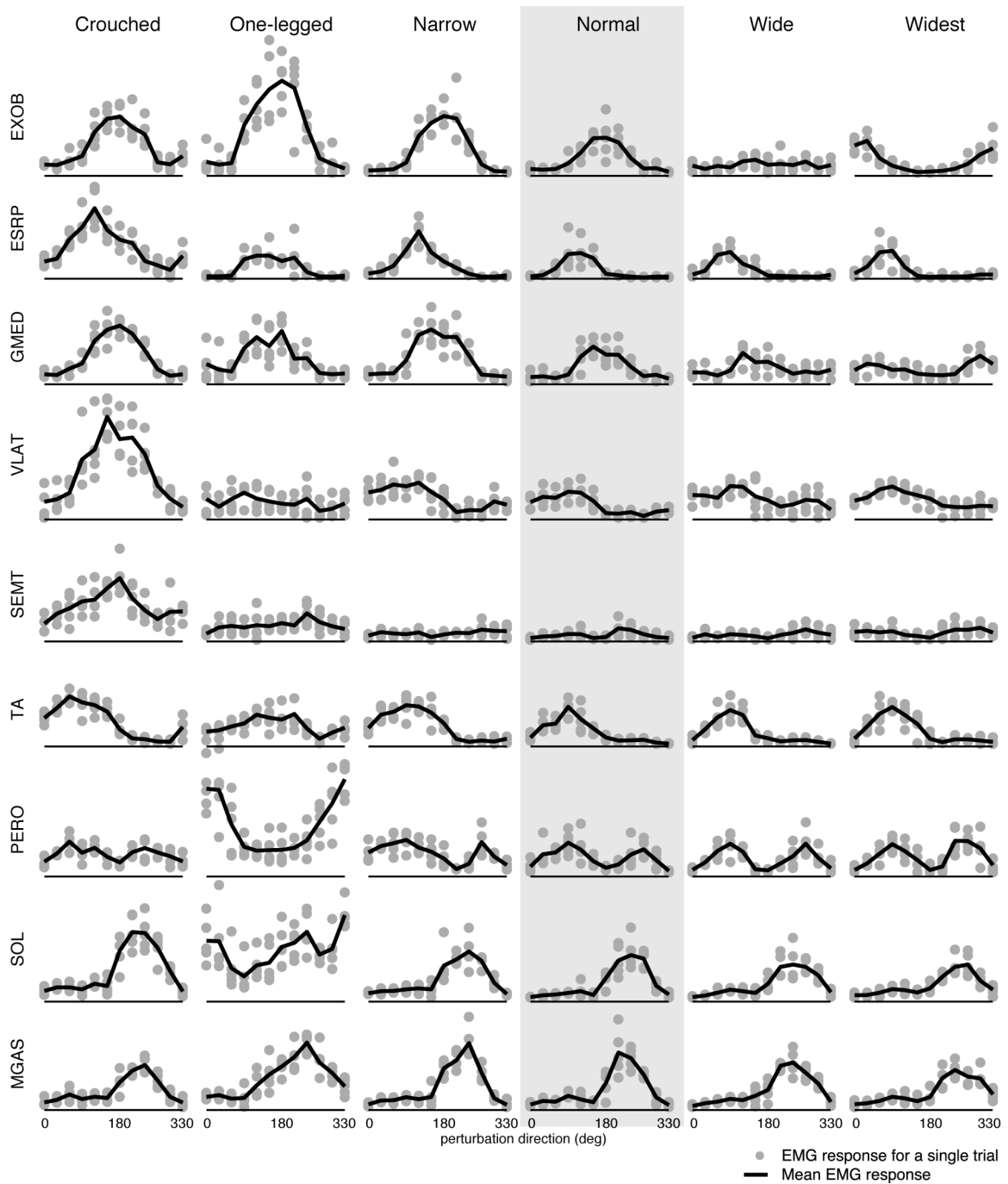


Figure 3.2. Tuning curves of multiple muscles in all stance conditions during one time bin. Magnitude and spatial variations in postural responses were observed when subjects stood in different stance configurations. Magnitude of responses increased when stance width decreased. Spatial changes in postural responses are observed in the one-leg, crouched, and widest stance conditions. Black traces indicate the mean response and gray dots represent responses in each trial. Inter-trial variations in postural responses were also observed in all stance conditions.

The directionality of all muscle tuning curves was consistent across most stance widths except for widest stance, in which directional tuning of GMED and EXOB reversed direction. They were activated in response to leftwards perturbation directions (0° - 30° and 300° - 330°) in the widest condition whereas they were activated in response to rightwards perturbation directions (120° - 270°) in the other stance conditions.

The one-leg stance altered the tuning of distal muscles from what was observed in the other stance conditions. For example, PERO was bimodally tuned, with maxima at 90° (forwards) and 270° (backwards) in all stance conditions except for the one-leg stance, for which its activity was unimodally tuned about 0° (rightwards). Similar changes were observed in SOL and TA (Fig 3.3), which changed from unimodal tuning in all stance conditions to bimodal tuning in the one-leg stance. Finally, all activated muscles in the crouched stance and MGAS in the one-leg stance broadened their tuning to include more perturbation directions (Fig 3.2). Inter-trial variations in postural responses of all muscles were also observed in all stance conditions (Fig. 3.2; gray dots).

Changes in onset latencies of postural response were observed in all subjects. Postural response onset latency varied across muscles, and the spatial tuning of a few muscles, such as GMED and REAB, varied across the three time bins of the APR (Fig. 3.3). In all stance conditions except for crouched stance, muscles seemed to be activated in a distal-to-proximal order. For example, thigh and trunk muscles, except for ERSP, EXOB, and GMED, were inactive or relatively weakly activated during APR1 but were highly activated during APR2 and APR3 (Fig. 3.3). This distal-to-proximal muscle activation order was not observed in the crouched stance (Fig. 3.3; red traces). The onset of thigh and trunk muscles in this stance condition was earlier than in the normal stance.

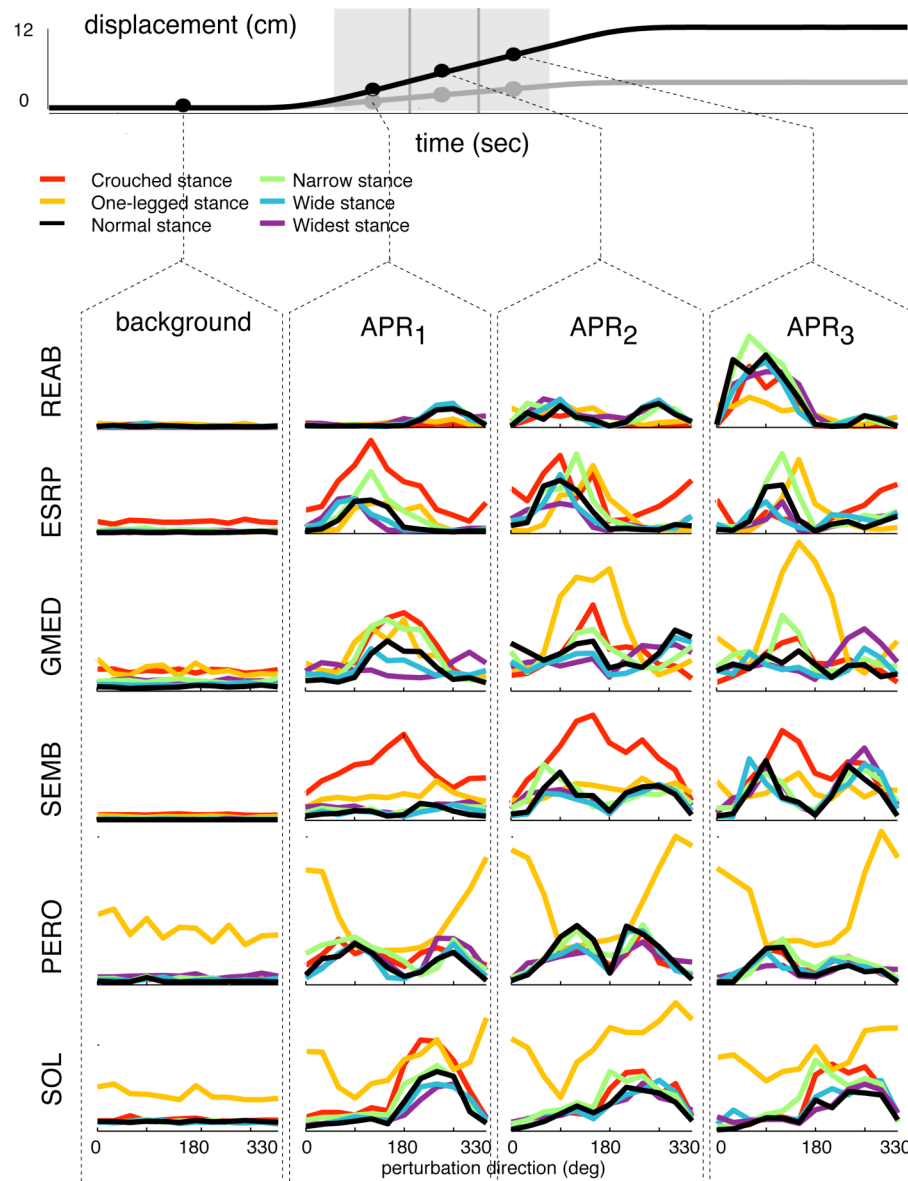


Figure. 3.3. Muscle activations of a sample subject during background and during responses evoked by all perturbation directions in all stance conditions. Directional tuning in the activation of all the muscles is observed in all stance conditions. Differences in muscle onset latencies and changes in directional tuning over time can be observed by comparing responses over the three time bins (APR₁, APR₂, and APR₃). Muscle onset latencies in all stance conditions are similar except for the crouched stance condition (red trace), in which proximal muscles are active during early time bins of the APR when they are normally inactive.

3.3.2 Identification of training and task-specific muscle synergies

Six or fewer muscle synergies extracted from the training condition were found to reproduce muscle activation patterns over all stance width conditions within the specified

parameters of acceptability. Additional muscle synergies were required to reconstruct the data from the one-leg and crouched stance conditions. As the specified number of training synergies was increased from one to sixteen, the reconstruction of both training and test conditions also increased (Fig. 3.4A). In the 9 subjects, the total mean VAF in the different stance conditions was $93 \pm 0.8\%$ (narrow), $93 \pm 1.4\%$ (normal), $93 \pm 1\%$ (wide), $92 \pm 1\%$ (widest), $84 \pm 9.9\%$ (crouched), and $84 \pm 4.7\%$ (one-leg). When four or fewer additional muscle synergies were used in the reconstruction of the crouched and one-leg stance conditions VAF increased to $91 \pm 3.6\%$ (crouched) and $92 \pm 1.3\%$ (one-leg). Background and APR responses of all muscles in all trials were well reconstructed, as determined by $VAF > 75\%$.

For example in the case of the representative subject 3, five muscle synergies reproduced 90% of the overall data variability collected under each stance width condition (Fig. 3.4A) and over 70% in the crouched and one-leg stance conditions. However, not all EMG activation patterns were adequately reconstructed (Fig. 3.4 B). Adding the sixth muscle synergy dramatically improved the reconstruction of REAB (Fig. 3.4C) and the directional profile of VAF in all stance width conditions, particularly at 0° - 90° during APR3 when this muscle was highly activated (Fig. 3.4 B). Similarly, adding one task-specific muscle synergy to the reconstruction of each of the crouched and one-leg stance conditions, dramatically improved the reconstruction of REAB and ERSP and the directional profile of VAF in these two stance conditions (Fig. 3.4 C).

In all subjects, the number of muscle synergies required to reproduce the postural responses in all stance width conditions varied between 4 and 6 (Fig. 2.6) and in the crouched and one-leg stance conditions varied between 6 and 9 (Fig. 3.11). The additional muscle synergies were either task-specific muscle synergies extracted from the specific testing data set or muscle synergies extracted from the training condition. The number of synergies chosen for each subject was corroborated by the fact that adding more synergies contributed evenly to the VAF of all muscles, suggesting that the extra

synergies reconstructed only random variations in the data. REFM from subject 10 was excluded from the analysis because its activity was erratic, as indicated by its lack of directional tuning in any experimental condition.

3.3.2.1 Muscle synergies extracted from the training condition reproduce responses in all stance width conditions

Changes in postural responses of individual muscles originated by changing the initial stance configuration were reproduced by a single set of muscle synergies extracted from the training condition. Each training muscle synergy, W_n^{Tr} , specifies the simultaneous activation of several muscles across the body (Fig. 3.5A), and each training muscle synergy was activated during specific perturbation directions and time bins, as specified by C_n^{Tr} (Fig. 3.5B). Training muscle synergies were distinct from each other in terms of muscle composition and spatiotemporal activation profile. Their muscle composition and directional tuning during normal stance condition were described in detail in Chapter 2. In Chapter 2 we concluded that because of their muscle composition and spatiotemporal activation W_1^{Tr} and W_6^{Tr} were considered muscle synergies relevant to the ankle strategy whereas W_{2-4}^{Tr} were considered muscle synergies relevant to the hip strategy. W_5^{Tr} contributed to medial-lateral stability muscle synergy and W_6^{Tr} might also constitute a muscle activation pattern used in a “knee” strategy.

3.3.2.2 Task-specific muscle synergies represent spatial activation patterns particular to the test condition.

Task-specific muscle synergies extracted from the one-leg or crouched stance conditions were needed to reproduce muscle activation patterns characteristic of these two conditions. For example in the representative subject 3 W_1^{Cr} , a task-specific muscle synergy used in the crouched stance, was mainly composed of VMED and was unimodally tuned about 180° (leftwards) when the leg was loaded (Fig. 3.6A).

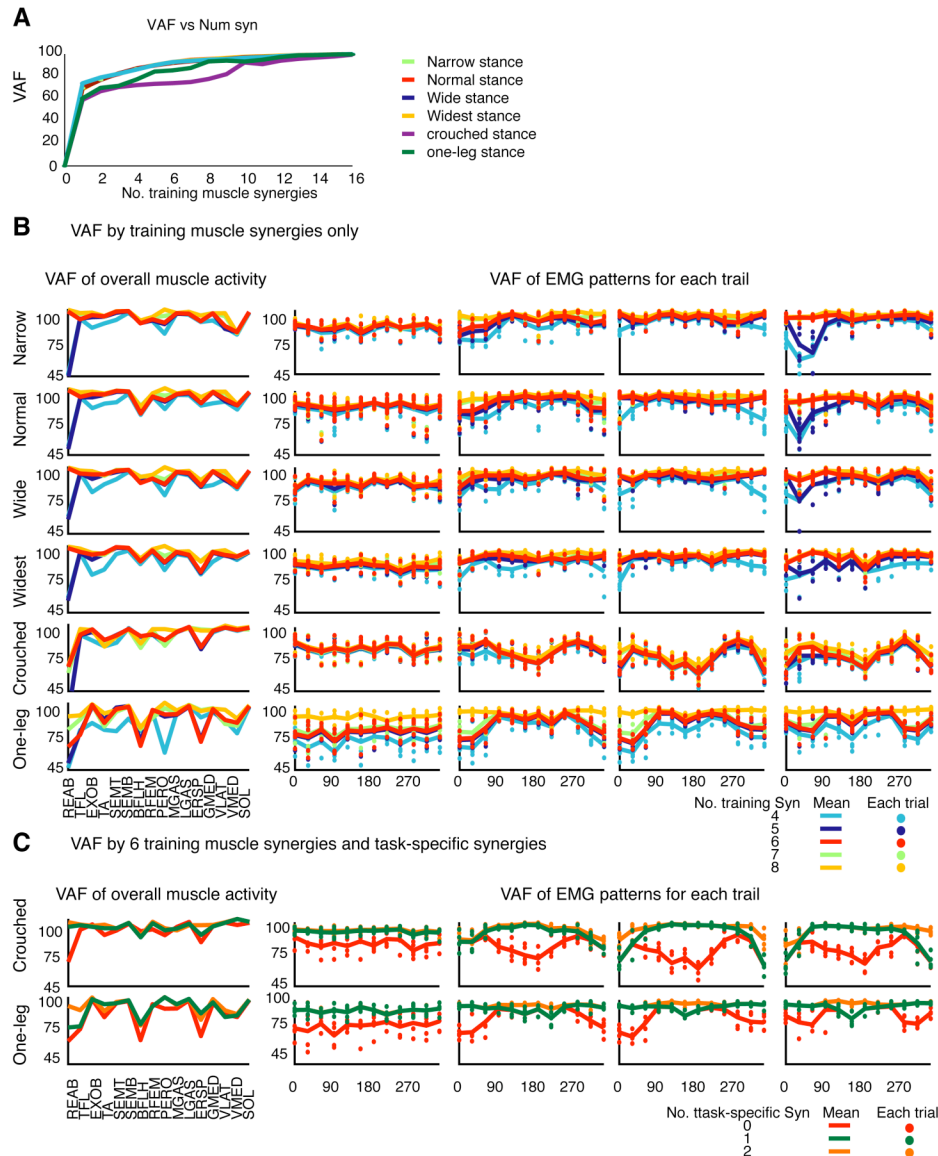


Figure 3.4. *A.* overall VAF for each stance condition by increasing numbers of synergies in a sample subject 3. Six muscle synergies extracted from the training condition accounted for 93% (narrow), 93% (normal), 92% (wide), 92% (widest), 84% (one-leg), and 73% (crouched), of total variability in each stance condition. *B.* VAF for each muscle's responses (left) and VAF as a function of perturbation direction during background and during the three time bins characterizing the APR (right) in all stance conditions. Colored lines indicate the VAF values when different number of training muscle synergies are used to reproduce each muscle responses. Dots indicate the VAF values characterizing the reconstruction of each trial. VAF >75% for all perturbation directions when six training muscle synergies are used for the data reconstruction in all stance width conditions (red traces). However additional muscle synergies are needed for the reconstruction of crouched and one-leg conditions. *C.* VAF when task-specific muscle synergies are included for the data reconstruction. One additional muscle synergy is needed to improve the directional profile of VAF in the crouched and one-leg stance conditions (dark green traces).

Similarly W_1^{1L} , a task-specific muscle synergy used in the one-leg stance, was formed by ankle evertor muscle PERO and was unimodally tuned about rightwards directions (0° - 30° and 300° - 330°), for which it was more challenging to maintain one-leg balance due to the missing support of the contralateral leg in this condition (Fig. 3.6A). Both W_1^{Cr} and W_1^{1L} were activated during the background period in the crouched or one-leg stances.

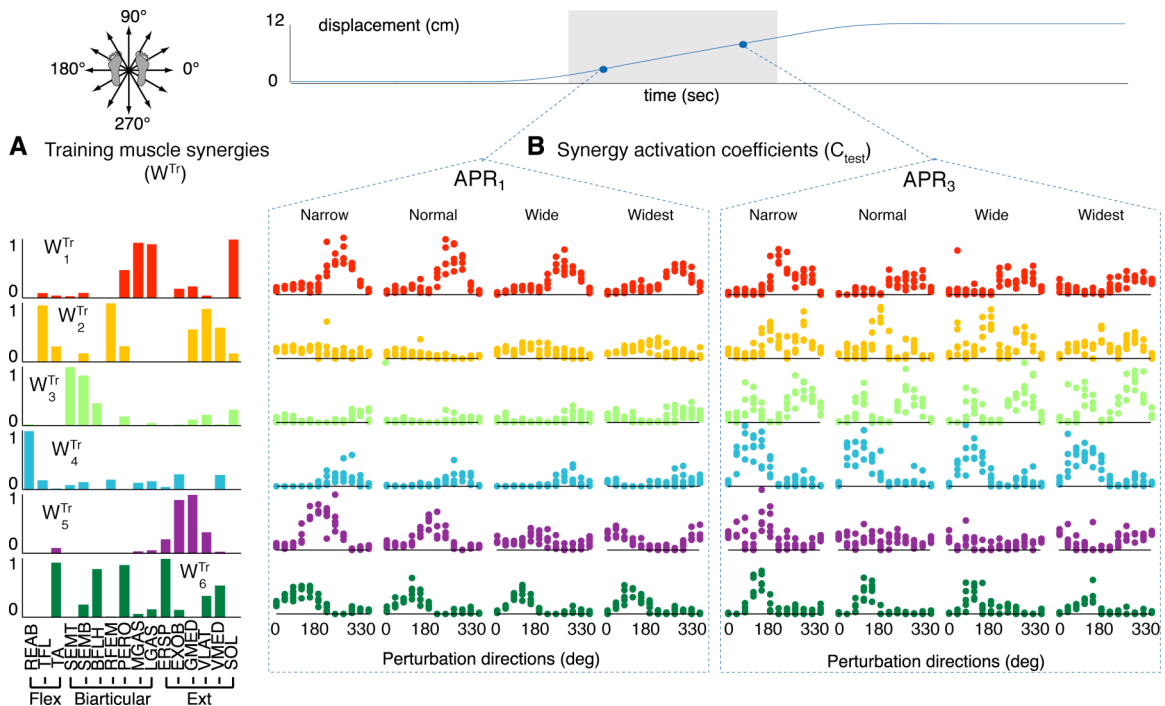


Figure 3.5 Muscle synergy vectors and synergy activation coefficients for a representative subject. *A.* Training muscle synergy vectors, W_i^{Tr} , extracted from EMG training data (normal stance condition data in this subject) during quiet stance and three APR time bins. Each bar represents the relative level of activation of each muscle within the synergy (see Methods section for muscle abbreviations). *B.* Activation coefficients, C_i^{Tr} , for each of the 6 synergies in all stance width conditions during two time bins in multiple perturbation directions. Each dot represents the activity of the muscle synergy in a single trial. Directional tuning of muscle synergies over the three time bins can be observed. Changes in magnitudes and spatial tuning of synergy activation coefficients were observed with stance width. For example, the activation of W_5^{Tr} increased when stance width decreased and its tuning curve changed in the widest stance condition. Inter-trial variation of muscle synergy activations are observed by the vertical spread of activation coefficients.

3.3.3 Magnitude and directionality of muscle synergy tuning curves change with stance

3.3.3.1 Training muscle synergy activations increase when stance width decreases

All training muscle synergies contributed to postural responses in all stance width conditions but the activation level of some muscle synergies decreased as stance width increased (Fig. 3.5B), similar to the modulation observed in individual muscles (Henry et al. 2001). W_5^{Tr} , characterized by the contribution of hip abductor GMED and lateral trunk muscle EXOB, varied the most in activation across stance widths. The C_5^{Tr} activations during APR1 about 120°-240° (leftwards) perturbations were significantly larger in the narrow stance than in all other stance widths (Fig. 3.5B; purple dots in APR1 panel). Also W_5^{Tr} shifted its spatial tuning by 180° in the widest stance, where C_5^{Tr} activations were significantly larger in response to rightwards perturbations (0°-30° and 300°-330°) as opposed to leftwards perturbations (120°-240°) like in all other stance width conditions (Fig. 3.5B. APR1 panel). W_1^{Tr} , formed by ankle plantar flexor muscles and primarily activated during APR1 in the normal stance, was more modulated with stance width during later time bins than during APR1. For example during APR3 the C_1^{Tr} activations about 210°-330° (backwards) perturbations were significantly larger in the narrow stance than in other stance widths (Fig. 3.5B red dots APR3 panel). In addition, W_1^{Tr} and W_6^{Tr} slightly shifted their maximum activation directions from backward and forward perturbations in the normal, wide, and widest stance to more leftward perturbation directions in the narrow stance. During all time bins W_1^{Tr} responses to a pure leftward perturbation (180°) were larger in narrow stance than in all other stance width conditions (Fig. 3.5B; red dots). Similarly, C_1^{Tr} activations about 120° and about 120°-180° (both forward-leftward) perturbations were significantly larger in narrow stance than in the other stance widths conditions during APR3 and during APR1, respectively (Fig 3.5B;

green dots). Finally, W_{2-4}^{Tr} , mainly composed of proximal muscles, maintained their directional tuning in all stance width conditions and were the least modulated with stance width. C_{2-4}^{Tr} only showed significant increased activations about 270°-330° (backwards) perturbations during APR3 in all stance width conditions compared to normal stance (Fig. 3.5B; yellow, light green, and blue dots, APR3 panel).

3.3.3.2 Training muscle synergy activations vary in a complex fashion in the one-leg and crouched condition

Training muscle synergies were recruited differently depending on the requirements of the postural task. For example, in the one-leg stance most of the muscle synergies were maximally activated in response to leftward or rightward perturbations to actively compensate for the lack of support from the contralateral leg. Namely, W_1^{Tr} , formed by ankle plantar flexors, increased its activation and changed its tuning in one-leg stance compared to normal stance. W_1^{Tr} was unimodally tuned about 270° (backwards) in normal stance but it was bimodally tuned with maxima at 180° (leftwards) and 270° (backwards) in the one-leg (Fig. 3.6B; dotted red traces). Similarly W_5^{Tr} , formed by hip abductor muscles, was significantly more activated in one-leg stance, although its unimodal spatial tuning about 180° (leftwards) perturbations was conserved (Fig 3.6B; dotted purple traces). During APR3 the spatial tuning of W_2^{Tr} changed from a unimodal tuning about 180° (leftward) in the normal stance to a bimodal tuning with maxima at rightwards (0° and 330°) and leftwards (180°) perturbations in one-leg stance (Fig 3.6B; dotted yellow line in APR3 panel). Hip flexor muscle synergy W_4^{Tr} slightly shifted its maximum activation from forward-rightward in normal stance to more forward-leftward in one-leg stance (Fig. 3.6B; dotted blue traces). The activations of W_3^{Tr} (unimodal, 30°-150°) and W_6^{Tr} (unimodal, 210°-330°) decreased in the one-leg condition (Fig. 3.6B;

dotted light green and green traces). Finally, W_1^{Tr} had a higher activation level during the background period in the one-leg condition.

In crouched stance all training muscle synergies maintained their spatial tuning but increased their activation magnitudes compared to normal stance. For example, W_1^{Tr} , formed by ankle plantar flexors, and W_2^{Tr} , formed by quadriceps, varied the most in activation in crouched stance. The averaged activation coefficients C_1^{Tr} and C_2^{Tr} were significantly larger in crouched stance than in normal stance (Fig. 3.6B; dashed red traces APR1 and APR3 panels and yellow dashed traces in all APR1 and APR2). W_3^{Tr} , W_5^{Tr} , and W_6^{Tr} also increased their activation magnitudes, particularly during APR1 (Fig 3.6 APR1 panel). On the other hand, W_4^{Tr} , mainly formed of hip flexors, was the only training muscle synergy that decreased in activation level in the crouched stance with respect to the normal stance.

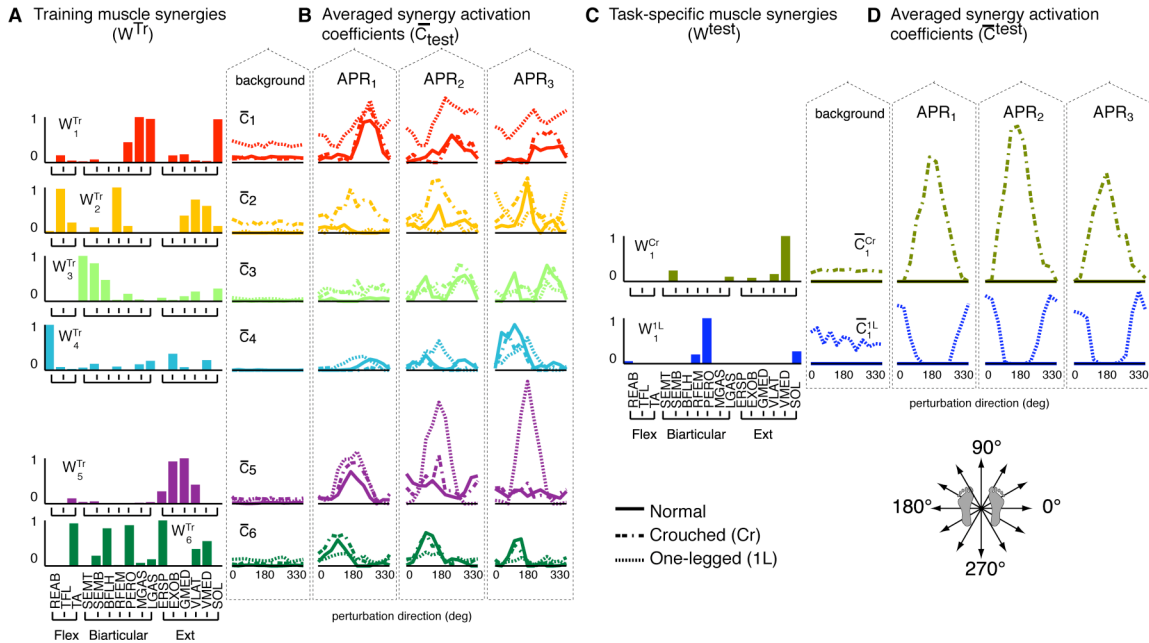


Figure 3.6 Training and task-specific muscle synergies with their correspondent averaged synergy activation coefficients across trials *A*. Training muscle synergy vectors, W_i^{Tr} , extracted from training EMG data during quiet stance and three APR time bins. Each bar represents the relative level of activation of each muscle within the synergy (see Methods section for muscle abbreviations). *B*. Averaged activation coefficients, \bar{C}_i , for each of the 6 synergies in normal, crouched, and one-leg stance

condition during one time bins in multiple perturbation directions. Directional tuning of training muscle synergies can be observed. *C.* Task-specific muscle synergies for crouched and one-leg stance condition. Task-specific muscle synergies are mainly formed by one single muscle highly activated. *D.* Averaged activation coefficients for each task-specific muscle synergy, $\overline{C_i^{test}}$. Task-specific muscle synergies were relevant to the specific test condition only. Each task-specific muscle synergy has a directional tuning maintained with time. Notice their activation coefficients are zero for the normal stance and other test condition.

3.3.4 Temporal features of synergy activations only change in drastically distinct stances

3.3.4.1 Onset latencies of training muscle synergies are maintained with stance width

Muscle synergy onset latencies were invariant over stance width and generally maintained a distal to proximal activation order. In all stance width conditions W_1^{Tr} and W_6^{Tr} , mainly composed of proximal muscles, were highly activated during the early time bins of the APR (APR1); whereas, W_{2-4}^{Tr} , mainly formed by trunk and proximal muscles, were active in later time bins (APR2 and APR3). W_5^{Tr} was active during the early time bins in all stance width conditions despite changes in spatial tuning in widest stance. In all stance width conditions only one muscle synergy, W_1^{Tr} , which included soleus, was active during the background period to provide antigravity support (Fig. 3.7B, red muscle synergy).

3.3.4.2 Temporal profiles and onset latencies of muscle synergies change in one-leg and crouched stance

Muscle synergies' temporal profiles and onset latencies were very similar in one-leg and normal stance except for those of W_4^{Tr} and W_5^{Tr} , which were muscle synergies stabilizing the hip. W_4^{Tr} was more active during APR2 in one-leg stance than in normal stance. Similarly, W_5^{Tr} was highly activated during APR2 and APR3 in one-leg stance whereas it was weakly or nearly inactive during these periods in normal stance.

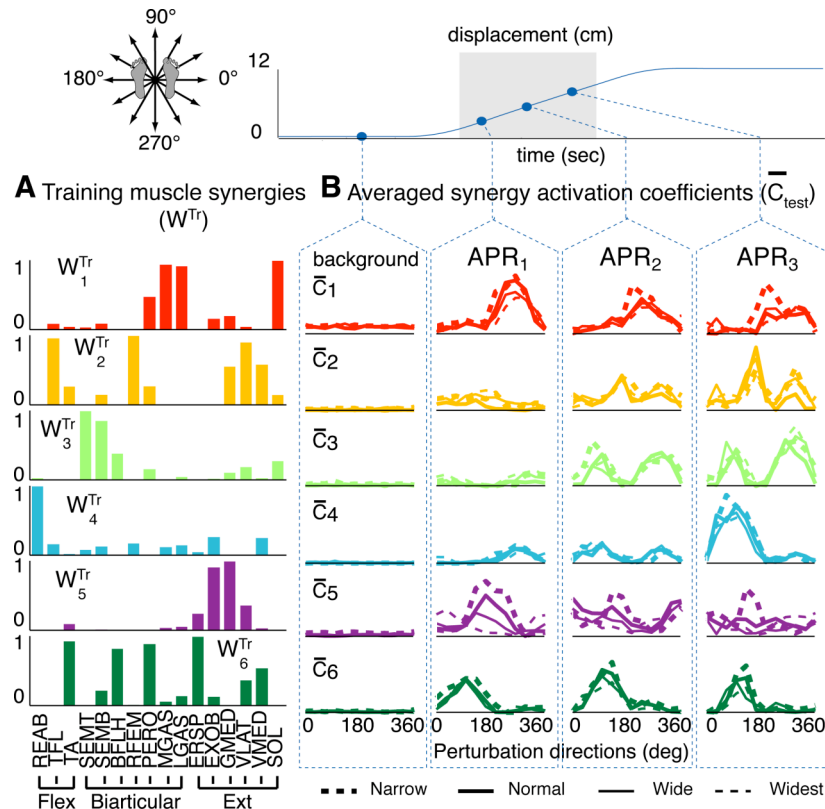


Figure 3.7 *A*. Training muscle synergy vectors, W_i^{Tr} *B*. Averaged activation coefficients, \bar{C}_i , for each stance width condition during three time in multiple perturbation directions. Directional tuning of training muscle synergies can be observed. Magnitude changes in muscle synergy activations are observed. In general muscle synergies are activated more in narrow than wide and widest stance conditions.

The onset latencies of muscle synergies formed by proximal muscles were reduced in crouched stance compared to normal stance. In crouched stance W_1^{Cr} , W_2^{Tr} , W_3^{Tr} , and W_5^{Tr} , formed by thigh and trunk muscles, initiated their activation during APR1 when W_1^{Tr} and W_6^{Tr} , formed by distal muscles, were also active. Only W_4^{Tr} , formed by hip flexor muscles, maintained the same temporal profile in the normal and crouched stance. Finally, in the crouched stance, both W_2^{Tr} and W_1^{Cr} were activated during the background period(Fig. 3.6B, red muscle synergy).

3.3.5 Similarities between task-specific muscle synergies and some training muscle synergies

Spatial tuning and muscle composition was similar among task-specific and training muscle synergies. For example, W_2^{Tr} and W_1^{Cr} in crouched stance responded to the same range of perturbations with maximum activation at 180° and the two muscles forming W_1^{Cr} (VMED and VLAT) were in the group of muscles forming W_2^{Tr} (Fig. 3.6). The similarities in the activations of both synergies suggest that task-specific muscle synergies might be activated by the same active command as some of the training muscle synergies; perhaps because of the non-linear activation of a few muscles within the training muscle synergies they might be erroneously identified by the algorithm as unique synergies. We hypothesize that similar tuning across synergies composed of similar muscles might possibly be used to identify non-linear activation in general.

3.3.6 Averaged EMG responses in all stance conditions are reproduced by training and task specific muscle synergies.

Using the muscle synergies from the training condition we were able to adequately reproduce the EMG tuning curves in all stance width conditions (Fig. 3.8). However, task-specific muscle synergies also contributed to reproducing EMG tuning curves of a few muscles in the one-leg and crouched stance conditions (Fig. 3.9). Individual muscle changes in tuning curve magnitudes and shapes across time periods and stance conditions were well reproduced by the activation of a few muscle synergies. The variability accounted for (VAF) exceeded 90% in 90% of the individual muscle tuning curves during all time periods in all stance conditions. During all time periods of the postural response only one muscle synergy contributed to the net activity of muscles like REFM, whereas two synergies contributed to the net activity of muscles like PERO and ERSP (Fig. 3.8). However, in some muscles such as BFLH, VMED, and, SOL different muscle synergies could contribute to their EMG responses during different time

periods (Fig. 3.8). For example, W_6^{Tr} contributed to the activation of BFLH during early time bin period APR1 but both W_6^{Tr} and W_3^{Tr} contributed to its activation during late time bin period APR3.

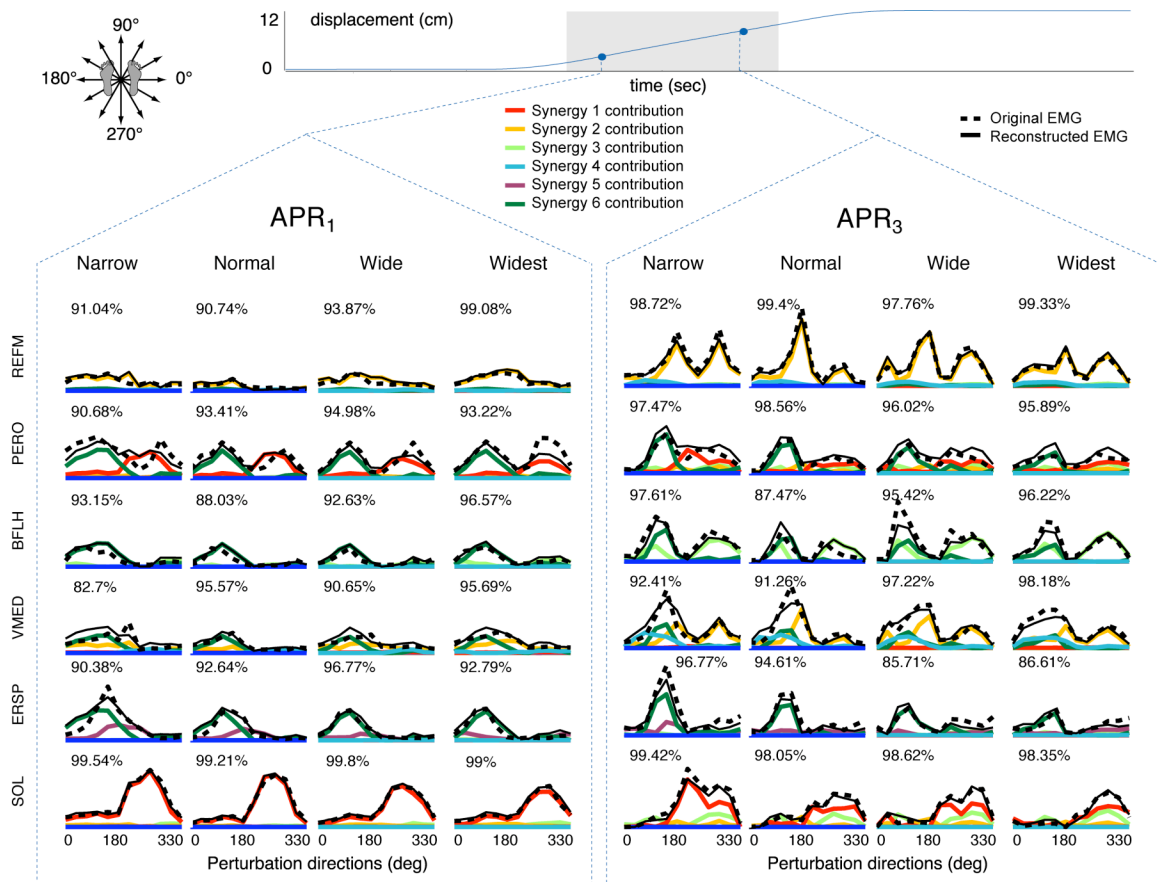


Figure 3.8 Tuning curves in a sample subject in all stance width conditions during two time bins. The original data are shown by the dashed black line and the reconstructed data by the solid black line. The contribution from each synergy to the reconstruction is shown by the corresponding colored line. This is computed by multiplying each training muscle synergy vector W by their corresponding averaged synergy activation coefficients across all trials (\bar{C}_i).

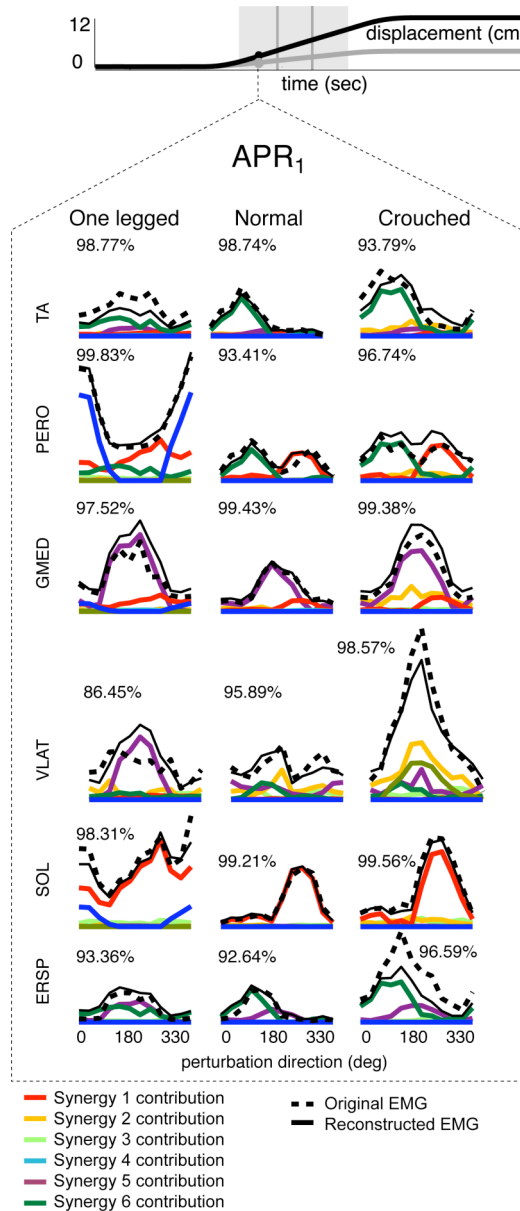


Figure 3.9 Tuning curves in a sample subject during in one-leg and crouched stance configuration during one time bin. The original data are shown by the dashed black line and the reconstructed data by the solid black line. The contribution from each synergy to the reconstruction is shown by the corresponding colored line. This is computed by multiplying each training muscle synergy vector W by their corresponding averaged synergy activation coefficients across all trials (\bar{C}_1).

Changes in magnitude with stance of individual muscles, such as ERSR and VMED, were reproduced by changes in the contribution of muscle synergies to the activation of each muscle. Similarly, spatial tuning changes with stance in the activation

of muscles like SOL were reproduced by spatial tuning changes of the entire muscle synergy W_1^{Tr} . Finally, the net activation of a few muscles such as PERO, SOL, VMED, and VLAT was accounted for by contribution of training and task-specific muscle synergies (Fig. 3.9). Only responses of BFLH of subject 10 and PERO of subject 7 were over predicted in crouched stance but their tuning curve reconstructions were within the parameters of acceptability (VAF>77%).

3.3.7 Inter-trial variations in EMG patterns in all stance conditions are accounted for by modulating muscle synergy activations

In all stance conditions inter-trial variations in EMG activity of individual muscles were not random, but instead corresponded to inter-trial variations in the activation of entire muscle synergies. In sample subject 4, TFL had different activation magnitudes in response to the same forward-rightward (60°) balance perturbation when standing in all stance conditions (Fig. 3.10). For example in trial 1 in the normal stance condition, TFL was highly activated whereas in trial 5 TFL activity was reduced. This difference was not simply a random variation in muscle activity, because all the other muscles belonging to W_3^{Tr} also showed a decreased in activity in trial 5 with respect to trial 1 (Fig. 3.10B, yellow bars). Similar trial-to trial variations of TFL responses were observed in other stance conditions such as widest stance and one-leg stance condition. However, in all stances the individual changes in activation of TFL were accompanied by similar changes in the activation of all other muscles belonging to W_2^{Tr} . Therefore, the muscle activation patterns specified by each muscle synergy were consistent across stance conditions and individual muscle inter-trial variations were explained by variations in the synergy activation coefficients, C (Fig. 3.5).

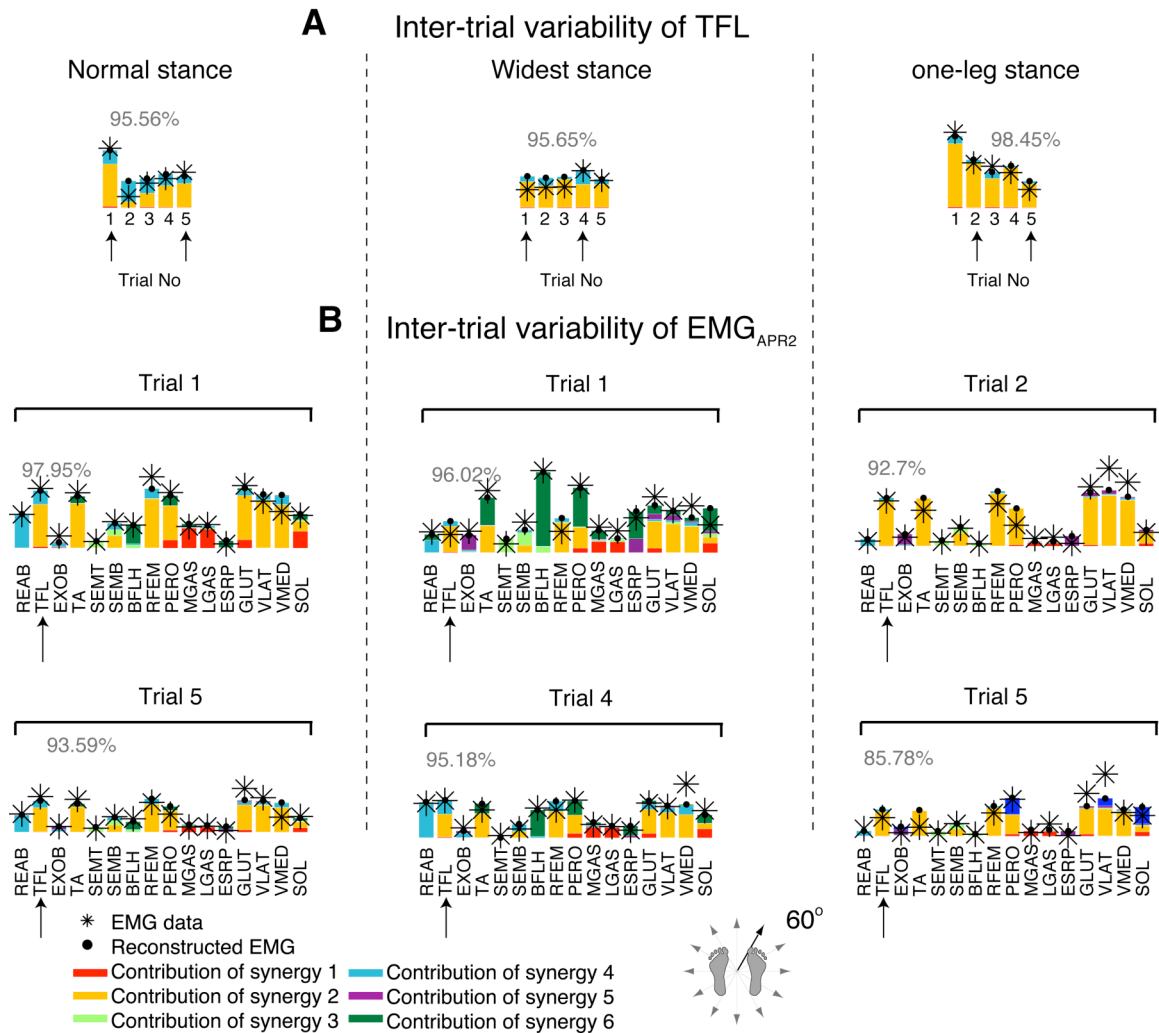


Figure 3.10 Inter-trial variations in the postural responses of one muscle in three sample stance conditions. *A*. TFL responses in APR2 to 5 randomly interspersed trials in the rightward-forwards (60°) direction in normal, widest, and crouched stance condition. The magnitude of the colored bars represents the contribution of each muscle synergy to the activation of TFL in these 5 trials. The recorded data are indicated by black stars and the reconstructed data by solid black dots. Percentage values indicate the variability accounted for by the muscle synergies (VAF) *B*. Muscle activation patterns across all muscles in APR2 (EMG_{APR2}) are shown. Trial-to-trial variations in TFL result from the variations in muscle synergies that activate multiple muscles. For example in normal stance (left column), all muscles belonging to W_2^{Tr} (green) and TFL activity increase in trial 1 and decrease in trial 5. Similar observations can be made in the other two sample stance conditions.

3.3.8 Similarities in muscle synergies across subjects

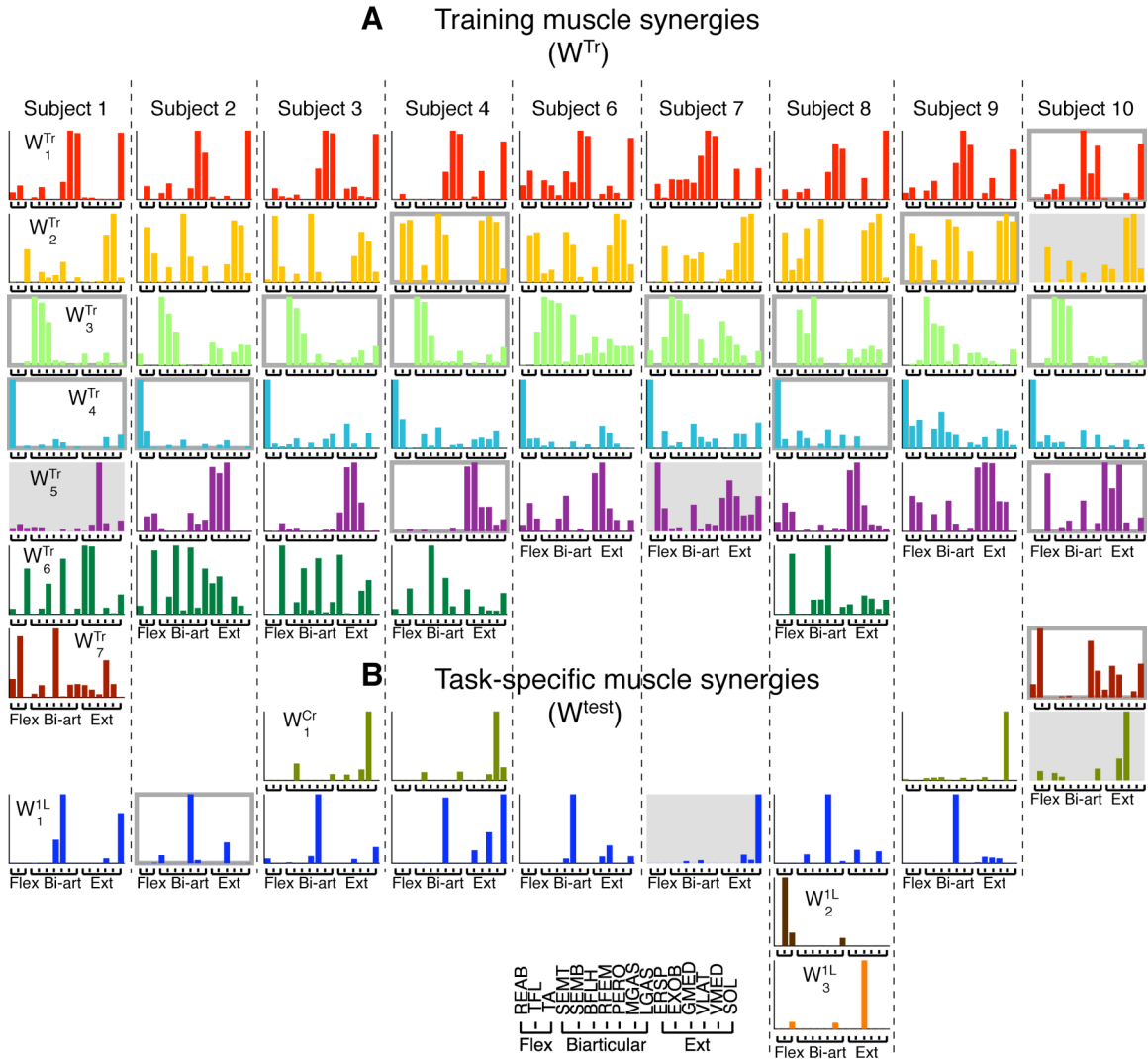


Figure 3.11 Training muscle synergies and task-specific muscle synergies for all subjects. *A*. 5 to 7 training muscle synergies were identified in each subject. Muscle composition of most of W_n^{Tr} was similar across subjects ($0.6 > r^2 > 0.96$); muscle synergies W_{1-5}^{Tr} are the most consistent across subjects. However, differences in muscle composition and synergy activation coefficients across subjects were also identified. Muscle synergies with a gray outline differ in their muscle composition from the other muscle synergies in the cluster but have very similar activation coefficients in all stance conditions. On the other hand muscle synergies on shaded background differ in their activations but have very similar muscle composition to the rest of the muscle synergies in the cluster. Not all the subjects used the same synergies; in particular muscle synergy W_6^{Tr} and W_7^{Tr} were only found in 5 and 2 subjects, respectively. Differences in muscle synergies across subjects indicate that subjects use different muscle activation patterns for maintaining balance in response to the same balance perturbations.



Figure 3.12 Averaged synergy activations coefficients for training muscle synergies of all subjects. The directional tuning of muscle synergy coefficients is similar across subjects, especially for “ankle” strategy synergy 1 (red traces) active during background and backwards perturbation directions (180° to 360°). Gray traces correspond are the averaged synergy activation coefficients of subjects having muscle synergies with very similar muscle composition but different activation coefficients from the other subjects. Differences in synergy activations of muscle synergies with similar muscle composition might indicate that subjects choose to activate their muscle synergies differently.

Training muscle synergy composition and recruitment across postural tasks with different stance configurations were similar across subjects (Fig. 3.11A; $0.6 > r^2 > 0.98$). $W_1^{Tr} - W_5^{Tr}$ were found in all subjects. Because of their muscle composition and their activations' spatiotemporal characteristics, W_{1-4}^{Tr} appear to quantify the classic muscle synergies observed during “ankle” and “hip” strategy and W_5^{Tr} suggests medial-lateral hip stability (Fig. 2.5B and 3.12; \bar{C}_1 through \bar{C}_5 traces). Muscle synergy activation coefficients were consistent across all subjects (Fig. 3.12; $0.6 > r^2 > 0.90$), especially \bar{C}_1 ($r^2 > 0.84$) indicating the regions of activation of the extensor ankle W_1^{Tr} . Since we wanted to determine the generality of muscle synergies across distinct biomechanical conditions and observe the effect of stance configuration on their muscle composition or activations, we recruited the same subjects that participated in our previous study to participate in this study. Only subject 5 did not participate in this study; data from subject 10 were not presented before. Therefore, most of the muscle synergies presented here have been shown in Chapter 2 (Fig. 2.5A).

The majority of muscle synergies used in normal stance were also used in one-leg and crouched stances. However, four additional muscle synergies patterns were unveiled during postural responses when standing in biomechanical configurations extremely different from the normal stance condition. These additional muscle synergies were either task-specific muscle synergies extracted from the test condition, such as W_1^{Cr} , W_1^{IL} , W_2^{IL} , and W_3^{IL} (Fig. 3.11B) or additional muscle synergies extracted from the training condition, such as W_7^{Tr} (Fig. 3.11A). In general, task-specific muscle synergies were formed by a single muscle with relatively high activation level and were unimodally tuned. In all subjects W_1^{Cr} was mainly composed of either VMED or VLAT and was unimodally tuned about 180° when the studied leg was loaded. Similarly W_1^{IL} , was formed by ankle evertor muscle PERO and ankle plantar flexor SOL and was unimodally tuned about rightward perturbations (0° - 30° and 300° - 330°), for which the contralateral

leg is loaded in two legged stances. In only subject 8, abductor hip muscles were highly activated with respect to other muscles in the one-leg stance condition. Thus, two task-specific muscle synergies were identified to account for their high activations in this test condition. W_2^{1L} , formed by TFL was highly activated in response to leftwards perturbations (150° - 210°) and W_3^{1L} formed by GMED was highly activated during background (Fig. 3.13).

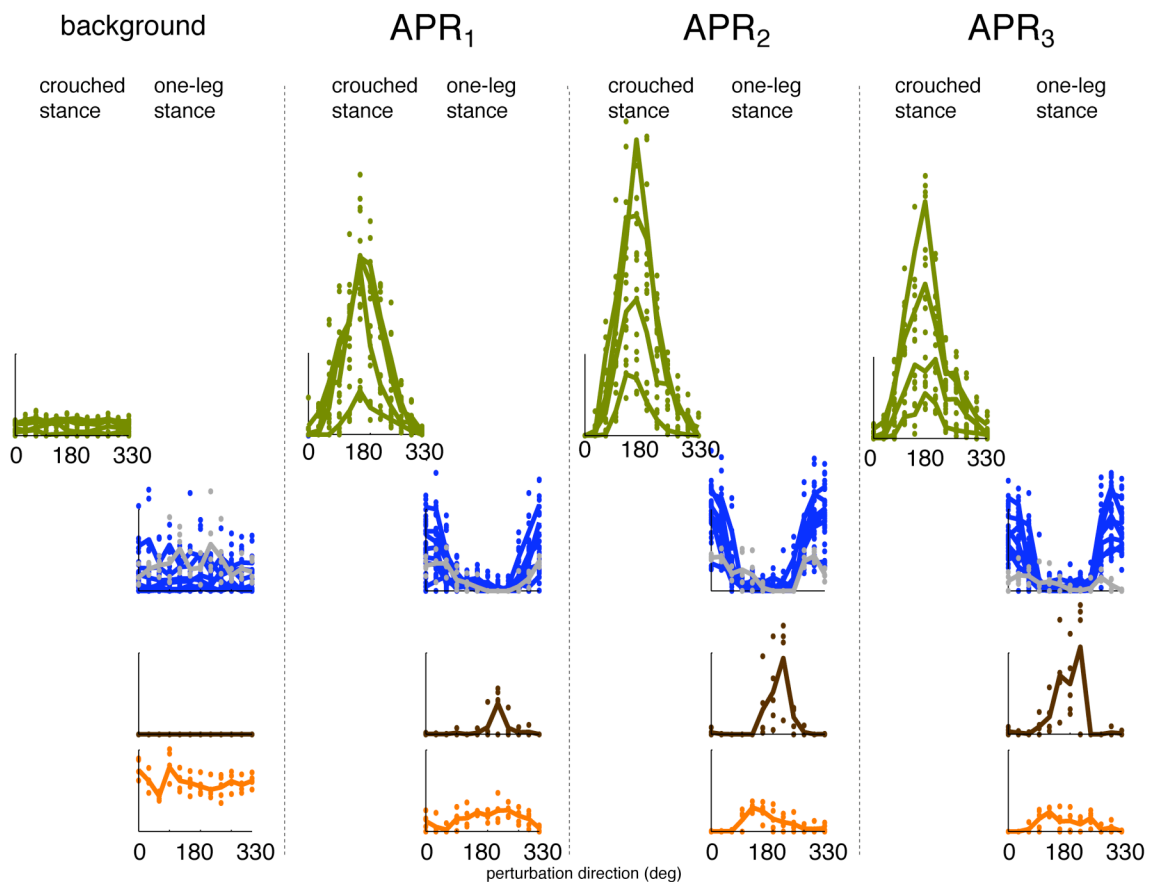


Figure 3.13 Averaged synergy activation coefficients of task-specific muscle synergies across subjects. The directional tuning of muscle synergy coefficients is similar across subjects for all time bins. W_2^{1L} , only identified in subject 8, was highly activated in response to medial balance perturbations as indicated by its spatial tuning curve W_2^{1L} . In addition W_3^{1L} was highly activated during background period when subject 8 was standing on one leg before the balance perturbation.

In addition, in four subjects muscle synergies used in crouched and one-leg stance were coactive in all stance width conditions. Thus these muscle synergies were identified as a single muscle synergy in the normal stance but as two different muscle synergies with distinct muscle composition and activations in the one-leg and crouched conditions. For example in subject 1, W_4^{Tr} and W_7^{Tr} had distinct activations in the one-leg stance condition where W_7^{Tr} was active in response to medial perturbation directions (120°-240°) and W_4^{Tr} was inactive. But these two muscle synergies had very similar spatial tuning in all stance width conditions. Thus they were identified as one single muscle synergy when only perturbation directions in the normal stance were analyzed (Fig. 2.5A). Muscle synergy pairs that were coactive in all stance width conditions but had distinct spatial tuning in the crouched and one-leg condition were $W_4^{Tr} - W_5^{Tr}$ in subject 6, $W_4^{Tr} - W_2^{Tr}$ in subject 9, and $W_2^{Tr} - W_6^{Tr}$ in subject 8. In general, changes in the responses of proximal muscles in crouched and one-leg stances required muscle synergies to split into two muscle activation patterns, suggesting that proximal muscles might be modulated more independently than distal muscles.

Differences in muscle synergy patterns and their activations were also identified across subjects. For example, one or two muscle synergies identified in subjects 1, 4, 7, and 10 (Fig. 3.11A; W^{Tr} s with gray outline) were very similar in their synergy activation coefficients compared to those of all subjects ($0.6 > r^2 > 0.90$) but differed in their muscle composition. Namely, W_5^{Tr} s were mainly composed of GMED and TFL in subject 1 and 7 whereas W_5^{Tr} s in all other subjects also had the contribution of hip extensors ERSP and EXOB. Despite these differences in muscle composition, W_5^{Tr} s in all subjects were highly activated in response to leftwards perturbations during early time bins especially in the narrow and one-leg stance. Thus, in all subject W_5^{Tr} s may have the consistent *function* of providing medial-lateral hip stability during postural perturbations.

Therefore, subjects might choose to use different muscle groups to perform the same function.

Besides, there were a few subjects whose muscle synergies were similar in muscle composition across subjects ($0.6 > r^2 > 0.98$) but differed in activation coefficients. For example all muscle synergies classified as W_3^{Tr} had very similar muscle composition but their tuning curves differed across subjects. These inter-subject differences in muscle synergy recruitment indicate that subjects might choose to activate their muscle groups differently. In this study we were able to identify specific differences in muscle activation patterns across subjects, which could constitute an important application for be important for clinical diagnosis or sports medicine.

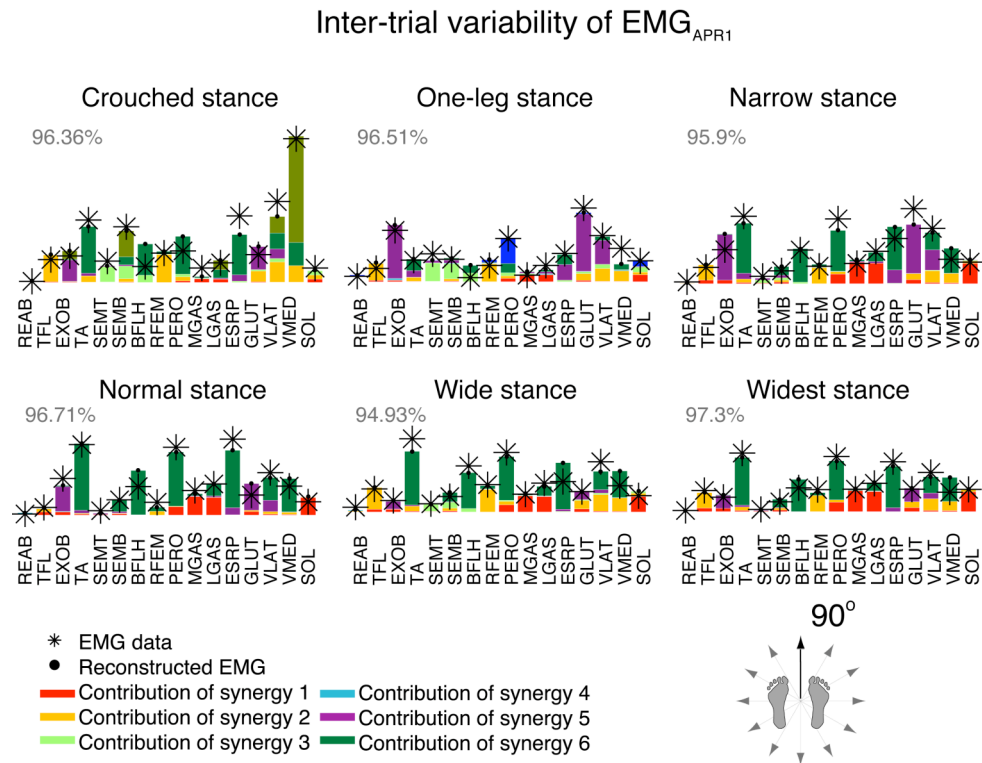


Figure 3.14 EMG activation patterns of sample subject 4 in response to one single perturbation direction in all stance conditions. Muscle activation pattern represented by W6 is consistently observed in EMG responses of this subject in all stance conditions.

Muscle synergies generalize across postural tasks more than across subjects. For example W_6^{Tr} s and W_7^{Tr} s were not general across subjects, but subjects that had them used consistently used them across all postural tasks. The muscle activation pattern represented by W_6^{Tr} was identified in EMG responses of subject 3 in all stance conditions (Fig. 3.14). Only the magnitude of W_6^{Tr} was modulated across stance conditions but muscles forming this muscle synergy were activated simultaneously maintaining fixed relative gains. Therefore, muscle synergies might represent a preferred set of muscle activation patterns used by each subject to maintain multidirectional postural control.

3.4 Discussion

We demonstrated that muscle synergies originally identified in one single stance condition reproduced responses in all stance width conditions and contribute to responses in one-leg and crouched conditions. Variations in synergy activation coefficients that are hypothesized to represent neural commands to the various muscle synergies were modulated to reproduce magnitude, temporal, and spatial changes in postural responses induced by changes in biomechanical context. Additional task-specific muscle synergies were required to reproduce large spatial and magnitude changes in postural responses observed in one-leg and crouched stances, respectively. Moreover, muscle synergies were very similar in muscle composition and spatiotemporal activations across subjects. Therefore, the identified muscle synergies are robust modules of motor output *generally* used to implement the postural strategies required for the postural task at hand.

3.4.1 Generality of muscle synergies in stance width conditions

The synergy activation coefficients, representing the high-level command to the muscle synergies, was the only parameter modulated with stance configuration, suggesting the classical postural strategies are used across stance width conditions. Similar postural strategies are used in all stance width conditions. Muscle synergies

identified in the normal stance condition could reproduce EMG responses in all other stance width conditions. In Chapter 2 we concluded that because of their muscle composition and spatiotemporal activations these muscle synergies might represent muscle activation patterns associated with the “ankle” and “hip” strategies previously described in human balance control (Horak et al. 1997; Horak and Macpherson 1996).

We demonstrated that modulation at the level of muscle synergy activations can account for EMG changes occurring with changes in base of support size. The effect of stance width on synergy activation coefficients is consistent with the changes in individual muscle activations previously reported (Henry et al. 2001). The magnitude of muscle synergy patterns increased as stance width decreased and in general tuning and temporal sequence of muscle synergy activations was maintained, consistent with previous studies in narrow and wide stance (Henry et al. 2001). Muscle synergies were mainly modulated in medial-lateral perturbation directions, which is not surprising since we altered base of support in a medial-lateral direction and not anterior-posterior direction.

The consistency in directional tuning of muscle synergies across postures suggests that they may perform functions that are generalized across tasks. For example, the identified muscle synergies might have the biomechanical function of displacing the CoM in a particular direction. Our prior work in feline postural control demonstrates robust muscle synergies across postures are associated to the consistent function of generating an end-point force in a particular direction (Torres-Oviedo et al. 2006). Similarly, other studies have shown that the activation of muscle synergies correlates to the control of task-level variable such as endpoint force (Ting and Macpherson 2005), or center of pressure displacement (Krishnamoorthy et al. 2003) in postural tasks, and endpoint foot kinematics during locomotion (Ivanenko et al. 2003).

The flexibility in recruitment of muscle synergies and generality of their function, suggest muscle synergies represent modules used for controlling task-level variables that

might be shared across motor behaviors. While the same muscle synergies are used in multiple tasks, their recruitment depends on the biomechanical context. For example W_5^{Tr} might have the general function of stabilizing the trunk in the frontal plane in all postures but its activation is required for distinct circumstances associated to each posture. In general W_5^{Tr} was active in response to leftward (180°) platform motions when the right leg was loaded. However, because changes in stiffness of the musculoskeletal system in the widest stance (Winter et al. 1998), the same perturbation directions caused a smaller displacement of the CoM in this condition; consequently the leg was not as loaded and W_5^{Tr} was inactive. On the other hand W_5^{Tr} was active in the widest stance in response to rightwards (0° - 30° and 300° - 330°) platform displacement that caused a destabilizing flexion of the trunk in this condition only. Therefore W_5^{Tr} serves the same purpose of stabilizing the trunk across postural tasks but it was active for different reasons depending on the distinct biomechanical contexts. Differences in recruitment of muscle synergies that might serve the same function are also observed in muscle synergies shared across locomotor tasks (d'Avella and Bizzi 2005).

3.4.2 Addition of task-specific muscle synergies in drastically distinct stances

Muscle synergies from the training condition were *general* since most of them were used in the one-leg and crouched conditions, which had very different biomechanical constraints. For example, in bipedal stance stabilizing forces are directed towards or away the subjects center of mass (Henry et al. 2001), which was proposed as a simplification strategy for maintaining balance (force constraint strategy) (Macpherson 1988a). However, in the absence of the contralateral leg in the one-leg condition the force constraint strategy cannot be applied, but also the base of support is drastically reduced. Muscle synergies formed by lateral muscles were highly activated to maintain balance in one-leg stance, consistent with previous studies (Tropp and Odenrick 1988; Van Deun et al. 2007). Similarly the distal-to-proximal sequence of activation of muscle

synergies in the normal stance was disrupted in the crouched stance, consistent with the effect of crouched posture in individual EMG responses (Burtner et al. 1998; Woollacott et al. 1998). In spite of those drastic differences in biomechanical context modulation of EMG patterns in the muscle synergy space accounted for changes in postural responses in these two conditions.

We found most muscle synergies recruited in normal stance were also used in the one-leg condition, suggesting common postural strategies to maintain balance are used in both stance configurations. To fully reproduce postural responses in one-leg stance, muscle synergies particular to this stance condition were identified. Because of the biomechanics of the postural task postural strategies not used in the normal stance might be required to maintain balance in the one-leg stance. Specifically, W_1^{1L} , formed by ankle evtor and plantar flexor muscles, was used to compensate for rightwards perturbations in the one-leg stance but not in the other stance conditions when the contralateral leg provided additional support. This is consistent with studies of standing balance on a single-limb quiet stance, demonstrating ankle torques are of primary importance to maintain single-leg balance (Riemann et al. 2003). The contribution of other *general* muscle synergies is also consistent with the increase in contribution of proximal knee and hip joints to one-leg stance balance under more challenging balance conditions induced by changing the support surface (Riemann et al. 2003). Although a standard clinical test to assess balance deficits consist of timing the duration of balancing on one leg, to our knowledge postural responses to balance perturbations by multidirectional support-surface translations, paradigm that has given insight for treatment of balance disorders (Horak et al. 1997), have not been characterized during one-leg stance.

Drastic changes in joint angle might alter the relative activation gains of muscles within a muscle synergy, which is consistent with studies demonstrating nonlinearities in motor neuron excitability with joint angles (Hyngstrom et al. 2007). In addition, it has been shown that heterogenic reflexes change with context (Nichols 1994; 1989; Nichols

et al. 1999; Wilmlink and Nichols 2003), suggesting that lower level processes might influence ongoing motor output patterns, specified by muscle synergies, depending on the biomechanics of the task. Thus, task-specific muscle synergies identified in crouched configuration might represent the nonlinear activation of muscles contributing to one of the *general* muscle synergies. In all subjects, W_1^{Cr} was composed of a single quadriceps muscle and had similar spatiotemporal activation as W_2^{Tr} , which included the muscle in question. Because of the large similarities between these two muscle synergies in terms of their muscle composition and activations, W_1^{Cr} and W_2^{Tr} might be the same muscle synergy but with the nonlinear amplitude scaling of quadriceps muscles in the crouched stance condition. Task-specific muscle synergies W_2^{LL} , and W_3^{LL} of subject 8 might also be examples of nonlinear recruitment of individual muscles within a muscle synergy as a function of posture.

Some subjects had muscle synergies that tended to covary in the training condition but acted independently in the test condition. Consequently, they were identified as a single muscle synergy in the training condition but their activation caused errors in the reconstruction of test condition data set. By extracting additional muscle synergies from the training condition we were able to improve the prediction of EMG responses in other stance conditions. Thus, muscle synergies that had independent activation in the test condition, such as W_4^{Tr} and W_7^{Tr} of subject 1 in crouched stance, could be identified in training data set even if they co-varied for most perturbation directions. A similar phenomenon was observed in simulation pedaling studies where two muscle groups used in the transition from extension to flexion and flexion to extension in forward pedaling were split into four muscle groups during backwards pedaling (Raasch and Zajac 1999; Zajac 2002).

Additional muscle synergies required to fully reproduce muscle activation patterns in the one-leg and crouched condition were either task-specific - extracted from

the specific test data set - or general - extracted from the training condition. This was necessary because the reformulated NMF algorithm could only isolate muscle activation patterns particular to the test condition that were totally absent in the training data, such as the activity of PERO particular to the one-leg condition. We overcame this problem by extracting additional muscle synergies from the training condition to reconstruct test condition data. As an alternate solution we could have used the data set for all conditions to extract shared and task-specific muscle synergies (Cheung et al. 2005). However we wanted to explicitly test the hypothesis of whether muscle synergies from one condition could reproduce the postural responses in all other stance conditions.

3.4.3 Mechanisms underlying muscle synergy activations

Muscle synergies might be activated by the direct projection from higher centers to multiple motorneuronal pools, as indicated by previous studies (Holdefer and Miller 2002; Schwartz et al. 1988). The directional tuning of muscle synergies might be encoded at different levels in the nervous system. For example, directional tuning is observed in activity of single motor units in arm muscles (Herrmann and Flanders 1998) and motor cortex (M1) cells while generating end-point forces (Georgopoulos et al. 1992) or end-point motions (Holdefer and Miller 2002; Schwartz et al. 1988; Scott and Kalaska 1997). Moreover, preferred directions in the arm-related M1 cell firing rates are modulated with arm posture (Scott and Kalaska 1997) and the activation magnitudes, or tuning gains, of wrist-related M1 cells are also modulated with posture (Kakei et al. 1999). In sum, shift in directional tuning and changes in activation magnitudes with posture observed at the level of muscle synergy activations are also observed at the level of M1 cellular activations.

Muscle synergies simplify the sensorimotor transformations required to produce the appropriate postural responses by producing “actions” invariant with context. Previous studies demonstrate each muscle synergy invariant with posture, like the ones

identified here, produces a function that is also invariant with posture (Torres-Oviedo et al. 2006). Therefore, the nervous system might regulate the activation of muscle synergies based on forward models indicating the “action” associated to the each modular motor output (Katsnelson 2003; Wolpert et al. 1998). In addition, the function associated to each muscle synergy is learned in intrinsic body coordinates (Shadmehr and Mussa-Ivaldi 1994). However, CoM displacement needed to recover balance is in an extrinsic reference frame. Therefore, sensorimotor transformations converting low-dimensional muscle synergy biomechanical functions from intrinsic to extrinsic coordinates are required to appropriately tailor muscle synergy activations to the postural task at hand.

3.4.4 Generality across tasks vs robustness across subjects

Generality of muscle synergies across tasks is more robust than generality in muscle synergies across subjects. Each subject used the same muscle synergies regardless of stance configuration. Thus, the underlying neuromechanical control for maintaining standing balance is conserved across subjects. However, differences in muscle synergies across subjects, in terms of their muscle composition and recruitment, demonstrate the existence of individual subject features associated to each subject’s neuromuscular system and experience.

The generality of muscle synergies across postural configurations indicates muscle synergies are preferred muscle activation patterns robustly used by each subject regardless of posture, yet they might not be optimized to each biomechanical condition. Recent studies have proposed muscle synergies represent optimal solutions for performing a motor task (Chhabra and Jacobs 2006; Scott 2004; Todorov and Ghahramani 2004). However, our results suggest they are not necessarily optimized to the biomechanical condition, if they were, we would expect to see changes with biomechanical context in motor output patterns specified by each muscle synergy, specially in conditions with very distinct biomechanical characteristics.

3.4.5 Clinical implications

The decomposition of EMG patterns into muscle synergies could be used to methodically evaluate changes in muscle coordination after clinical interventions, rehabilitation, or injury. We demonstrated that in all postures EMG variability is generated at the level of muscle synergies and not in individual muscle activations. Thus, we can use factorization techniques like the one presented here to explicitly identify changes in muscle activation patterns in the context of muscle synergy composition or recruitment after learning and adaptation. Studies have demonstrated muscles' preferred direction of activation changes with posture (Flanders and Soechting 1990) and adaptation to a kinetic disturbance (Thoroughman and Shadmehr 1999; 2000). However, these studies could not discriminate between changes in *composition* of preferred muscle activation patterns, represented by muscle synergies, or changes in the *contribution* of muscle synergies to the activation of each muscle.

Results presented here might give us insight into postural control of cerebral palsy (CP) patients with chronic crouched posture. We observed similar changes in EMG postural responses to those reported in CP patients and matched healthy subject standing in a crouched posture, suggesting that abnormalities in postural responses of CP patients are caused by biomechanical constraints associated to the crouched posture (Burtner et al. 1998; Woollacott et al. 1998). However, the dimensionality of EMG data, that is the number of muscle synergies, of some of our healthy subjects is maintained in crouched and preferred stance. Therefore although differences in timing and magnitude of muscle synergies activations are observed between crouched and preferred stance, muscle synergies underlying postural control are invariant in the two conditions. This suggest that CP patients might have the same muscle synergies underlying standing postural control as typically developed children. Nonetheless a rigorous study following the methodology presented here would have to be performed in CP subjects to test this hypothesis. Therefore, understanding the effect of posture in the context of muscle

synergies might give us insight into muscle coordination for postural control of patients adopting postures different from healthy subjects.

In all biomechanically distinct stance conditions a few muscle synergies reproduced the directional tuning of individual EMG patterns, temporal difference in muscle onset latencies, and inter-trial variations in postural strategies. Similarly, the flexible combination of muscle synergies reproduced additional spatial, temporal, and magnitude changes in postural responses induced by changes in biomechanical context. Task-specific muscle synergies were identified in postures characterized by drastic biomechanical differences. Task-specific muscle synergies in the one-leg stance represent muscle activation patterns particular to this stance, whereas task-specific muscle synergy in crouched stance might represent the nonlinear activation of muscles forming one of the *general* muscle synergies. Muscle synergies may therefore provide a *general* simplifying mechanism by which descending neural commands influence postural strategy selection for maintaining standing balance.

CHAPTER 4

ROBUSTNESS OF FUNCTIONAL MUSCLE SYNERGIES IN CATS

We recently showed that four muscle synergies can reproduce multiple muscle activation patterns during postural responses to support surface translations (Ting and Macpherson 2005). We now test the robustness of *functional* muscle synergies, which specify muscle groupings and the active force vectors produced during postural responses under several biomechanically distinct conditions. We aimed to determine whether such synergies represent a generalized control strategy for postural control, or if they are merely specific to each postural task. Postural responses to multidirectional translations at different fore-hind paw distances, and to multidirectional rotations at the preferred stance distance were analyzed. Five synergies were required to adequately reconstruct responses to translation at the preferred stance distance -- four were similar to our previous analysis of translation while the fifth accounted for the newly added background activity during quiet stance. These five control synergies could account for >80% total variability or $r^2 > 0.6$ of the electromyographic and force tuning curves for all other experimental conditions. Forces were successfully reconstructed, but only when they were referenced to a coordinate system that rotated with the limb axis as stance distance changed. Finally, most of the functional muscle synergies were similar across all of the six cats in terms of muscle synergy number, synergy activation patterns, and synergy force vectors. The robustness of synergy organization across perturbation types, postures, and animals suggests that muscle synergies controlling task-variables are a general construct used by the central nervous system for balance control.

4.1 Introduction

Recent findings suggest that the CNS simplifies motor control by constraining muscles to be activated in fixed groups, or synergies, where each synergy is defined as a

set of muscles recruited by a single neural command signal. Complex muscle activation patterns in a wide range of motor tasks including locomotion, finger spelling, and postural tasks, can be decomposed into the summed activation of just a few muscle synergies (d'Avella and Bizzi 2005; d'Avella et al. 2003; Ivanenko et al. 2003; Ivanenko et al. 2004; Krishnamoorthy et al. 2003; Poppele and Bosco 2003; Poppele et al. 2002; Ting and Macpherson 2005; Tresch et al. 1999; Weiss and Flanders 2004). A muscle synergy control structure provides an attractive simplifying strategy for the control of complex movements because it reduces the number of output patterns that the nervous system must specify for a large number of muscles, yet allows flexibility in the final expression of muscle activation.

A synergy control structure not only simplifies the motor output pattern for muscle activation but may also be functionally related to high-level control parameters -- global biomechanical variables that are important for movement control. For example, Ting and Macpherson (2005) demonstrated that four muscle synergies could account for the spatial tuning patterns of the automatic postural response elicited by support surface translations in multiple directions in the horizontal plane. These synergies appear to specify the appropriate endpoint forces at the ground that are required to maintain balance (Ting and Macpherson 2005). Muscle synergy recruitment has also been correlated to center of mass shifts in standing (Krishnamoorthy et al. 2003), foot and limb kinematics in walking (Ivanenko et al. 2003; Ivanenko et al. 2004), foot acceleration in pedaling (Ting et al. 1999) and hand kinematics in finger spelling (Weiss and Flanders 2004). Muscle synergies may therefore reflect a neural control strategy at the level of functional variables specific to the particular motor task at hand.

In order for a muscle synergy structure to be useful in reducing the degrees of freedom to be controlled during movement, the observed synergies must be limited in number and robust across behavioral tasks and subjects. Only a few studies have directly examined these features of robustness and generality. Studies in frogs demonstrate

synergies that are shared for walking, jumping, and swimming and those that are unique to each locomotor mode (d'Avella and Bizzi 2005). In addition, simulations and experiments in human pedaling show that the same functional muscle groups can be used to perform variations within the task such as fast or slow, smooth or jerky, forward, backward, or one-leg pedaling (Raasch and Zajac 1999; Raasch et al. 1997; Ting et al. 2000; 1999; Ting et al. 1998). On the other hand, Krishnamoorthy et al. (2004) showed that postural synergies are specific to the task since they change with changes in stability conditions during standing, and new muscle synergies (M-modes) emerge to account for changes in the postural responses.

The current study explicitly addresses both robustness and generality by examining the extent to which muscle synergies and their biomechanical functions described for postural responses in the cat (Ting and Macpherson 2005) generalize across tasks and subjects. We chose to modify the conditions under which postural responses were elicited in two ways: 1) Altering the configuration of the limbs during support surface translations by varying the stance distance between the fore- and hind-paws, and 2) Changing the perturbation characteristics such that the support surface was rotated in combinations of pitch and roll rather than horizontal plane translations.

Because these experimental manipulations induce variability in the automatic postural response, the tolerance of synergies to this variability is a reasonable test of their robustness. First, in both humans and cats, changing the stance distance has been shown to modify the forces and EMGs produced during postural responses and quiet stance (Fung and Macpherson 1999; Henry et al. 2001; Macpherson 1994). In particular, the force responses in the horizontal plane change from being constrained to two directions (force constraint strategy) at long stance distances to a more uniform distribution at short distances (Henry et al. 2001; Macpherson 1994). Second, translations and rotations of the support surface produce similar EMG responses in extensors, but not flexors (Ting and Macpherson 2004). Moreover, extensor responses during rotations and translations are

elicited during disparate kinetic and kinematic conditions. For example, extensors are activated when the hindlimb is initially loaded in translations, but also when it is unloaded in rotations. Thus, the extensors are activated when joint angles undergo flexion in translation vs. extension in rotation, and the extensors are stretched in translation vs. shortened in rotation.

We hypothesized that the synergy organization for postural control is robust such that a single set of functional muscle synergies underlies a variety of automatic postural responses under differing conditions. Our results show that for all limb postures and perturbation types, the same set of muscle synergies and endpoint force vectors could reproduce the entire range of muscle and force responses observed during quiet stance, and during multidirectional balance perturbations. We also hypothesized that the synergy organization is generalized across subjects. Our results show considerable similarity in both synergy composition and endpoint force across animals. Our findings of robustness and generality suggest that muscle synergies controlling endpoint forces represent a general control structure used for maintaining balance, independent of the particular postural conditions.

4.2 Methods

4.2.1 Experimental setup

To investigate the effect of limb configuration and perturbation type on muscle synergies used during postural control in the cat, we analyzed previously collected postural responses to 1) multidirectional support surface translations at different fore-hindlimb stance distances (Macpherson 1994) and 2) multidirectional platform rotations and translations (Ting and Macpherson 2004). Functional muscle synergies were extracted from the control condition of multidirectional translation at the preferred stance distance, and used to reconstruct all of the other test conditions. Detailed experimental

and training procedures were described previously (Macpherson et al. 1987). A brief overview of the experimental setup and data collection procedures is presented here.

Cats were trained to stand freely with one foot on each of four triaxial force plates. Each plate was mounted on the perturbation platform using a magnet and double-sided tape, thus allowing the position of each plate to be easily manipulated between experimental sessions, to effect a change in stance distance. Translation perturbations consisted of ramp-and-hold displacements of 5 cm amplitude, 370 ms duration, and 15 cm/s mean peak velocity in 12 or 16 directions, evenly spaced in the horizontal plane. Rotation perturbations consisted of ramp-and-hold platform tilts in 16 combinations of pitch and roll of 6° amplitude, 200 ms duration and 40°/s mean peak velocity. Platform rotation amplitude was chosen to produce similar rotation about the metacarpophalangeal (MCP) and metatarsophalangeal (MTP) joints as was observed during translation. The coordinate systems used to describe rotation and translation directions were defined such that the direction of the horizontal displacement of the cat's center of mass (CoM) relative to the feet was the same at the end of each translation or rotation (Fig. 4.1).

After training was completed, muscles in each cat were implanted with indwelling bipolar wire electrodes (Teflon-coated multi-stranded stainless steel, Cooner AS632) under general anesthesia using aseptic technique (see Macpherson 1988b). Electrode wires were accessed through 2 connectors mounted on the cat's head. EMG activity was recorded from a subset of eight to fifteen left hindlimb muscles in each of six cats. Table 4.1 contains an inclusive list of all the recorded muscles. Cats were allowed to recover fully from the surgery before participating in experiments.

Three recording sessions for each experimental condition were performed on separate days. For three cats, postural responses to translations were measured when cats were standing at 3 or 4 different inter-paw distances. The anterior-posterior (AP) distance between the fore-and-hind paws was varied from 48 to 138% of the preferred distance of each cat. The preferred distance was defined as the fore-hind paw separation assumed by

an individual cat while standing unrestrained on the lab floor. For a given stance distance, five trials were collected at each of 12 evenly spaced perturbation directions. Kinematic data from body segments were collected at 100 Hz using an Optotrak (Northern Digital, Waterloo, Ontario, Canada) system.

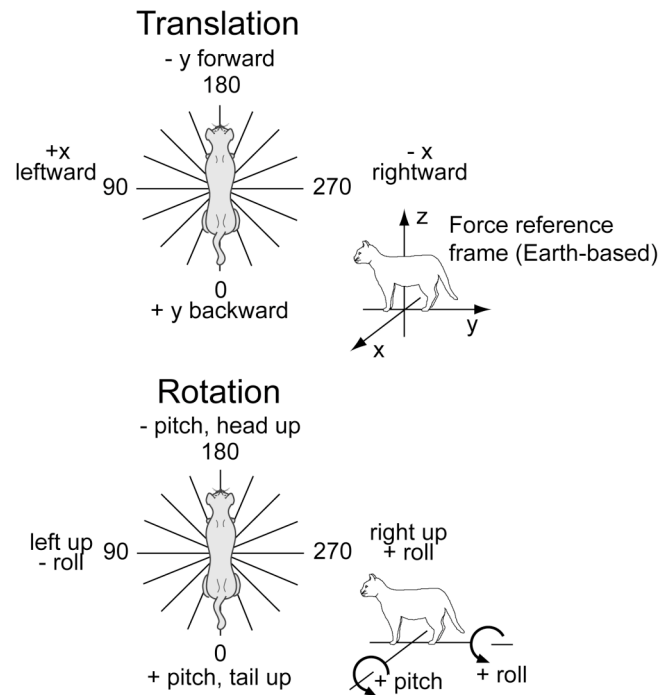


Figure 4.1 Coordinate system for support surface translations and rotations in 16 evenly spaced directions around the horizontal plane. The coordinate systems used to describe rotation and translation directions were defined such that the horizontal displacement of the cat's CoM relative to the feet was in the same direction at the end of each translation or rotation. For example, a backwards platform translation and a head down rotation are defined as perturbations in same 0° direction because both displace the cat's CoM forward, relative to the feet. The coordinate system of force plate recordings is also shown.

For three other cats, postural responses to 16 directions of translation and rotation at the preferred stance distance were recorded (5 trials per direction). Ground reaction forces and EMGs were collected at 1000 Hz for translation and 1200 Hz for rotation, using an Amlab system (Amlab Technologies, Lewisham, NSW, Australia). Kinematic data from body segments were collected at 120 Hz using a Vicon system (Vicon, Lake Forest, CA). Data were filtered and processed offline using a set of custom MATLAB

routines. Forces were low-pass filtered at 100 Hz, and EMG data were high-pass filtered at 35 Hz, de-measured, rectified, and then low-pass filtered at 30 Hz.

Table 4.1 Inclusive list of the muscles recorded from the left hindlimb across cats.

Label	Muscle name	Label	Muscle name
GLUT	Gluteus medius		
GLUP	Posterior gluteus medius	SRTM	Medial sartorius
GLUA	Anterior gluteus medius	STEN	Semitendinosus
VLAT	Vastus lateralis	BFMA	Anterior biceps femoris
VMED	Vastus medialis	BFMM	Medial biceps femoris
SOL	Soleus	BFMP	Posterior biceps femoris
PLAN	Plantaris	REFM	Rectus femoris
EDL	Extensor digitorum longus	SEMA	Anterior semimembranosus
ILPS	Iliopsoas	SEMP	Posterior semimembranosus
TFL	Tensor fasciae latae	GRAA	Anterior gracilis
FDL	Flexor digitorum longus	GRAP	Posterior gracilis
TIBA	Tibialis anterior	MGAS	Medial gastrocnemius
SRTA	Anterior sartorius	LGAS	Lateral gastrocnemius

4.2.2 Data processing

In summary, for each perturbation direction, we generated data vectors consisting of the mean EMG activity and forces generated during a background period (BK) and during the automatic postural response (APR). Thus each experimental condition was characterized by a matrix of data where the rows represent muscles and forces, and the columns represent their activity during background and APR period for each perturbation direction.

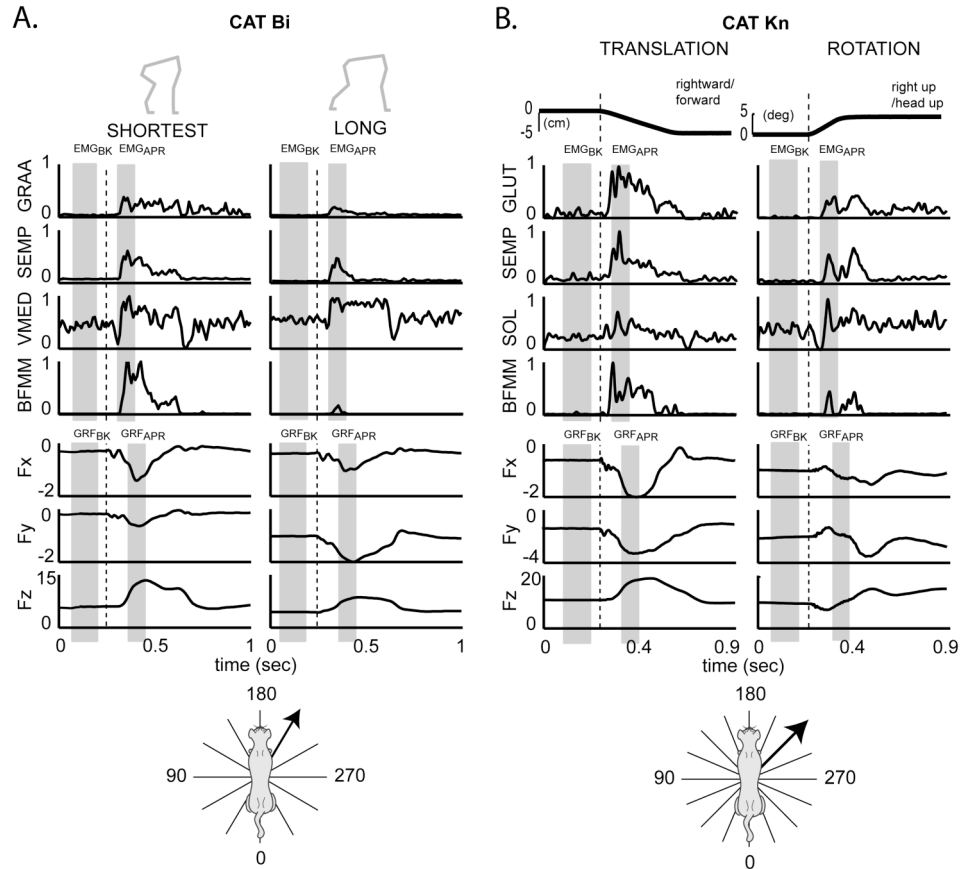


Figure 4.2 Left hindlimb EMG and force responses of two cats during different experimental conditions. *A*: Responses of cat Bi to 210° platform translation at shortest (13cm) and long (34cm) stance distances. Overall, the EMG activity of most of the recorded muscles was higher at short stance compared to long. *B*: Responses of cat Kn to 225° translation and rotation. Note the overall smaller amplitude of response for rotation compared with translation. Vertical dashed lines mark onset of platform motion. In all cats, the EMG_{BK} and GRF_{BK} responses during background, were quantified by the mean activity over the shaded area before platform onset. Similarly, EMG_{APR} and GRF_{APR} were quantified by the mean activity over the time window indicated by the shaded areas following platform onset. Note the time offset between the EMG_{APR} period and the GRF_{APR} period. Passive changes in force due to platform motion are observed between the dashed line and the gray area indicating the GRF_{APR} window. In the case of platform rotation, note that passive changes in force are relatively large and in the opposite direction to changes in force during the GRF_{APR} window.

To obtain the mean EMG and force data for the data matrix, the first step was to average trials by perturbation direction within each session. From each set of averages, the EMG background (EMG_{BK}) was computed as the mean EMG during a 200 ms window that ended 50 ms prior to perturbation onset. Similarly, the EMG of the postural

response (EMG_{APR}) was computed as the mean EMG during an 80 ms window beginning 60 ms after perturbation onset (Macpherson 1988b) (Fig. 4.2). EMG_{APR} amplitude varies as a function of perturbation direction and represents the muscle tuning curve (e.g., Fig. 4.6). Background forces (F_{BK}) during quiet stance were computed as the mean ground reaction force under the left hindlimb in the same period as EMG_{BK} . The active force during the postural response (F_{APR}) was computed as the change in force from background levels during an 80 ms window that began 60 ms after EMG_{APR} onset, or 120 ms following perturbation onset (Jacobs and Macpherson 1996), to accommodate excitation-contraction coupling time. This definition of active force was used in our previous work in which only change in force from background was related to EMG (Macpherson 1988a,b; Jacobs and Macpherson 1996; Ting and Macpherson 2005).

We separated out the positive and negative components of the forces (x , y , and z) to match the functional characteristics of muscle, in that muscles and muscle synergies can produce forces in only one direction along an axis. The generation of force in positive and negative directions is accomplished by different synergies as demonstrated by our previous studies (Ting and Macpherson 2005; Jacobs and Macpherson 1996; Macpherson 1988b). Thus, the F_{BK} during quiet stance was expressed as six values corresponding to absolute values of the positive and negative directions of the force vector components (F_{BKx+} , F_{BKx-} , F_{BKy+} , F_{BKy-} , and F_{BKz+} , F_{BKz-}). The F_{APR} of the postural response was expressed as six values corresponding to the absolute values of the positive and negative change in force from background levels (F_{APRx+} , F_{APRx-} , F_{APRy+} , F_{APRy-} , and F_{APRz+} , F_{APRz-}) (Fig. 4.3). Expressing the force components as absolute values was a requirement of the non-negative analysis method that we chose (see below, Extraction of Functional Muscle Synergies).

The treatment of APR forces from rotation trials was slightly different from that of translation. Unlike translations, rotations cause large changes in passive force between the onset of the platform motion and the APR, primarily due to the projection of the

weight-support force (F_z) into the x-y plane of the force plates as the platform tilts (Ting and Macpherson 2004). Thus, the change in force of the APR was computed with respect to the passive force level and not the background force. The maximum passive force was defined as the peak force level (in platform-based coordinates, Ting and Macpherson 2004) that occurred at 80 ms after perturbation onset. The passive forces in translations (observed only in the x and y components) are small ($< 5\%$ of the F_{APR} amplitude) and dominated by the motion artifact due to the platform acceleration. Because of the small amplitude and the difficulty in accurately estimating the passive force in translation, we did not subtract passive forces from the F_{APR} in translations.

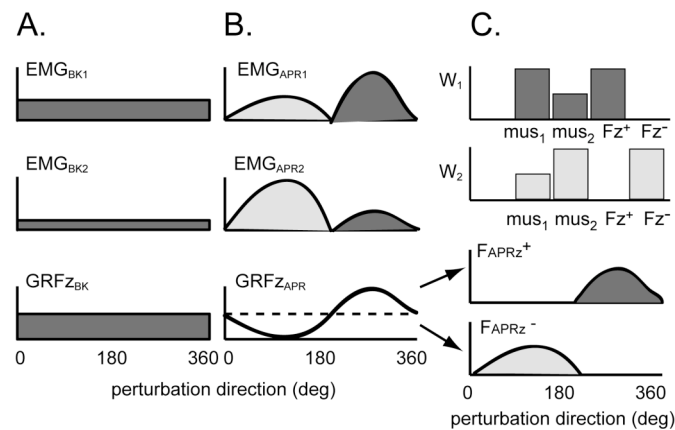


Figure 4.3 Schematic diagram of EMG and force analysis procedure. *A*: Example of background EMG from 2 muscles, EMG_{BK} , and vertical force, GRF_{ZBK} during quiet stance prior to each perturbation direction. *B*: Example tuning curves for the postural response, EMG_{APR} , of the two muscles, and force tuning curve for the vertical component during the postural response, GRF_{ZAPR} . In this example, the two muscles are co-activated at each direction while GRF_{ZAPR} decreases below background levels for directions 0-180° and increases for 180-360°. *C*: W_1 and W_2 represent functional muscle synergies extracted from the example data. Both muscles (mus_1 and mus_2) are active in each synergy, but with different relative levels of activation (dark and light shaded areas under the EMG tuning curves in B correspond to the activation of synergies 1 and 2, respectively). Before synergy extraction, the active force is decomposed into the absolute values of positive and negative changes from background levels (bottom two plots). Synergy 1 is associated with a change in the positive z-force (F_{APRz^+}) and synergy 2, with the negative z-force (F_{APRz^-}).

In summary, for each experimental condition, the data pool consisted of a vector for each muscle in which the elements represented EMG_{BK} and EMG_{APR} across perturbation directions, and a vector for each of the 6 force components in which the elements represented F_{BK} and F_{APR} for each perturbation direction. For display and data inspection prior to synergy analysis, EMGs and forces were normalized to their respective maximum response amplitude across all experimental conditions so that all values were between 0 and 1. Then, each data vector consisting of either an EMG signal or a force component was normalized to have unit variance in the control condition, which allowed the different data types to be combined. EMG and force data from the test conditions were normalized with the same factors as the control condition to maintain consistent units across conditions.

4.2.3 Extraction of Functional Muscle Synergies

The matrix for extracting functional muscle synergies consisted of both muscle [EMG_{BK} , EMG_{APR}] and force data [F_{BK} , F_{APR}]. Therefore, a functional muscle synergy consists of pairs of covarying patterns of muscle activation (muscle synergies, W_{EMG}) and force generation (synergy force vectors, W_F) and each muscle synergy is assumed to have the function of generating a synergy force vector. This approach differs from a previous study, in which muscle synergies and endpoint forces were extracted separately and then correlated (Ting and Macpherson 2005).

By extracting synergies conjointly from muscle and force data, we tested the hypothesis that the force data could be reconstructed using a set of force vectors whose magnitudes scale with the activation of muscle synergies. The synergy force vectors represent the forces most likely to be generated by muscle synergy activation, they may not be orthogonal or independent vectors, and may not span the entire force space. The conjoint method has the further effect of ignoring components of force not directly

generated by muscle activation in the limb, such as those due to dynamic or inertial forces or to forces generated by muscles in a different limb.

Because the main purpose of this study was to explore dimensionality of the muscle activations and the robustness of muscle synergy composition, we tested whether the presence of force data in the data matrix influenced the composition of the resultant muscle synergy vectors. Synergies extracted from the EMG data both with and without the force data showed the same dimensionality (5) and very similar muscle composition ($r^2 > 0.9$ for all synergies across all cats). Therefore, addition of the forces to the data set changed neither the dimensionality of the synergies nor their composition.

We used a linear decomposition technique called non-negative matrix factorization (NMF) to extract functional muscle synergies (Lee and Seung 2001). This formulation is mathematically identical to that presented in both Tresch et al (1999) and Ting and Macpherson (2005), but uses a more efficient algorithm. For each perturbation direction k , the vector X_k represents a concatenation of all of the muscle and force responses during quiet stance or during the APR period. Thus, 32 data vectors, X_k , were generated from 16 perturbation directions (16 BK and 16 APR vectors). A functional muscle synergy is represented as a vector W_n formed by a group of muscles and the endpoint force generated by their activation. The data vectors, X_k , for each given perturbation direction, k , can be reconstructed using a weighted sum of functional muscle synergy vectors:

$$X_k \cong \sum_{n=1}^{N_{syn}} c_{nk} W_n$$

Where $X_k = [EMG_{BK} \ F_{BK}]_k$ or $[EMG_{APR} \ F_{APR}]_k$, c_{nk} is a non-negative coefficient representing the activation level of synergy n in direction k , and W_n is composed of muscle and force individual gains (w_{ni} and f_{nj}) that specify the activation level of each muscle, i , within the synergy and of each component, j , of the synergy force vector for each functional synergy. All the elements of each functional synergy are constrained to

be positive and constant over all conditions. For each synergy n , the set of activations c_{nk} across all perturbation directions during quiet stance and during the APR period is the vector C_n . The C_n components during the APR period represent the tuning curve that describes how the activation of the functional muscle synergy W_n changes as a function of perturbation direction.

The number of functional muscle synergies that best characterized the data was determined by one global criterion and two local criteria: 1) total % variability accounted for (%VAF) $> 90\%$ in the control condition, 2) a roughly uniform distribution of errors as a function of perturbation direction within each condition, as determined by evaluating the effect of adding an additional synergy, and 3) adequate reconstruction of each muscle tuning curve for each perturbation direction in all conditions, as determined by either $r^2 > 0.6$ or %VAF $> 80\%$.

%VAF is defined as $100 \times$ uncentered Pearson correlation coefficient, which requires the regression to pass through the origin (Zar 1999). This is a similarity metric that is used to quantify exact matches between two patterns such as genomic sequences (Alizadeh et al. 2000; Eisen et al. 1998). The definition of both r^2 and VAF is (1-sum of squared errors/total sum of squares). However, in the standard Pearson correlation coefficient (r^2) the total sum of squares taken with respect the mean value of y , whereas in the uncentered case (VAF) it is taken with respect to zero.

VAF is a more stringent criterion than r^2 because it evaluates both shape and magnitude of the measured and reconstructed curves. VAF is equal to 100% when the two curves are perfectly matched, that is, the regression between them has a slope of 1 and offset of 0. r^2 is only sensitive to the similarity in shape of the curves without constraining the slope or offset of the regression. r^2 provided a better assessment of the reconstruction in the case where the tuning curve shapes were well-matched, but the amplitude was not, whereas VAF was higher for muscles with high baseline activity and

noisy tuning curves (e.g., LGAS in Fig. 4.9). If a muscle tuning curve was flat (i.e., muscle activation was constant across direction) the r^2 and VAF values from that muscle were not included in the criteria for selecting the number of functional muscle synergies, because such muscles were not selectively activated during postural responses.

The combination of both global and local variability criteria ensured that each pattern of muscle activation measured for a given perturbation direction, and each muscle tuning curve over all directions was well-reconstructed. This allowed identification of functional muscle synergies that may account for only a small percentage of the total data variability but are essential to reproduce the responses to a specific range of perturbation directions (Ting and Macpherson 2005).

4.2.4 Data Analysis

Functional muscle synergies were first extracted from the control data set of multidirectional translations at the preferred stance distance. These control synergies were then tested for robustness within subjects by using them to reconstruct the test data from 1) translations at non-preferred stance distances, and 2) rotation perturbations. Finally, synergy vectors were compared across cats, to test the generality of the synergy structure across individuals.

In the first test, functional muscle synergies extracted from control data were used to reconstruct EMG and force responses to platform translation at all stance distances by performing a non-negative least square fit. Using custom MATLAB routines, we determined the coefficients C_{shortest} , C_{short} , $C_{\text{preferred}}$ and C_{long} that would best reconstruct the translation data at each distance using the control synergies.

In the second test, functional muscle synergies extracted from the control data of translations were used to reproduce EMG and force responses to platform rotations. The reverse procedure of using the rotation synergies to reconstruct the translation responses was not done because rotation does not activate the full muscle set, with the most notable

absence being the flexors (Ting and Macpherson 2004). Therefore, flexor responses to translation perturbations could not be reconstructed using rotation synergies extracted from data where flexor responses are smaller or nonexistent. Similar to the stance distances analysis, a non-negative least squares fit of the translation vectors to the rotation data set was performed to find the coefficients C_{rot} that would best reconstruct the rotation data.

To test the generality of synergy structure, the features of the synergies were compared across cats that followed the same experimental paradigm. Functional synergy vectors (W), muscle synergies (W_{EMG}), synergy force vectors (W_{F}), and synergy activation coefficients (C) were compared by calculating the coefficients of determination between cats. The muscles that were not common to all the cats were excluded from the muscle synergy vectors before correlation analysis.

4.3 Results

For each cat, a set of 5 functional muscle synergies extracted from the control data was found to account for the muscle activation patterns associated with quiet stance and with the automatic postural response for all 5 test conditions: multidirectional support surface translations at four non-preferred stance distances, and multidirectional rotations. When muscle activation in a test condition varied from the control condition, this was achieved by changes in the directional tuning of the activation coefficients for the various synergies, with some synergies varying more than others. Each functional muscle synergy was characterized by a unique synergy force vector. Forces recorded in the test conditions were well-reconstructed from the control synergy force vectors, but only when the force data were referenced to a coordinate system that rotated with the hindlimb axis (defined by the vector from the MTP to hip joints). In other words, the net direction of force produced in space by each muscle synergy rotated with the limb axis. Finally, all

animals exhibited similar functional muscle synergies in terms of muscular patterns, force direction, and activation.

4.3.1 Five synergies extracted from preferred stance reproduce responses at all stance distances

A minimum of 5 functional muscle synergies extracted from the control condition was found to reproduce muscle activation patterns and forces over all perturbation conditions within the specified parameters of acceptability. As the specified number of control synergies was increased from one to eight, the reconstruction of both control and test conditions also increased (Fig. 4. 4A). Across the three cats in the stance distance group, 5 synergies accounted for a total mean VAF of $96.6 \pm 0.8\%$ in the control dataset at the preferred distance. The total mean VAF accounted for in the test dataset was $84.6 \pm 8\%$ (shortest), $89.7 \pm 3.5\%$ (short), and $79.6 \pm 9.8\%$ (long). The fore-hindpaw stance distances from cat Bi, whose data are illustrated in this section, were 13 cm (shortest), 20 cm (short), 27 cm (preferred), and 34 cm (long). Three functional muscle synergies reproduced 90% of the overall data variability in Bi at the preferred stance (Fig. 4.4A) but not all directions were adequately reconstructed (Fig. 4. 4B). Adding the fourth and fifth synergy dramatically improved the directional profile of VAF, particularly at 0° and 150° . For example, when the synergy number was increased from 4 to 5, the VAF for the 150° perturbation direction at the shortest stance distance increased from about 60% to over 80% in cat Bi (Fig. 4.4B, preferred to shortest). Five synergies from the preferred stance dataset were also required to reconstruct all EMG tuning curves to $r^2 > 0.6$ (Table 4.2). The only EMG tuning curve excluded from the analysis was from cat Ru at long stance where SRTM was inactive. A minimum of 5 synergies was needed to adequately reconstruct the EMG responses across all directions as well as quiet stance. For more than 5, the added synergies contributed about evenly to the reconstruction of

responses across all perturbation directions, suggesting that the extra synergies represented random variations in the data.

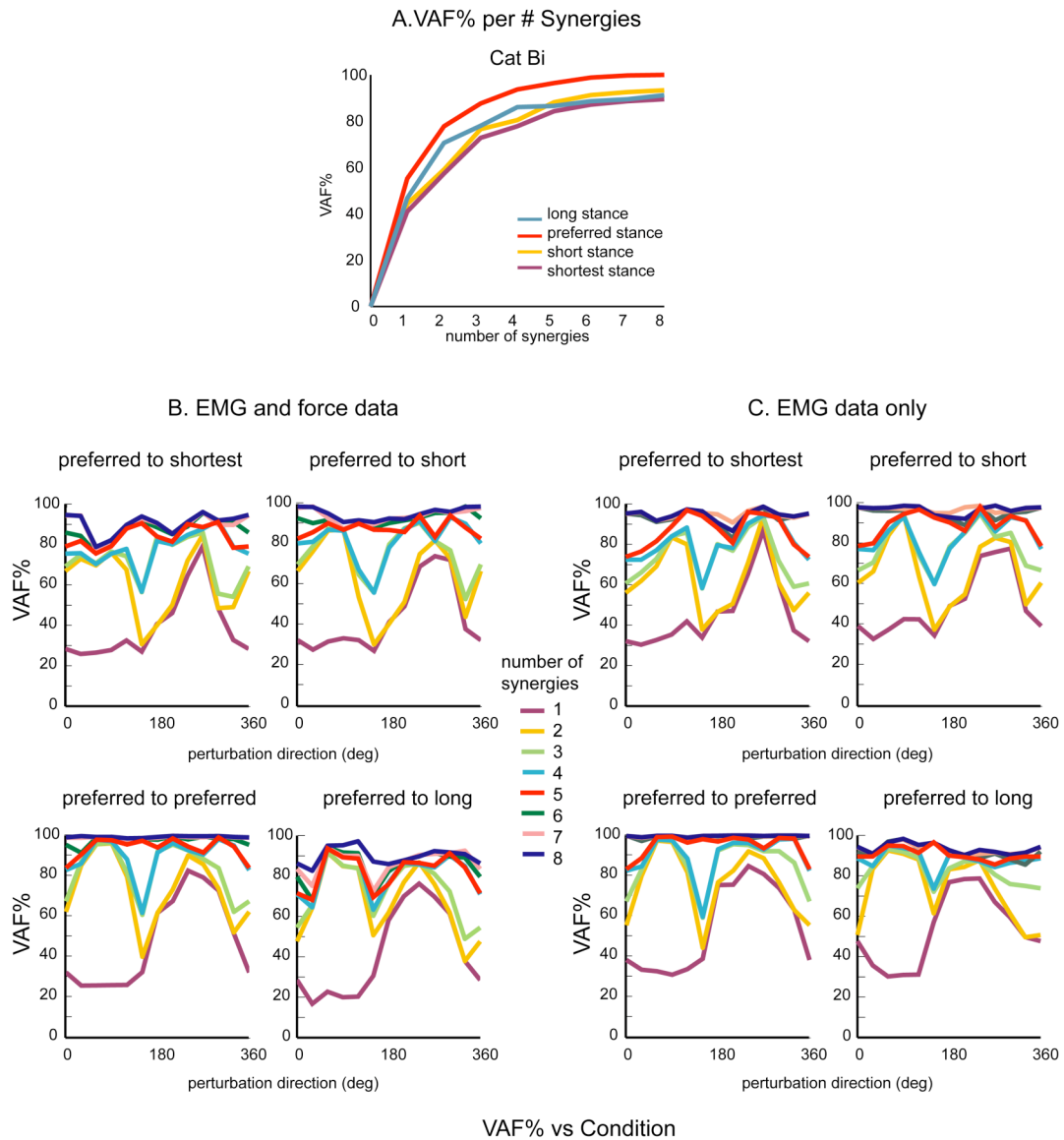


Figure 4.4 *A.* Variability accounted for by increasing numbers of synergies for entire datasets at each stance distance for cat *Bi*. 5 synergies accounted for 96% of total variability in translation at the preferred stance (red line). These same 5 synergies accounted for 84%, 88%, and 87% of the total data variability at shortest, short, and long stance, respectively. *B.* Variability accounted for at each stance distance as a function of perturbation direction for cat *Bi*. The synergies used to obtain these VAF values were extracted from EMG and force responses during background and APR periods. *C.* Variability accounted for at each stance distance of cat *Bi* when synergies were extracted from EMG data only. The dimensionality of the synergy set used to characterize muscle postural responses was the same whether or not forces were included in the synergy extraction analysis.

Table 4.2 r^2 values of EMG and force tuning curve reconstructions in the stance distance group

Summary of EMG reconstruction												
Cat	r^2 Shortest			r^2 Short			r^2 Preferred			r^2 Long		
	min	max	avg	min	max	avg	min	max	avg	min	max	avg
Ru	0.69	0.98	0.90	0.73	0.99	0.93	0.88	1.00	0.96	0.61	0.99	0.88
Bi	0.63	0.98	0.86	0.73	0.99	0.87	0.88	0.99	0.94	0.73	0.95	0.88
Ni	0.57	0.98	0.88	0.81	0.99	0.91	0.81	1.00	0.94	na	na	na
Summary of Force reconstruction												
Cat	r^2 Shortest			r^2 Short			r^2 Preferred			r^2 Long		
	min	max	avg	min	max	avg	min	max	avg	min	max	avg
Ru	0.74	0.95	0.84	0.59	0.96	0.82	0.56	0.96	0.85	0.60	0.92	0.77
Bi	0.55	0.96	0.79	0.59	0.98	0.81	0.81	0.99	0.90	0.75	0.97	0.88
Ni	0.74	0.96	0.88	0.84	0.96	0.90	0.87	0.98	0.91	na	na	na

The inclusion of the force data in the synergy analysis did not alter the muscle composition of each synergy or the number of muscle synergies required to adequately reconstruct the EMG data (Fig. 4.4C). Therefore the dimension and composition of the functional synergies primarily reflects variability within the muscle activation pattern, and not the forces.

Each synergy, W_n , was reasonably distinct in terms of muscle composition (Fig. 4.5A) and directional tuning of the activation coefficients, C_n , (Fig. 4.5B; cf. Ting and Macpherson 2005). Only one synergy, W_1 was active during the background period to provide antigravity support and consisted primarily of the vasti muscles in cat Bi (Fig. 4.5, red synergy). During the APR, the activity of W_1 was decreased from that of quiet stance for perturbations between 210 and 300° when the left hindlimb was loaded (increased vertical force) and shut down completely for all other directions. W_2 (Fig. 4.5, yellow synergy) was active from 330 to 120°, when the left hindlimb was unloaded, and contained the uniarticular hip flexor iliopsoas, as well as biarticular muscles with a knee

flexion moment arm such as sartorius, semitendinosus, and posterior biceps femoris. The composition of W_3 (Fig. 4.5, green synergy) included many hip extensors, such as anterior and posterior gluteus, middle biceps femoris, posterior semimembranosus, and gracilis. W_4 (Fig. 4.5, blue synergy) was dominated by rectus femoris, a hip flexor and knee extensor, with activity from the synergist, anterior sartorius, hip extensors vastus lateralis and medialis and moderate activity from the uniarticular hip flexor iliopsoas; its tuning curve overlapped with that of the flexors in W_2 , but was phase-shifted to the right. W_5 (Fig. 4.5, purple synergy) was dominated by the hamstring muscles and especially gracilis, and its activation overlapped with the flexors in W_2 but with a phase-shift to the right.

4.3.2 Activation of functional muscle synergies changes with stance distance

All 5 control synergies contributed to translation postural responses at all stance distances, however the activation level of some synergies decreased as stance distance increased (Fig. 4.5B). W_3 and W_5 , formed largely by biarticular muscles, varied the most in activation across stance distance. The peak activations in W_3 and W_5 at the longest stance were 32.5% and 13% of their respective peak activations at the shortest stance. W_4 and W_2 , the flexor-dominated synergy, were less modulated with distance (peak at the long stance was 74.5% and 59.4% of their respective peak activations at the shortest stance). Activation of W_1 during the background period and the postural responses was little affected by stance distance. W_5 broadened its activation to include more directions at long stance, W_4 shifted its activation to the right at short and shortest stances, and W_2 and W_3 maintained the same directional tuning with stance.

The EMG tuning curves were adequately reconstructed at all stance distances using the five synergies from the control condition (Fig. 4.6). Overall, tuning curve shape was well reconstructed for all EMGs, whereas amplitude was less well reconstructed for a subset of muscles. The coefficients of determination (r^2) between the original and the

reconstructed data exceeded 0.8 in 97.9% of the muscle tuning curves across all stance distances and all cats while the variance accounted for (VAF%) exceeded 96.5% in 80% of the individual muscle tuning curves. In some muscles of cat Bi (anterior gracilis, middle biceps femoris, and anterior sartorius) EMG amplitude was greater at the short stances than was predicted by the linear modulation of the muscle synergy (Fig. 4.6). However, the direction at which peak activation occurred and the tuning curve shapes were well predicted, suggesting that these muscles might still be activated by the same synergies, but with a nonlinear amplitude scaling.

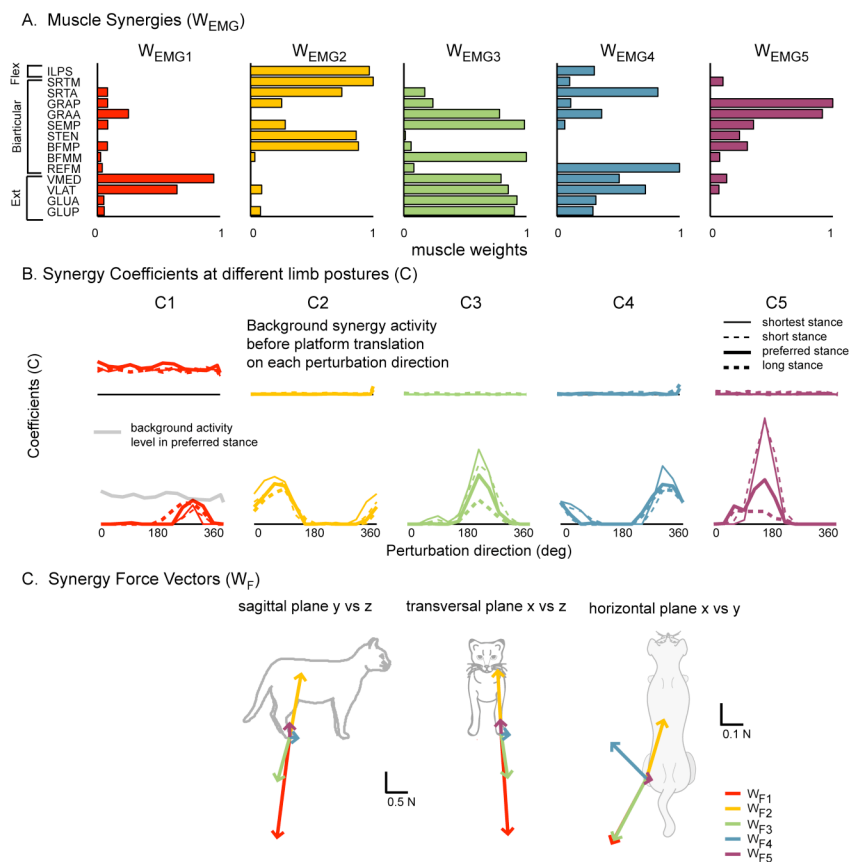


Figure 4.5 *A.* Muscle synergy vectors, W_{EMG} , extracted from translation at the preferred stance distance for cat Bi. Each bar represents the relative level of activation for each muscle within the synergy (see Table 4.1 for muscle abbreviations). *B.* Activation coefficients, C_i , for each of the 5 synergies at 4 stance distances. Upper traces show background, quiet stance activation levels across direction. Lower traces show the response to translation across direction. *C.* Synergy force vectors, W_F , associated with each muscle synergy (same color coding), drawn in the sagittal, frontal, and horizontal planes. Vectors are expressed as forces applied by the limb against the support. Note that the scale for the horizontal plane has been magnified for easier viewing.

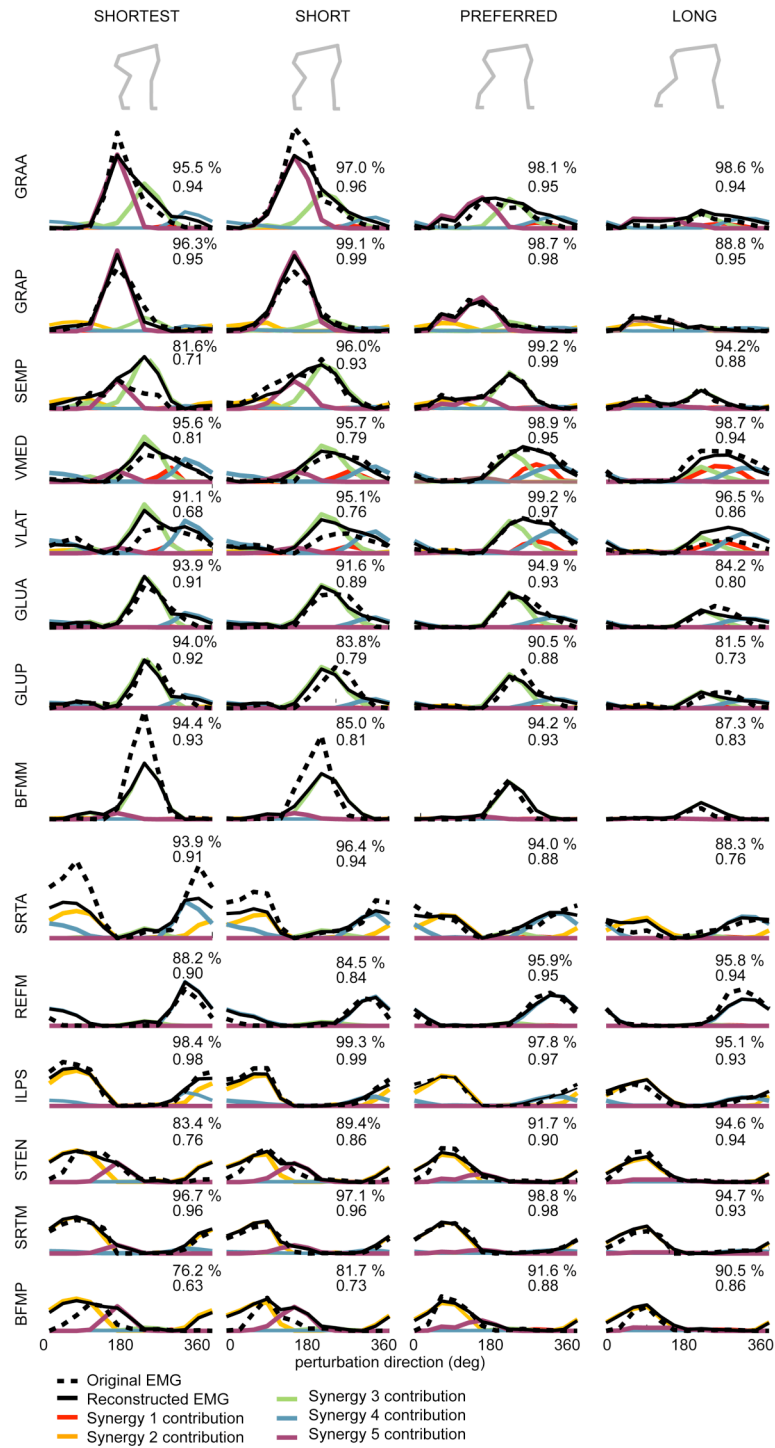


Figure 4.6 EMG tuning curves of the automatic postural response in cat Bi for translations at 4 stance distances. The original data are shown by the dashed black line and the reconstructed data by the solid black line. The contribution from each synergy to the reconstruction is shown by the corresponding colored line. This is computed by multiplying each functional synergy vector W by its activation coefficient C .

4.3.3 Synergy force vectors are consistent with respect to the limb axis

Each of the five control synergies was characterized by a distinct force vector (W_F) (Fig. 4.5C). Initial attempts to reconstruct GRF responses to platform translation using this control set of synergy W_F 's were successful only at reconstructing data from the preferred stance distance and not from the other distances. We attributed the difficulty in force reconstruction to the large change in GRF vector orientation that accompanies changes in stance distance.

Our previous study showed that during quiet stance, the angle of both the limb axis and the GRF vector changed linearly with stance distance, with the GRF vector angle having a slightly smaller gain than that of limb axis angle (Fung and Macpherson 1995). Therefore, we transformed the original force data into the coordinate system of the average GRF vector that was measured during quiet standing at each stance distance, named here the F-frame (Fig. 4.7A,B). Once transformed, acceptable reconstruction of all the force data was achieved at the $r^2 > 0.6$ level (Table 4.2) using control synergy force vectors, except for F_x - ($r^2 = 0.55$ and $r^2 = 0.59$) of cat Bi at the short and shortest stance and F_x - ($r^2 = 0.58$ and $r^2 = 0.56$) of cat Ru at the short and preferred stance. This result suggests that synergies produce consistent forces in a limb-referenced coordinate system. As shown in Fig. 4.7A, the z-axis was specified as the mean GRF vector during quiet stance and the x-axis was defined to be collinear with the X-axis of the Earth coordinate system (a vector pointing laterally). The GRF vector and the hindlimb axis varied mainly in the sagittal plane with stance distance. As a result, the force data in each configuration were rotated about the x-axis by an angle θ , defined as the angle between the z-axis of the Earth coordinate system and that of the hindlimb GRF coordinate system. When expressed in the hindlimb coordinate system, the anterior-posterior (F_y) forces show consistent phasing relative to perturbation direction across stance distance, unlike the tuning curves of the same F_y forces in the Earth coordinate system (Fig. 4.7D). The angles of rotation for each stance configuration in all the cats are reported in Table 4.3.

Table 4.2 r^2 values of EMG and force tuning curve reconstructions in the stance distance group

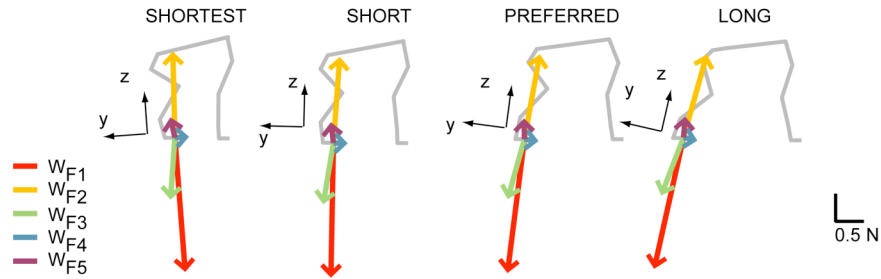
Summary of EMG reconstruction												
Cat	r^2 Shortest			r^2 Short			r^2 Preferred			r^2 Long		
	min	max	avg	min	max	avg	min	max	avg	min	max	avg
Ru	0.69	0.98	0.90	0.73	0.99	0.93	0.88	1.00	0.96	0.61	0.99	0.88
Bi	0.63	0.98	0.86	0.73	0.99	0.87	0.88	0.99	0.94	0.73	0.95	0.88
Ni	0.57	0.98	0.88	0.81	0.99	0.91	0.81	1.00	0.94	na	na	na
Summary of Force reconstruction												
Cat	r^2 Shortest			r^2 Short			r^2 Preferred			r^2 Long		
	min	max	avg	min	max	avg	min	max	avg	min	max	avg
Ru	0.74	0.95	0.84	0.59	0.96	0.82	0.56	0.96	0.85	0.60	0.92	0.77
Bi	0.55	0.96	0.79	0.59	0.98	0.81	0.81	0.99	0.90	0.75	0.97	0.88
Ni	0.74	0.96	0.88	0.84	0.96	0.90	0.87	0.98	0.91	na	na	na

Table 4.3 Mean angle of GRF rotation, θ , for all cats at all stance distances

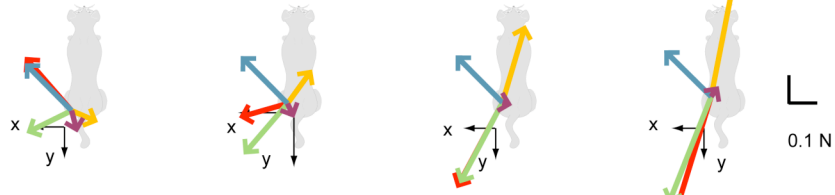
Cat	Shortest	Short	Preferred	Long
Bi	-4.1	1.4	7.5	12.9
Ru	-4.5	0.35	6.9	18.5
Ni	-3.3	1	7	NA

When viewed in the F-frame coordinate system, the five W_F 's, appear to have a consistent function across all stance distances. In the sagittal plane (Fig. 4.7A), W_{F1} and W_{F2} were aligned approximately with the limb axis, with W_{F1} having a downward, or loading component and W_{F2} an upward component, which corresponds with the respective antigravity and flexor functions of the associated muscle synergies. W_{F3} produced a downward and posterior force relative to the limb axis which was similar to the quiet stance support vector, W_{F1} , at the preferred and long distances but less so at the shorter distances. W_{F4} produced an anterior force related to the anterior biarticular muscles, rectus femoris and anterior sartorius of W_4 . Finally, W_{F5} produced an upward and medial force relative to the limb axis, consistent with the presence in W_5 of muscles with knee flexor action and the hip extensor/adductor, gracilis.

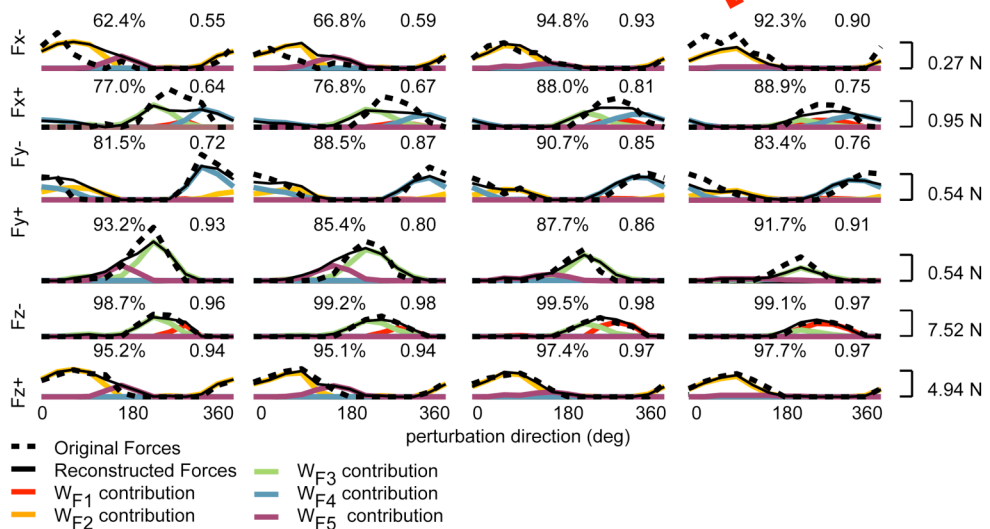
A. Synergy Force Vectors in Sagittal Plane



B. Synergy Force Vectors in Horizontal Plane



C. Force Tuning Curves Reconstruction



D. Force Tuning Curves expressed in Earth and leg reference frames

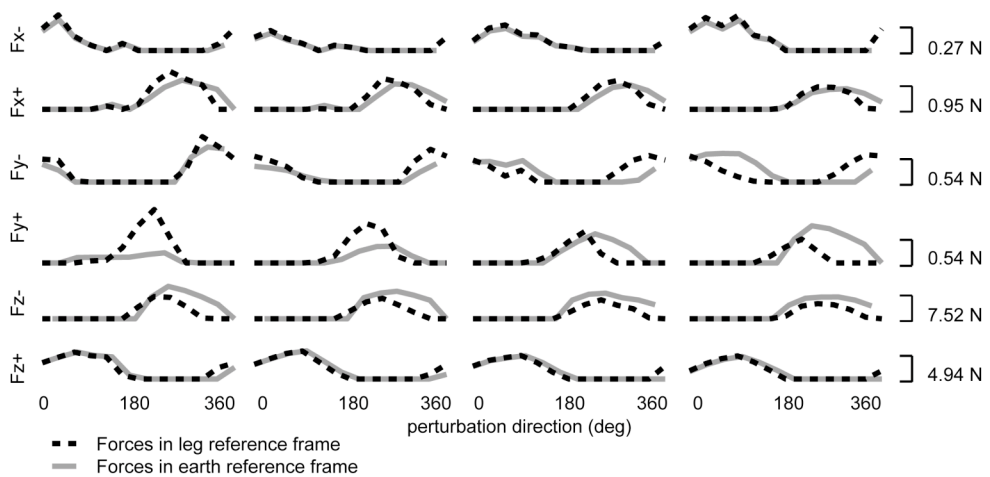


Figure 4.7 A,B. Synergy force vectors extracted from translation data at the preferred stance distance, for cat Bi. Vectors are expressed as forces applied by the limb

against the support, and are rotated in the sagittal plane such that the z-axis is collinear with the mean GRF vector observed during quiet standing, which itself rotates with stance distance. Coordinate axes of the F-frame are shown at each stance distance. *C.* Applied force tuning curves for translation at 4 stance distances for cat Bi, expressed in the F-frame coordinate system. Black dashed lines indicate the original experimental data, black solid lines the reconstructed data and colored lines the contributions from each synergy force vector. *D.* Tuning curves of the recorded force amplitude data from cat Bi for 4 stance distances. The forces have been separated into components as described in the text. The same data are drawn in two different coordinate reference frames, Earth-based (solid gray lines) and F-frame based (dashed black lines). Note that the phase of the F_y force tuning curves remains constant when expressed in limb coordinates, but changes in Earth coordinates.

The synergy force vectors were able to account for the active forces during the postural response at all stance distances provided the ground reaction forces were rotated according to the angle of the background force during quiet standing, as illustrated in Fig. 4.7C by the reconstruction of each force component across stance distance. The shapes of the tuning curves were well reconstructed in most cases ($r^2 > 0.7$ in 81.8% of all force tuning curves in all cats at all stance distances). As stance distance decreased the F-frame referenced anterior-posterior forces (F_y) increased in magnitude whereas the dorso-ventral (F_z) and lateral (F_x) forces were relatively consistent (Fig. 4.7C, Original Force traces). At short stances, the limb is protracted and the F_y^+ component contributes to weight support (see coordinate frame for the short distance in Fig. 4.7A), which accounts for the change in amplitude with stance distance. These force changes parallel the increased magnitude in many of the EMGs at short compared to long stances.

4.3.4 Functional muscle synergies extracted from translation data reproduce rotation data

In a separate set of cats, functional muscle synergies extracted from translations could be used to successfully reproduce EMG and force responses during rotation perturbations. The representative data of cat Wo are presented. Activation coefficients of the functional muscle synergies were different in rotation and translation across direction.

The tuning curves of synergies W_1 and W_2 were the most similar, exhibiting only a small phase difference (Fig. 4.8).

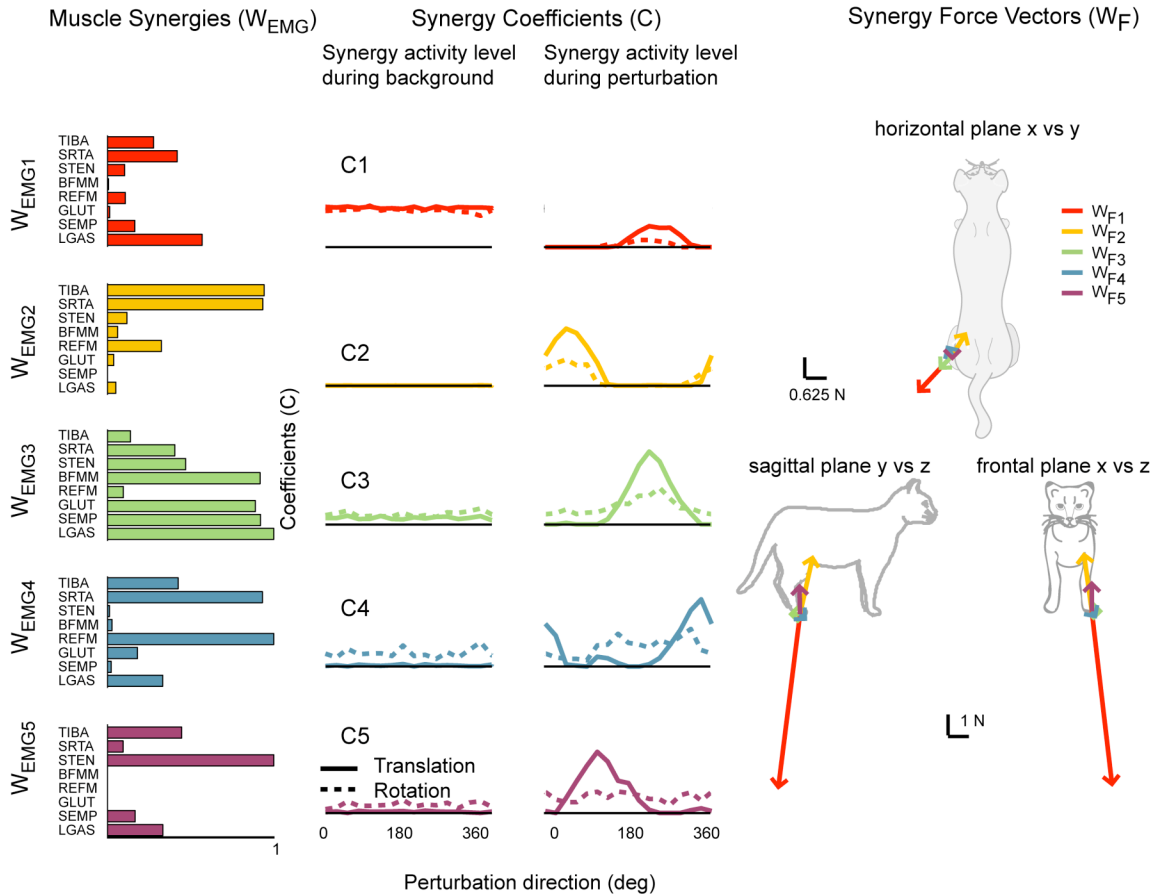


Figure 4.8 Translation synergies applied to platform rotation data. Left panel: synergy vectors, W , extracted from translation data of cat W_0 . Center panel: activation coefficients, C , of each synergy for background activity during quiet stance and for the response to translation (solid lines) and rotation (dashed lines). Right panel: synergy force vectors associated with each of the 5 muscle synergies, drawn in 3 planes.

The activity level of synergies W_2 , W_4 and W_5 which were dominated by biarticular muscles with a flexion moment arm at the hip or knee such as sartorius, semitendinosus and rectus femoris, were effectively lower in rotations, consistent with the fact that many flexor muscle are not activated in response to rotations (Ting and Macpherson 2004). The direction of peak activation in W_3 was similar to translation, but the tuning curves for rotation were wider and flatter, and overall lower in amplitude. Finally, there was higher background activity in W_4 , and W_5 compared to translation, suggesting that cats had a slightly different strategy for standing on the rotating platform.

The total mean VAF across all 3 cats was $>98.9 \pm 0.07\%$ and $>86.6 \pm 7.29\%$ for translations and rotations, respectively. The muscle synergies extracted from the translation data accounted well for most of the EMG tuning curves for rotation, which differed significantly in shape and amplitude from those evoked by translation in the identical muscles (Table 4.4 and Fig. 4.9A). Because some of the muscles had a relatively flat tuning curve where a high level of activation was present for all perturbation directions, r^2 was not always a good measure of the reconstruction fit. The VAF criterion $> 80\%$ provided a better assessment of degree of reconstruction of the original data (e.g. LGAS and TIBA in Fig. 4.9). In all the cats, the EMG tuning curve reconstructions matched the original data with $\text{VAF}\% > 90\%$ in 91% of muscle tuning curves (in all the muscles of Wo). Force tuning curves for rotation were well reconstructed using the synergy force vectors extracted from the control condition, with $r^2 > 0.9$ in 75% of all force tuning curves in all the cats (Table 4.4; $r^2 > 0.88$ for all force tuning curves of Wo) (Fig. 4.9B).

Table 4.4. r^2 or VAF% values of EMG and force tuning curve reconstructions in translation-rotation group

Summary of EMG reconstruction						
Cat	VAF% Translation			VAF% Rotation		
	min	max	avg	min	max	avg
Kn	95.6	99.8	98.7	87.6	99.9	95.8
Wo	96.7	99.5	98.7	90.3	99.2	95.6
An	93.7	99.8	98.6	84.3	99.9	96.7
Summary of Force reconstruction						
Cat	r^2 Translation			r^2 Rotation		
	min	max	avg	min	max	avg
Kn	0.94	1.00	0.97	0.73	0.99	0.89
Wo	0.95	0.98	0.97	0.88	0.99	0.96
An	0.73	0.97	0.92	0.73	0.92	0.84

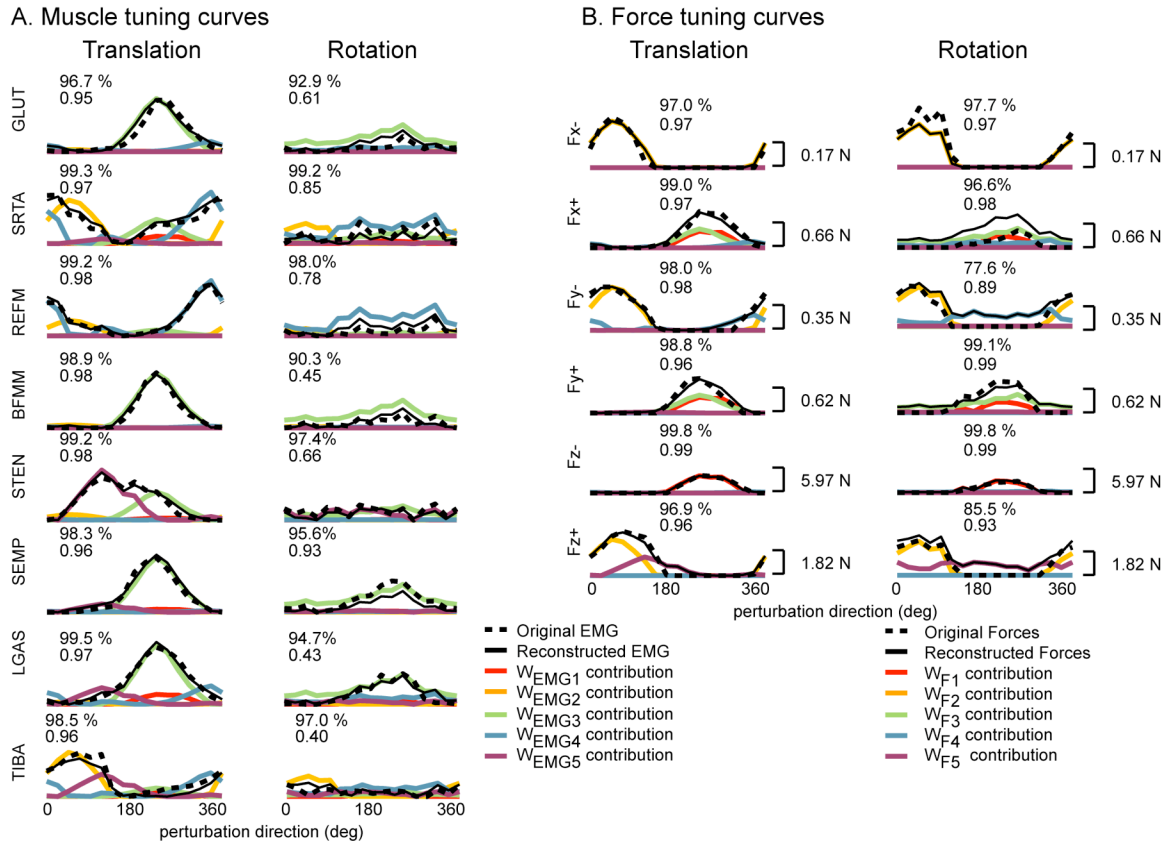


Figure 4.9 Muscle (A) and force (B) tuning curves of the automatic postural response to translations (left column) and rotations (right column). Details as in Figure 7. Force tuning curves are expressed in the Earth reference frame because cats stood at their preferred stance distance during both types of perturbation.

4.3.5 Muscle synergies and synergy force vectors are similar across cats

In all cats, the same number (5) of functional muscle synergies could reproduce the postural responses during all experimental conditions, and synergy composition, recruitment, and output was similar across cats (Fig. 4.10). Some differences in muscle synergy vectors and their activation coefficients across cats were found; nevertheless, all cats seem to follow the same postural control and biomechanical simplification strategy.

In the stance distance group, the muscle synergy vectors were similar across cats (Fig. 4.10A; $r^2 > 0.6$) except for W_{EMG3} , which had low correlation across cats, and W_{EMG1} of N_i , which had a low correlation when compared to the corresponding synergy of B_i ($r^2=0.47$). Nevertheless, the corresponding muscle synergies were activated for the

same range of perturbation directions ($r^2 > 0.83$), except for C_5 of Ni, which was slightly phase-shifted relative to the other two cats (correlations $0.48 < r^2 < 0.54$). The synergy force vectors of Bi had similar directions to the corresponding synergy force vectors of the other two cats ($r^2 > 0.74$) except for W_{F3} , when compared to Ru, and W_{F5} , when compared to Ni (Fig. 4.10A). Ru's synergy force vectors were similar to the corresponding synergy force vectors of the other cats except for W_{F3} ($r^2 < 0.48$), and both W_{F5} and W_{F4} when compared to the corresponding W_F 's of Ni ($r^2 < 0.52$). In all the cats, the end-point forces specified by each synergy were consistent across stance distance when rotated to the F-frame coordinate system.

Likewise in the translation-rotation group (Fig. 4.10B), all 5 muscle synergy vectors were similar across cats (Fig. 4.10A; $r^2 > 0.67$) except for W_{EMG3} , which had low correlation across cats, and W_{EMG1} of Kn, which had a low correlation when compared to the corresponding synergy of the other two cats. In all cats, the comparable muscle synergies were activated for the same range of perturbation directions ($r^2 > 0.6$) with the exception of the tuning coefficient C_5 ($r^2 < 0.58$) of An when compared to the corresponding coefficients of the other two cats. The synergy force vectors were very similar for two cats, An and Wo ($r^2 > 0.92$) with the exception of W_{F4} and W_{F5} ($r^2 < 0.58$). Kn's synergy force vectors differed somewhat from those of the other two cats ($r^2 < 0.34$), except for W_{F1} ($r^2 > 0.99$) and W_{F2} ($r^2 > 0.99$).

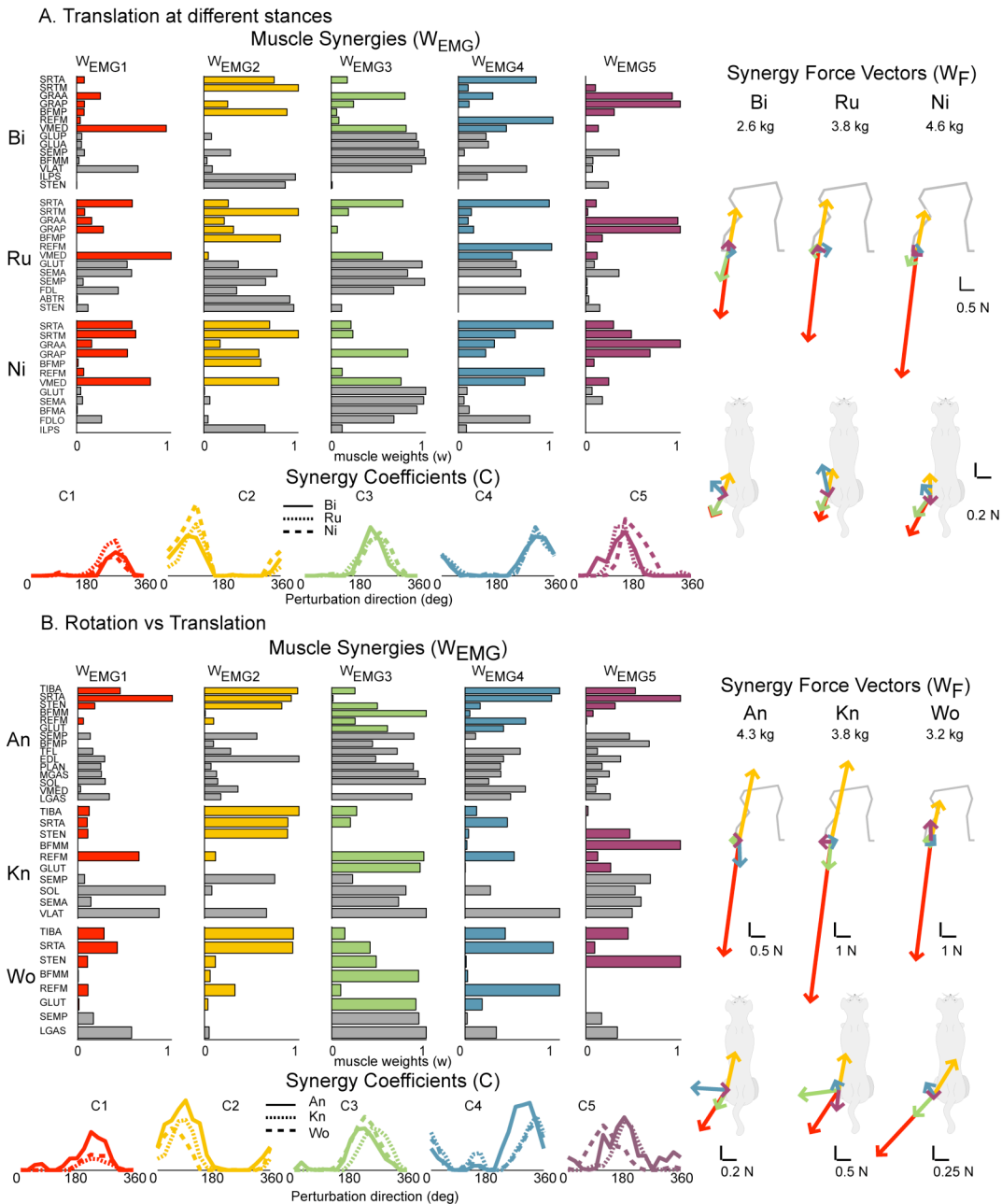


Figure 10 Functional muscle synergies, synergy activation coefficients, and synergy force vectors across subjects. In all cats, 5 synergies accounted for >96% of the variability in response to translation at the preferred stance. The directional tuning of muscle synergy coefficients is similar across the 6 cats ($r^2 > 0.6$ except for C_5 of cat Ni and An). Muscle synergies are similar across cats ($r^2 > 0.6$) except for W_{EMG3} of the 6 cats and W_{EMG1} of cat Ni and cat Kn ($r^2 < 0.47$). The direction of three synergy force vectors, W_{F1} (red), W_{F2} (yellow), and W_{F4} (blue) is similar across cats ($r^2 > 0.74$) with the exception of W_{F4} of cat Ru and Kn (when compared to Ni). W_{F3} (green) and W_{F5} (purple) are only similar in some cases. Only those muscles recorded in common (indicated by colored bars) were used for calculating r^2 in the comparison of muscle synergies across cats. Gray bars indicate the remainder of muscles recorded in each subject.

4.4 Discussion

Our results show first, that muscle synergy structure is robust across a variety of postural tasks and second, postural synergies generalize across subjects. Thus, we conclude that muscle synergies and their related force vectors reflect a global control mechanism rather than an arbitrary outcome of the analysis technique. We will first discuss the validity of our methods, followed by the physiological significance in terms of a general scheme for the neural control of balance.

4.4.1 Methodological Considerations

We believe that the basic characteristics of our five functional muscle synergies would emerge independent of the method of factorization or data analysis. Recent studies have demonstrated that many different factorization algorithms such as factor analysis (FA), independent components analysis (ICA), and NMF all produce similar results in terms of dimensional reduction and basic muscle synergy structure (Ivanenko et al. 2005; Tresch et al. 2006)

The number and characteristics of the functional synergies revealed in our NMF analysis was determined by the EMG patterns and not the force data, lending confidence to the conclusion that these synergies represent a basic organizational principle of neural control. Co-extraction of force with EMG was driven by our primary interest in identifying the set of force synergy vectors that is most closely related to the muscle synergies, with the underlying assumption that muscle synergies reflect the output structure of the neural control system and produce task-related biomechanical effects (forces at the ground). Five synergies were required to reconstruct the data, whether EMG data were tested alone or in combination with the forces while inclusion of forces in the dataset had little effect on muscle synergy composition.

While EMG data is inherently positive and reflects the unidirectional nature of force generation by a muscle, GRF components may have positive and negative values.

The challenge was to represent the force responses in a way that is physiologically relevant. We chose to separate the force APRs into 6 components comprised of the absolute value of positive and negative change from background, consistent with our previously published synergy studies (Jacobs and Macpherson 1996; Macpherson 1988a; b; Ting and Macpherson 2005). This approach obeys the non-negative constraint of the NMF technique and resulted in physiologically meaningful synergy force vectors. For example, our previous studies showed that the limb unloading during translation is mediated by active flexion. By partitioning the forces into positive and negative changes, the activity of the flexor synergy can be represented as a flexor force at the endpoint of the limb. Moreover, our results distinguish this flexor activation from the decrease in the extensor activity producing antigravity support, which has a different synergy tuning curve that is not merely the inverse of the flexor one.

In theory, many different sets of force vectors could be found to adequately reconstruct the force space, but it would be difficult to determine the physiological significance of any particular force set in terms of neural output. We encountered this issue in our previous study in which force data were analyzed independent from EMG (Ting and Macpherson 2005). Some of the resultant force vectors did not correlate well with muscle synergy activation, leading us to speculate that such forces arose from other sources such as forces generated by a different limb.

It is possible that the reconstruction of the forces using NMF is not unique and a different set of synergy force vectors might be found with a different algorithm. However, muscle synergy characteristics were not affected by presence or absence of forces in the NMF analysis and we obtain a consistent set of force vectors from the analysis. These results demonstrate that the set of force vectors that was extracted can reproduce the variations in the force data when the vector amplitudes are modulated exactly as the muscle synergies. Therefore, we believe that the extracted forces reflect a plausible biomechanical function of each synergy.

A shortcoming of segmenting the forces is the possibility of under-estimating the VAF in reconstruction of the net force. For example, during translation at 180° in long stance, the total F_x was close to zero (Fig. 4.7C). At this direction, synergies W_3 and W_5 were co-active such that W_3 (green trace) produced a small F_{x+} and W_5 (purple trace) produced a small F_{x-} . The summed effect was the correct net F_x of zero, but both F_{x+} and F_{x-} were overestimated, leading to a reduced VAF for both components. Fortunately, these effects were minimal in our data set, but would need to be addressed for a data set containing more co-activation of muscle synergies. We did not find any muscle synergies that represented only co-contraction and that would have produced no net force, although antagonistic muscle activity was represented in each of the muscle synergies. Thus, co-contraction independent of force production was not found.

We acknowledge that combining changes in force with total EMG in the APR portion of the dataset may introduce some small uncertainty in the parsing of EMG and force contributions between the quiet stance synergy (W_1) and the extensor synergy (W_3). However, by analyzing the total EMG during the background and during the postural response, we demonstrated that the response to translations includes not only the activation of various synergies, but also the shutting down of the quiet stance synergy, W_1 ; this would not have emerged if we had analyzed the change in EMG. Therefore, the errors that may have been introduced to accommodate the algorithm were minimal and far outweighed the physiological interpretations we gained from using NMF. Nonlinearities in the negative and positive changes in force and EMG are inherent in the musculoskeletal physiology and without a mechanistic model of EMG to force generation, may be difficult to handle mathematically, whatever algorithm is used.

4.4.2 Functional significance of muscle synergies

Our data show that 5 synergies are sufficient to account for a wide variety of EMG and force patterns associated with changing task demands, in this case due to

changes in limb configuration or to changes in perturbation type. Variation in EMG and force was accomplished by modifying either the activation levels of synergies (altered stance distance) or the shape of their tuning curves (changing perturbation type). Some tasks may not require the full set of synergies (e.g., rotation used 4 synergies). Similarly, it has been shown that new synergies can arise when postural task mechanics change in humans (Krishnamoorthy et al. 2004), or in different types of locomotor tasks in frogs (d'Avella and Bizzi 2005).

By including the background muscle activity in our analysis, we were able to identify two muscle synergies that were associated with similar extensor force vectors yet had different roles for balance control and could represent differences in muscle synergy composition at the motor unit level. Our analysis revealed an explicit representation of an extensor synergy (W_1) which not only assumes the primary role for antigravity weight support during quiet stance but also drops out during the dynamic postural response, even when the limb is loaded. The second extensor synergy (W_3) recruits several muscles in common with W_1 and generates a similar force, but it is recruited during the postural response and not during quiet stance. It is possible that the two extensor synergies activate different sets of motor units within a given muscle with slow twitch units for quiet standing, and faster twitch units for the rapid response to perturbation. Analysis at the single motor unit level is required to test this idea. Nevertheless, the separation of weight support and of the dynamic response to perturbation into two separate synergies suggests some level of independence in the neural control of these two functions, as previously suggested from our study of postural responses in the spinally-transected cat (Macpherson and Fung 1999).

There was evidence of nonlinear recruitment of individual muscles within a synergy as a function of stance distance. This was evident in biarticular thigh muscles where the correct spatial pattern but an incorrect magnitude was predicted. For example, BFMM was activated more than predicted for long stance and less than predicted for

short stance. One explanation concerns the change in muscle length with change in limb orientation that accompanies variations in stance distance. Some muscles, particularly those crossing more than one joint, may be significantly shortened or lengthened at the extremes of stance distance, such that the relationship between EMG and force is no longer within the linear range assumed by our analysis method. Another explanation is that under certain conditions, the relationship between the descending command to a muscle synergy and the magnitude of change in EMG could differ for various specific muscles within the synergy. This could occur due to the additional influence of position-dependent sensory feedback altering the excitability of individual muscles at different stance distances. For example, static joint angle changes can alter H-reflex and stretch reflex gains in humans (Knikou and Rymer 2003; Knikou and Rymer 2002; Stein and Kearney 1995), and muscle activation amplitude in response to direct spinal cord stimulation in the cat (Lemay and Grill 2004).

4.4.3 Functional consequences of limb-referenced synergy force vectors

Our previous studies of the postural response to translation described variations in the force constraint strategy with stance distance (Macpherson 1994) which we believe can now be explained in terms of functional muscle synergies and their relationship to limb-referenced force vectors. The force constraint strategy (Macpherson 1988a) refers to the forces produced by a single limb during multi-directional postural perturbations, which are constrained to act along a diagonal axis directed roughly towards and away from the CoM. At long stance distances, this alignment is augmented, and at short stance distances, the force directions are more evenly distributed (Macpherson 1994). It has not been clear whether the source of this constraint is neural or mechanical. The use of a force directed towards the CoM appears to be advantageous for coordinating forces across many limbs, in order to provide stability and minimize torques at individual joints, as well as those that rotate the body (Full et al. 1991). Therefore, at the preferred stance

distance, the most useful muscle synergies would be those directed roughly along this stabilizing axis. However, because the same muscle synergies are used at all postures, the contributions of the synergy forces in the horizontal plane change as the limb rotates. At long stance distances, 4 of 5 synergy force vectors are aligned along the diagonal axis in the Earth-based horizontal plane (Fig. 4.7B), leaving few options for generating forces in other directions. At short stance distances, the synergy forces rotate away from the diagonal axis and have projections in many directions, which can account for the relaxation of the force constraint. Therefore, the change in the force constraint strategy with stance distance is an emergent property which arises naturally from a neural strategy of using the same functional muscle synergies at all stance distances. The endpoint force generated depends on the production of synergy forces that are consistent within the limb reference frame, but are used to stabilize the CoM in the extrinsic reference frame.

Expressing the synergy force vectors in limb axis coordinates also explains the decrease of EMG activity in many muscles as well as the decrease in synergy coefficients, C , with increase in stance distance. The longer the stance distance, the larger are the horizontal plane force components of the synergy force vectors along the antero-medial to postero-lateral axis (primarily W_1 , W_3 and W_5). Thus, correspondingly less activation of these functional muscle synergies is required to generate the same horizontal force magnitude in the limb for long compared to short stance distances. Furthermore, at short stance distances, W_3 (green) and W_5 (purple), which contain many of the posterior thigh muscles, must be activated to achieve a net force in the posterior and downward direction. However, the component of these synergy forces in the posterior direction is quite small; therefore a relatively higher activation level is required, to generate an adequate horizontal force. Similarly, in human postural responses, muscle activity is reduced when stance width is increased (Henry et al. 2001).

4.4.4 How are synergies encoded in the nervous system?

The robustness of the set of 5 synergies suggests that this output organization does not arise from reflex pathways, nor from biomechanically imposed constraints. The various types of postural perturbations examined in the current study evoked widely differing sensory input signals, even when the disturbance propelled the body center of mass in the same direction. A good example is rotation and translation which evoked similar EMG_{APR} 's, yet caused widely different patterns of sensory inputs in muscle spindles, Golgi tendon organs, and vestibular organs due to the opposite mechanical effects on muscle length, joint angle change, and head acceleration (Nashner 1976; Ting and Macpherson 2004). The commonality between rotation and translation perturbations that elicit similar postural responses is the center-of-mass kinematics with respect to the feet, which is probably represented in the nervous system as a derived variable based on multisensory integration of cutaneous and other inputs from many body regions (Ting and Macpherson 2004). Thus it is unlikely that functional muscle synergies are simply a reflexive response due to a particular set of sensory inputs, but rather that they represent a central mechanism for coordination of motor outputs.

Muscle synergies provide a modular control mechanism whereby higher neural control centers need only specify the desired task-level function such as force at the ground, and not the detailed coordination of muscles across multiple joints. This scheme could include the activation of spinal synergies through simple higher-level commands, as has been suggested from locomotor studies (Hart and Giszter 2004; Saltiel et al. 2005; Saltiel et al. 2001). More generally, one might predict the existence of neuronal networks or populations that specify the synergy activation patterns (C), and whose outputs are distributed (perhaps multisynaptically) to the motoneurons of muscles within the synergy. The consistency of synergy activation and force vectors across individuals suggests that a neural organization encoding low dimensional variables is a basic component of the motor control system. However, the variation in muscle synergy composition (W_{EMG})

across subjects suggests a flexibility of expression within the set of equivalent solutions present in a redundant musculoskeletal system. Because each individual has a stable muscle synergy composition across postural condition and days, the particular composition of muscle synergies may be tuned to the body morphology and mechanics of each individual but modifiable through learning and experience.

In the context of postural control, muscle synergies are likely to be coordinated in supraspinal structures such as brainstem or cerebellum, because of the need to integrate multimodal sensory inputs from somatosensory, visual, and vestibular sources. Postural responses to translation are notably absent in the hindlimbs of cats with spinal cord transection at the T6 level (Macpherson and Fung 1999), yet weight support for quiet standing can still be achieved (Edgerton et al. 2001; Macpherson and Fung 1999). Perhaps the extensor synergy (W_1), or some vestige of it, can be accessed in the isolated spinal cord, whereas the other synergies require connectivity to higher centers. The horizontal plane force components of the extensor synergy for quiet stance may account for the ability of the spinal cat to withstand small perturbations, by virtue of the stiffness of the activated muscles and the resultant force vector along the diagonal axis. Therefore, muscle synergies encoded in the spinal cord (Giszter et al. 1993; Lemay and Grill 2004; Saltiel et al. 2001) may not play a role in directional balance control. Reticulospinal neurons branch to innervate many different spinal levels and could send synergy commands to many muscles spanning multiple joints (Matsuyama et al. 2004). Or, synergies may be accessed from a variety of neuronal networks, which could account for differences in their modulation and changes with neurological impairments. Evidence from stroke and spinal cord patients during locomotion also suggest that higher centers may be necessary for appropriate synergies to arise (Bourbonnais et al. 1989; Brown et al. 1997; Ivanenko et al. 2003).

The organization of motor outputs according to task-level variables provides a parsimonious symmetry with the integration of sensory inputs in the nervous system. In a

feedback control loop, the sensory information would first be transformed into task-level variables, for example center of mass displacement and velocity, which would then cause a functional muscle synergy to be activated. Such an organization is consistent with the fact that structures throughout the nervous system appear to integrate both sensory inputs (Bosco and Poppele 1997; Poppele et al. 2002), and motor commands (Georgopoulos et al. 1992; Georgopoulos et al. 1986) to reflect task-level variables. Specifically, limb axis orientation is encoded by ascending neurons in the dorsospinal-cerebellar tract (DSCT) and is therefore a readily available derived variable (Bosco and Poppele 1997; Bosco et al. 1996) that has been hypothesized to be an important task-level variable for the neural control of stance in the cat (Lacquaniti and Maioli 1994). Such information would be necessary to activate functional muscle synergies that are encoded in a limb-axis reference frame.

In conclusion, we identified a set of 5 functional muscle synergies that was robust across a range of dynamic postural tasks as well as quiet stance, and generalized across subjects. This finding suggests that a synergy organization forms part of the neural control structure for the motor system. This type of neural mechanism effectively reduces the musculoskeletal redundancy inherent in the multisegmented limb and allows for rapid activation of functionally appropriate responses for automatic postural adjustments. It is likely that such a control structure underlies other types of automatic as well as voluntary movements. Similar sharing of motor output units has been demonstrated in rhythmic tasks such as paw shake and locomotion (Baev et al. 1991; Carter and Smith 1986a; b; Stein 2005). The identification of functional muscle synergies may provide a means for understanding the task-level variables that are used by the nervous system to encode sensory inputs as well as motor outputs (d'Avella and Bizzi 2005; Poggio and Bizzi 2004).

CHAPTER 5

DISCUSSION

5.1 Conclusions

5.1.1 Functional muscle synergies simplify motor control

We conclude muscle synergies represent a simplifying mechanism for muscle coordination not only because it is a strategy for reducing the number of actuators to be controlled, but because it represents a mechanism for controlling task-level variables. Our results demonstrate the low dimensional muscle coordination during standing postural control. Since the flexible modulation of low dimensional muscle synergies is sufficient for reproducing spatial, temporal and inter-trial variations in individual muscle activations in response to support surface motions under different biomechanical contexts. Furthermore, these *preferred* modules of motor output, called muscle synergies, are associated with a biomechanical function in the cat and possibly in the human. Therefore, muscle synergies represent a mechanism that facilitates a hierarchical scheme for motor control because the nervous system can control task-level variables through the simple modulation of low dimensional neural commands activating muscle synergies.

Muscle synergies may represent a simplifying mechanism for higher centers to directly influence the strategy for the motor task. Our results demonstrate the inherent muscle noise when producing a task is not random but coordinated in muscle synergy patterns. Thus, inter-trial variations in muscle synergy activations reflect inter-trial variations in the selection of a postural strategy. Therefore muscle synergies appear to be combined in different proportions in order to implement the strategy needed according to the context of the task such as mental state of the subject, sensory cues, or prior experience.

Finally, muscle synergies appear to simplify the sensorimotor transformation required to perform the motor task. We demonstrated functional muscle synergies produce same biomechanical output in the body reference frame –regardless of body biomechanical context. Therefore, the activation of functional muscle synergies would reduce the computation required by the nervous system for implementing the mechanical strategies needed for achieving the task at hand. Since a single transformation from intrinsic to extrinsic reference frame would be required to generate the stabilizing forces needed for the postural task. In other words, muscle synergies might be a mechanism for reducing the transformations that the nervous system needs to perform to convert muscle activations into joint torques, and subsequent end-point forces and body motion.

5.1.2 Sensorimotor transformations for postural control

Although our results indicate the flexible activation of muscle synergies reproduce the large variability in muscle activation patterns during different postural tasks, it remains to be determined the sensorimotor transformations required for producing the adequate postural responses to the different contexts of the task. Several studies have proposed that the nervous system utilizes internal models, possibly stored in the cerebellum, to perform these sensorimotor transformations (Kawato 1999; Wolpert et al. 1998). Following the “reafference principle”, the difference between the afferents information and the anticipated afferent signals (“efference copy”) predicted by the internal model are used as an error signal to modify the efferent commands for performing the movement (von Holst and Mittelstaedt 1950).

Characteristics of postural response cannot be attributed to cues from a single sensory input but to the integration of multiple sensory signals, suggesting similar dimensional reductions in sensors and actuators occur in the sensorimotor transformation process. Several studies have shown that postural responses cannot be predicted by the correlations to a particular sensory signal (Allum et al. 1998; Allum and Carpenter 2005;

Carpenter et al. 1999; Inglis and Macpherson 1995; Keshner et al. 1988; Runge et al. 1998; Ting and Macpherson 2004). However, postural responses are modulated as a function of the CoM displacement, suggesting multiple sensory signals are integrated to provide information about the CoM kinematics, which is the controlled task-level variable in posture. Similar reduction in sensory signals is observed in visual systems (Poggio and Bizzi 2004). Therefore, same neurophysiological principles might underlie afferents and efferent signals.

5.1.3 What factors determine the characteristics of *preferred* muscle activation patterns specified by muscle synergies?

Muscle synergies might actually be encoded at the motor-unit, rather than muscle, level. Descending input can simultaneously activate motor pools of different muscles throughout the body (Björklund and Skagerbæg 1982). Additionally, motor-units are orderly recruited following the size principle even across different muscles (Cope and Sokoloff 1999a; b; De Luca and Erim 2002; Sokoloff et al. 1999). Thus, this self-organizing principle at the motor unit level might facilitate the coordination of multiple muscles to produce appropriate smooth muscle forces. Moreover, anatomically defined muscles are compartmentalized since motor-units forming a single muscle can be assembled into distinct tasks groups recruited differently depending on their functions (Chanaud et al. 1991a; b). This muscle compartmentalization might constitute the biological basis for muscles that belonged to more than one muscle synergy in our studies.

Afferent pathways might play an important role in the muscle activation patterns represented by each muscle synergy. Several studies have demonstrated force and length feedback pathways facilitate the coordination of multiple muscles across the body (Nichols 1994; 1989; Nichols et al. 1999). Additionally, recent studies have demonstrated afferent information regulates descending neuromodulatory drive diffused

to motor pools of multiple muscles throughout the body (Hyngstrom et al. 2007). Our results show changes in relative gains of one muscle within a synergy occur with drastic changes in joint angles. Therefore, the muscles and their relative gains forming the muscle synergy structure might be influenced by afferent information. Further studies need to be performed to determine the effect of specific sensory pathways on both, muscle synergy composition and recruitment of multiple muscle synergies.

It remains unclear whether the consistency in muscle activation patterns represented by muscle synergies is attributable to biomechanical and/or neural constraints. Results from Chapter 3 and 4 indicate that a single set of muscle synergies can reproduce postural responses in different biomechanical contexts, including responses in one-legged and crouched stance when the biomechanics of the legs are very different. This consistency in motor output patterns constructing the postural responses can be attributed to the musculoskeletal structure of the body. For example, it has been demonstrated that the biomechanics of the hand constrains the variability in muscle activation patterns generating submaximal end-point finger force (Valero-Cuevas 2000). Alternatively, muscle synergies might be hardwired neural structures encoded in the nervous system, as demonstrated by the task-independent synchronous activation of muscles elicited from focal stimulation of sites within the spinal cord of frogs (Seltiel et al. 2001).

5.1.4 Development of muscle synergies

Muscle synergies represent a simplification strategy for muscle coordination robustly used across species. Previous studies have demonstrated common sensorimotor principles for postural control across species, specifically between cats and humans, despite differences in stance configuration and biomechanics (Dunbar et al. 1986; Horak and Macpherson 1996). We present further evidence of common sensorimotor principles since muscle synergies for postural control were identified in both species and muscle

synergies used during background activity in cats and humans standing in the crouched condition were similar.

Individual features of each subject might influence the *preferred* muscle activation patterns represented by muscle synergies. In all our subjects a consistent set of muscle synergies were used for a variety of postural tasks. However, subject-specific differences were observed in terms of the muscle composition and recruitment of each synergy. These inter-subject differences might be associated with subject's neuromuscular system. For example, it has been proposed that a rule for muscle coordination may be to minimize the energy required to perform the task (Dul et al. 1984a; Dul et al. 1984b). Therefore, muscle synergy composition and their activations might be optimized based on the neuromuscular features and motor skill of each subject.

The development of muscle synergies is not well understood. Recent studies have proposed the existence of a slow and a fast motor learning rate. We believe that the slow motor learning would induce changes in composition of muscle synergies or the generation of new muscle synergies; whereas the fast motor learning would generate changes in the contributions of each muscle synergy to the new motor task. Our studies indicate preliminary evidence for this hypothesis since we observed that subjects consistently used muscle synergies from the normal stance, or overtrained condition, in all other postural tasks including those with very distinct biomechanical features such as standing in a crouched posture. The only parameter that varied when standing in the less frequently experience conditions was the activation of muscle synergies, meaning a fast adaptation to the new postural task was performed by modulating existing muscle synergies. However in the one-leg stance conditions a new and different muscle synergy was observed in the one-leg stance conditions. This muscle synergy has presumably been developed with subjects' experience standing on one leg.

5.2 Study limitations

5.2.1 A two-dimensional paradigm

Experimental and theoretical studies have shown that biomechanical constraints, such as requiring both feet are in contact with a support surface during balance maintenance, limit the choice of joint coordination choices available to the nervous system (Kuo 1995). Moreover, the muscle synergy hypothesis has been questioned because the co-activation patterns across muscles observed during motor tasks have been attributed to the restricted body motion in experimental environments (Buchanan et al. 1989). Therefore, although we designed our experiments to induce as much variation as possible, the variability in muscle activation patterns may have been limited by the characteristics of the studied task. Recent studies have shown the existence of muscle synergies in reaching movements in a 3-D space (d'Avella et al. 2006) and in natural frog behaviors (d'Avella and Bizzi 2005), but it remains to be determined whether the muscle synergy organization described here is robust in more dynamical motor behaviors such as postural responses during walking or 3-D postural tasks (leg drop). Particularly, it would be very interesting to determine whether muscle synergies change in a dynamic context since it has been shown that postural responses are tuned to the phase of step cycle when the balance perturbation occurs (Nashner 1980). A few studies have identified similarities in individual muscle responses evoked in the stance leg during standing and walking (Misiaszek 2003; Misiaszek et al. 2000). Therefore it is possible that the modulation of muscle synergies used for postural control during static conditions might account for the postural responses evoked during walking.

5.2.2 Robustness of muscle synergies over time

The studied burst of activity in response to balance perturbations (APR) is an involuntary, stereotypical response (Horak and Macpherson 1996). The postural

response after APR is more variable. Thus, variability in the entire time course of the postural response provides a reasonable test of robustness of the synergy concept. Although we observed consistency in muscle synergy organization over the initial 325ms of the human postural response, it remains to be determined whether the muscle synergies used to reproduce the postural responses during the APR can reproduce the entire time course of the postural response. In other words, we have yet to see whether muscle synergies are consistent over time. Based on preliminary postural control studies in cats we expect that muscle synergies used for the APR are robust across the entire course of the postural response (cf. Appendix A).

5.2.3 Methodological improvements

To date, there is no standard method to determine the number of muscle synergies that would best characterize the data (Tresch et al. 2006). We implemented local and global criteria to determine this parameter as accurately as possible but our criteria were subject to thresholds that could lead to overestimation or underestimation of the number of synergies. Since further analysis such as muscle synergy classification or comparison of muscle synergies across subjects is sensitive to this parameter, different methods should be implemented to determine in a more systematic way the number of muscle synergies that characterize the data in each subject. Once this is resolved, statistical tests on muscle synergy composition and muscle synergy activations could be performed to determine the effect of training or injury, for example.

5.3 Future directions

5.3.1 Functions of muscle synergies

In Chapter 2 and 3 we identified human muscle synergies robustly used to recover balance for specific range of perturbation directions. Based on the muscle synergy composition and its spatiotemporal activations, we concluded every synergy had the

function of generating the joint torques required to displace the CoM to a particular position. However, it remains to determine explicitly the functionality of muscle synergies identified here through biomechanical models or inverse dynamics experimental studies.

5.3.2 Muscle synergies reflect biomechanical or neural constraints?

Studies of amputees with dramatically altered whole-body biomechanics could help us determine whether muscle synergies are attributable to biomechanical constraints. If muscle synergies are purely due to biomechanics we would expect that muscle synergies from controls and amputees in the healthy leg would be the same since musculoskeletal biomechanics are maintained in the intact limb, even if the biomechanical context of the body has changed and they have adapted to the new condition.

On the other hand, bilateral muscle synergies during one-leg stance perturbations could help us determine whether muscle synergies are hardwired neural structures. Dietz and Berger (1989) showed unilateral limb perturbations evoked EMG responses in the same muscle of both legs when the balance perturbation was received unilaterally, suggesting the activation of inter-limb muscle synergies. However, in this study, subjects were standing on both legs; therefore although perturbations were unilateral, both legs received somatosensory information. Thus, further studies are required to determine whether muscle synergies are activated bilaterally when one leg is not in contact with the ground.

5.3.3 Optimality of muscle synergies

Recent studies have proposed muscle synergies represent optimal solutions for performing a motor task such that the nervous system minimizes total muscle activation (Chhabra and Jacobs 2006; Kurtzer et al. 2006; Scott 2004; Todorov and Ghahramani

2004). However, we observed generality in the activation of muscle synergies even during postural tasks with very distinct biomechanical characteristics. Therefore, our results raise the question whether the observed *preferred* muscle activation patterns are optimal for maintaining balance in all postures. The optimality hypothesis underlying muscle synergies remains to be tested. To test this hypothesis we need to investigate whether variations in context of the motor task would induce changes in muscle synergies over time in order to minimize a cost function such as energy expenditure. In other words, it remains to be determined whether muscle synergies are formed following homeostasis principles.

5.3.4 Changes in muscle synergies with motor learning

We hypothesize long term changes in muscle synergies would be indicated by changes in muscle activation patterns represented by each muscle synergy; whereas short term changes in muscle synergies would be indicated by changes in the activation of each muscle synergy. Possible experiments to test this hypothesis would be to determine whether athletes that have developed specialized motor skills have different muscle synergies while performing a motor task than control subjects or whether patients that have undergone traumatic biomechanical injuries, such as amputees, also developed different muscle synergies than control subjects.

5.3.5 Clinical applications

Understanding the effect of biomechanical context in postural responses might give us insight into why patients adopt postures different from healthy subjects to achieve balance control. For example, stance biomechanics similarly affect postural responses in healthy and CP patients and muscle synergy composition seems to be independent of biomechanics in normal subjects. Thus, it is tempting to think that muscle synergy organization in patients with crouched posture would be similar to those in patients with

normal posture. However, in the case of CP children the neurological disorder induces the biomechanical changes in posture. Therefore we cannot conclude that the neural control of posture in CP and typically developed subjects is similar since CP subjects might lack muscle synergies that allow them to stand upright.

Since it is possible that slow and fast adaptation rates might be reflected by changes in muscle synergy composition and muscle synergy recruitment, respectively, we can speculate that during the initial stage of neurological disease patients with neurological disorders might have muscle synergies similar to those in healthy subjects but with different temporal patterns. We observed in healthy subjects that the temporal changes in postural responses induced by a crouched stance (similar to CP patients natural posture) are reproduced by the same muscle synergies used in normal stance, albeit with altered recruitment timing. However, more permanent changes in muscle synergies may occur with training and in later stages of neurological disease when patients learned to use compensatory mechanisms to perform the motor task.

All our studies were performed in a population of young healthy adults; therefore, it remains to be determined the effect of aging and pathological conditions in muscle synergies. We speculate that the number of muscle synergies accessible to accomplish motor tasks would be reduced with aging and with pathologies. For example, the absence of “ankle” strategy in postural responses in the elderly demonstrates the decreased in strategies that can be used for performing motor behaviors (Horak et al. 1997). However, changes in muscle synergies as a function of pathological features would have to be investigated.

In conclusion, the work presented here constitutes a framework for understanding biomechanical consequences of altered muscle coordination due to pathological disorders or adaptation in typically developed subjects. Our current results represent the ground research for future studies that may serve as a guide to improve rehabilitation techniques.

APPENDIX A

ROBUSTNESS OF MUSCLE SYNERGIES OVER ENTIRE TIME COURSE OF POSTURAL RESPONSES

A.1 Introduction

In both cats and humans, postural responses to support surface translations are characterized by different EMG patterns for each direction of perturbation (Macpherson 1988, Henry et al. 1998). It has been shown that complex EMG patterns of the initial automatic postural response (APR) can be composed of a limited set of muscle synergies (Ting and Macpherson 2002). We investigated whether muscle synergies can characterize the variability in muscle activation for the entire postural response including background, transient, automatic, and voluntary activity. We *hypothesize* that the functional muscle synergies that reproduce the postural responses during the automatic postural response (APR) period, initial stereotypical involuntary response, can reproduce the entire time course of the postural response. To test our hypothesis cat balance was perturbed by multidirectional support surface translations in their natural stance. We extracted muscle synergies from the APR period and use them to reconstruct the entire course of the muscles postural response. Our results show muscle synergies used for the APR are robust across the entire course of the postural response.

A.2 Methods

3 freely standing cats were translated in 12 directions while standing with the paws at 62 to 135.5% of preferred anterior-posterior stance distance. EMG activity in 14 left hindlimb muscles was recorded before, during, and after perturbations. EMGs were binned every 10 ms over a 1 s duration.

Each synergy was represented as a vector of constant positive-valued components indicating the relative activity level of each muscle within that synergy (Tresch et al. 1999). A synergy is thus defined as a group of muscles whose relative activity level is fixed. Synergies are scaled independently by synergy coefficients. Varying synergy coefficients provides the flexibility needed to reconstruct muscle patterns.

The synergies and coefficients that best reconstructed EMG responses over time were computed using a nonnegative matrix factorization algorithm (Lee and Seung 2001). Synergy vectors extracted from EMG at the shortest stance distance were used to reconstruct EMG data at all other stances.

A.3 Results

In all cats, only 5 synergies were required to reproduce > 96% of the muscle activity at the shortest distance (Figure A.1). Therefore, synergy vectors can reconstruct not only the initial APR (EMG activity from 60 to 140 ms after perturbation onset) but also background, early, and late activity, which could have voluntary components. Synergies were very similar to those extracted from the initial APR ($0.6 < r^2 < 0.98$).

Two synergies were dominated by either flexor or extensor muscles, another synergy by adductors, and two synergies by biarticular muscles. Each synergy vector responds to a preferred range of perturbation directions 60 – 300 ms following perturbation onset (Figure A.2). However, only the ‘extensor synergy’ (synergy 1) was active in the background period of 0 to 120 ms. This synergy was also activated during 180 to 360° perturbations and was inhibited during 0 to 180° perturbations, when the ‘flexor synergy’ (synergy 5) was active. Finally, at the end of platform displacement only the extensor synergy was active again.

Moreover, the same 5 synergies reproduced >91% of the muscles EMGs at all stance distances (4 postures x 14 muscles x 12 directions x 100 time bins). The muscle

activity before, during, and after postural perturbations can be accounted for by 5 muscle synergies even at different stance distances.

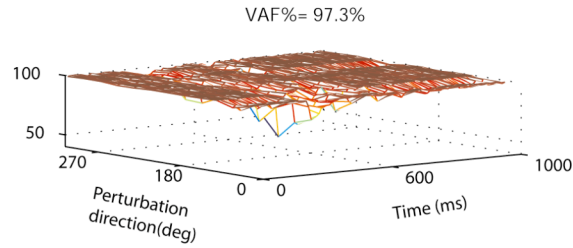


Figure A. 1: Percent EMG variability accounted for by 5 synergies over time and perturbations in cat Ru.

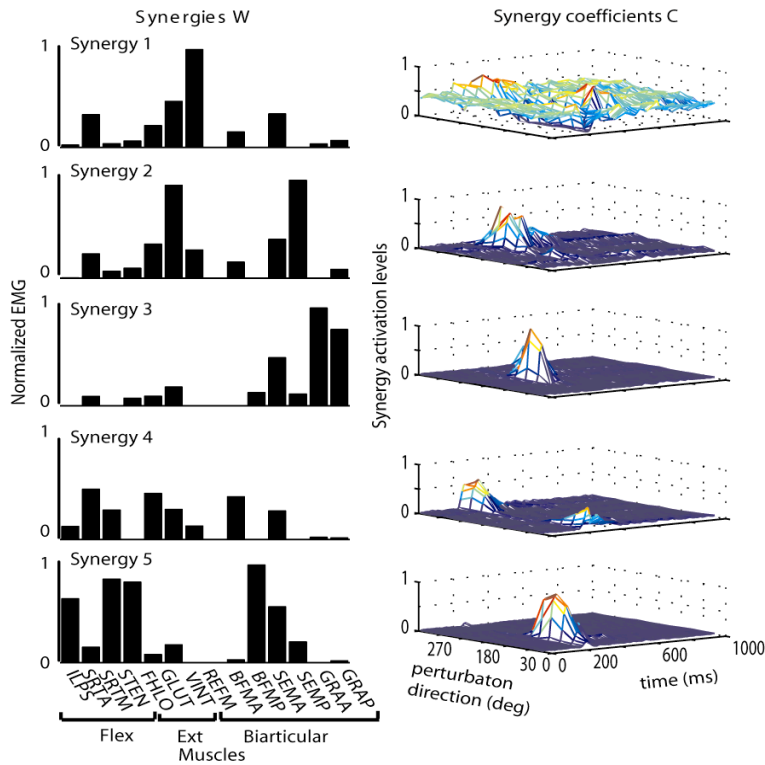


Figure A.2: Muscle synergies and synergy activation levels versus perturbation direction and time.

A. 4 Conclusions

This robustness suggests that synergies can characterize not only the initial automatic postural response, but also EMG patterns during quiet standing, early reflex response, and voluntary behaviors.

REFERENCES

- Alexandrov A, Frolov A, and Massion J.** Axial synergies during human upper trunk bending. *Experimental Brain Research* 118: 210-220, 1998.
- Alexandrov AV, Frolov AA, Horak FB, Carlson-Kuhta P, and Park S.** Feedback equilibrium control during human standing. *Biol Cybern* 1-14, 2005.
- Alexandrov AV, Frolov AA, and Massion J.** Biomechanical analysis of movement strategies in human forward trunk bending. I. Modeling. *Biol Cybern* 84: 425-434, 2001a.
- Alexandrov AV, Frolov AA, and Massion J.** Biomechanical analysis of movement strategies in human forward trunk bending. II. Experimental study. *Biol Cybern* 84: 435-443, 2001b.
- Allum JH, Bloem BR, Carpenter MG, Hulliger M, and Hadders-Algra M.** Proprioceptive control of posture: a review of new concepts. *Gait Posture* 8: 214-242, 1998.
- Allum JH, and Carpenter MG.** A speedy solution for balance and gait analysis: angular velocity measured at the centre of body mass. *Curr Opin Neurol* 18: 15-21, 2005.
- Allum JH, Carpenter MG, and Honegger F.** Directional aspects of balance corrections in man. *IEEE Eng Med Biol Mag* 22: 37-47, 2003.
- Allum JH, Carpenter MG, Honegger F, Adkin AL, and Bloem BR.** Age-dependent variations in the directional sensitivity of balance corrections and compensatory arm movements in man. *J Physiol* 542: 643-663, 2002.
- Baev KV, Esipenko VB, and Shimansky YP.** Afferent Control of Central Pattern Generators - Experimental-Analysis of Locomotion in the Decerebrate Cat. *Neuroscience* 43: 237-247, 1991.
- Bernstein N.** *The Coordination and Regulation of Movements*. New York: Pergamon Press, 1967.

Bosco G, and Poppele RE. Representation of multiple kinematic parameters of the cat hindlimb in spinocerebellar activity. *J Neurophysiol* 78: 1421-1432, 1997.

Bosco G, Rankin A, and Poppele R. Representation of passive hindlimb postures in cat spinocerebellar activity. *J Neurophysiol* 76: 715-726, 1996.

Bourbonnais D, Vandennoven S, Carey KM, and Rymer WZ. Abnormal Spatial Patterns of Elbow Muscle Activation in Hemiparetic Human-Subjects. *Brain* 112: 85-102, 1989.

Brown DA, Kautz SA, and Dairaghi CA. Muscle activity adapts to anti-gravity posture during pedalling in persons with post-stroke hemiplegia. *Brain* 120 (Pt 5): 825-837, 1997.

Buchanan TS, Rovai GP, and Rymer WZ. Strategies for Muscle Activation during Isometric Torque Generation at the Human Elbow. *Journal of Neurophysiology* 62: 1201-1212, 1989.

Burtner PA, Qualls C, and Woollacott MH. Muscle activation characteristics of stance balance control in children with spastic cerebral palsy. *Gait Posture* 8: 163-174, 1998.

Cappellini G, Ivanenko YP, Poppele RE, and Lacquaniti F. Motor patterns in human walking and running. *Journal of Neurophysiology* 95: 3426-3437, 2006.

Carpenter MG, Adkin AL, Brawley LR, and Frank JS. Postural, physiological and psychological reactions to challenging balance: does age make a difference? *Age Ageing* 35: 298-303, 2006.

Carpenter MG, Allum JHJ, and Honnegger F. Directional sensitivity of stretch reflexes and balance corrections for normal subjects in the roll and pitch planes. *Experimental Brain Research* 129: 93-113, 1999.

Carter MC, and Smith JL. Simultaneous Control of 2 Rhythmical Behaviors .1. Locomotion with Paw-Shake Response in Normal Cat. *Journal of Neurophysiology* 56: 171-183, 1986a.

Carter MC, and Smith JL. Simultaneous Control of 2 Rhythmical Behaviors .2. Hindlimb Walking with Paw-Shake Response in Spinal Cat. *Journal of Neurophysiology* 56: 184-195, 1986b.

Cheung VCK, d'Avella A, Tresch MC, and Bizzi E. Central and sensory contributions to the activation and organization of muscle synergies during natural motor behaviors. *J Neurosci* 25: 6419-6434, 2005.

Chhabra M, and Jacobs RA. Properties of synergies arising from a theory of optimal motor behavior. *Neural Comput* 18: 2320-2342, 2006.

Creath R, Kiemel T, Horak F, Peterka R, and Jeka J. A unified view of quiet and perturbed stance: simultaneous co-existing excitable modes. *Neurosci Lett* 377: 75-80, 2005.

d'Avella A, and Bizzi E. Shared and specific muscle synergies in natural motor behaviors. *Proc Natl Acad Sci U S A* 102: 3076-3081, 2005.

d'Avella A, Portone A, Fernandez L, and Lacquaniti F. Control of fast-reaching movements by muscle synergy combinations. *J Neurosci* 26: 7791-7810, 2006.

d'Avella A, Saltiel P, and Bizzi E. Combinations of muscle synergies in the construction of a natural motor behavior. *Nat Neurosci* 6: 300-308, 2003.

Day BL, Steiger MJ, Thompson PD, and Marsden CD. Effect of vision and stance width on human body motion when standing: implications for afferent control of lateral sway. *J Physiol* 469: 479-499, 1993.

Diener HC, Horak FB, and Nashner LM. Influence of stimulus parameters on human postural responses. *J Neurophysiol* 59: 1888-1905, 1988.

Dietz V. Human Neuronal Control of Automatic Functional Movements - Interaction between Central Programs and Afferent Input. *Physiological Reviews* 72: 33-69, 1992.

Dimitrova D, Horak FB, and Nutt JG. Postural muscle responses to multidirectional translations in patients with Parkinson's disease. *J Neurophysiol* 91: 489-501, 2004a.

Dimitrova D, Nutt J, and Horak FB. Abnormal force patterns for multidirectional postural responses in patients with Parkinson's disease. *Exp Brain Res* 156: 183-195, 2004b.

Dunbar DC, Horak FB, Macpherson JM, and Rushmer DS. Neural control of quadrupedal and bipedal stance: implications for the evolution of erect posture. *Am J Phys Anthropol* 69: 93-105, 1986.

Edgerton VR, Leon RD, Harkema SJ, Hodgson JA, London N, Reinkensmeyer DJ, Roy RR, Talmadge RJ, Tillakaratne NJ, Timoszyk W, and Tobin A. Retraining the injured spinal cord. *J Physiol* 533: 15-22, 2001.

Flanders M, and Soechting JF. Arm muscle activation for static forces in three-dimensional space. *J Neurophysiol* 64: 1818-1837, 1990.

Flash T, and Hochner B. Motor primitives in vertebrates and invertebrates. *Curr Opin Neurobiol* 15: 660-666, 2005.

Fonseca ST, Holt KG, Fethers L, and Saltzman E. Dynamic resources used in ambulation by children with spastic hemiplegic cerebral palsy: relationship to kinematics, energetics, and asymmetries. *Phys Ther* 84: 344-354; discussion 355-348, 2004.

Full RJ, Blickhan R, and Ting LH. Leg design in hexapedal runners. *J Exp Biol* 158: 369-390, 1991.

Fung J, and Macpherson JM. Attributes of quiet stance in the chronic spinal cat. *Journal of Neurophysiology* 82: 3056-3065, 1999.

Fung J, and Macpherson JM. Determinants of postural orientation in quadrupedal stance. *J Neurosci* 15: 1121-1131, 1995.

Georgopoulos AP, Ashe J, Smyrnis N, and Taira M. The motor cortex and the coding of force. *Science* 256: 1692-1695, 1992.

Georgopoulos AP, Kalaska JF, Caminiti R, and Massey JT. On the Relations between the Direction of Two-Dimensional Arm Movements and Cell Discharge in Primate Motor Cortex. *Journal of Neuroscience* 2: 1527-1537, 1982.

Georgopoulos AP, Schwartz AB, and Kettner RE. Neuronal population coding of movement direction. *Science* 233: 1416-1419, 1986.

Giszter SF, Mussa-Ivaldi FA, and Bizzi E. Convergent force fields organized in the frog's spinal cord. *J Neurosci* 13: 467-491, 1993.

Graziano M. The Organization of Behavioral Repertoire in Motor Cortex. *Annu Rev Neurosci* 2006.

Gruneberg C, Bloem BR, Honegger F, and Allum JH. The influence of artificially increased hip and trunk stiffness on balance control in man. *Exp Brain Res* 157: 472-485, 2004.

Gruneberg C, Duysens J, Honegger F, and Allum JH. Spatio-temporal separation of roll and pitch balance-correcting commands in humans. *J Neurophysiol* 94: 3143-3158, 2005.

Hart CB, and Giszter SF. Modular Premotor Drives and Unit Bursts as Primitives for Frog Motor Behaviors. *J Neurosci* 24: 5269-5282, 2004.

Henry SM, Fung J, and Horak FB. Effect of stance width on multidirectional postural responses. *J Neurophysiol* 85: 559-570, 2001.

Henry SM, Fung J, and Horak FB. EMG responses to maintain stance during multidirectional surface translations. *Journal of Neurophysiology* 80: 1939-1950, 1998.

Herrmann U, and Flanders M. Directional tuning of single motor units. *J Neurosci* 18: 8402-8416, 1998.

Hogan N, Bizzi E, Mussa-Ivaldi FA, and Flash T. Controlling multijoint motor behavior. *Exerc Sport Sci Rev* 15: 153-190, 1987.

Holdefer RN, and Miller LE. Primary motor cortical neurons encode functional muscle synergies. *Exp Brain Res* 146: 233-243, 2002.

Horak FB. Adaptation of automatic postural responses. In: *The Acquisition of Motor Behavior in Vertebrates*, edited by Bloedel JR, Ebner TJ, and Wise SP. Cambridge: The MIT Press, 1996, p. 57-85.

Horak FB, Dimitrova D, and Nutt JG. Direction-specific postural instability in subjects with Parkinson's disease. *Exp Neurol* 193: 504-521, 2005.

Horak FB, Henry SM, and Shumway-Cook A. Postural perturbations: new insights for treatment of balance disorders. *Phys Ther* 77: 517-533, 1997.

Horak FB, and Macpherson JM. Postural orientation and equilibrium. In: *Handbook of Physiology, Section 12*. New York: American Physiological Society, 1996, p. 255-292.

Horak FB, and Nashner LM. Central programming of postural movements: adaptation to altered support-surface configurations. *J Neurophysiol* 55: 1369-1381, 1986.

Hynstrom AS, Johnson MD, Miller JF, and Heckman CJ. Intrinsic electrical properties of spinal motoneurons vary with joint angle. *Nat Neurosci* 10: 363-369, 2007.

Inglis JT, and Macpherson JM. Bilateral labyrinthectomy in the cat: effects on the postural response to translation. *J Neurophysiol* 73: 1181-1191, 1995.

Ivanenko YP, Cappellini G, Dominici N, Poppele RE, and Lacquaniti F. Coordination of locomotion with voluntary movements in humans. *J Neurosci* 25: 7238-7253, 2005.

Ivanenko YP, Grasso R, Zago M, Molinari M, Scivoletto G, Castellano V, Macellari V, and Lacquaniti F. Temporal components of the motor patterns expressed by the human spinal cord reflect foot kinematics. *Journal of Neurophysiology* 90: 3555-3565, 2003.

Ivanenko YP, Poppele RE, and Lacquaniti E. Five basic muscle activation patterns account for muscle activity during human locomotion. *Journal of Physiology-London* 556: 267-282, 2004.

Jacobs R, and Macpherson JM. Two functional muscle groupings during postural equilibrium tasks in standing cats. *Journal Of Neurophysiology* 76: 2402-2411, 1996.

Jing J, Cropper EC, Hurwitz I, and Weiss KR. The Construction of Movement with Behavior-Specific and Behavior-Independent Modules. *J Neurosci* 24: 6315-6325, 2004.

Jo S, and Massaquoi SG. A model of cerebellum stabilized and scheduled hybrid long-loop control of upright balance. *Biol Cybern* 91: 188-202, 2004.

Jonsson E, Seiger A, and Hirschfeld H. One-leg stance in healthy young and elderly adults: a measure of postural steadiness? *Clinical Biomechanics* 19: 688-694, 2004.

Takei S, Hoffman DS, and Strick PL. Muscle and movement representations in the primary motor cortex. *Science* 285: 2136-2139, 1999.

Katsnelson A. Current approaches to the study of movement control. *PLoS Biol* 1: E50, 2003.

Kawato M. Internal models for motor control and trajectory planning. *Curr Opin Neurobiol* 9: 718-727, 1999.

Keshner EA, Allum JH, and Pfaltz CR. Postural coactivation and adaptation in the sway stabilizing responses of normals and patients with bilateral vestibular deficit. *Exp Brain Res* 69: 77-92, 1987.

Keshner EA, Woollacott MH, and Debu B. Neck, trunk and limb muscle responses during postural perturbations in humans. *Exp Brain Res* 71: 455-466, 1988.

Knikou M, and Rymer WZ. Static and dynamic changes in body orientation modulate spinal reflex excitability in humans. *Exp Brain Res* 152: 466-475, 2003.

Knikou M, and Rymer Z. Effects of changes in hip joint angle on H-reflex excitability in humans. *Exp Brain Res* 143: 149-159, 2002.

Krakauer JW, Mazzoni P, Ghazizadeh A, Ravindran R, and Shadmehr R. Generalization of Motor Learning Depends on the History of Prior Action. *PLoS Biol* 4: 2006.

Krishnamoorthy V, Latash ML, Scholz JP, and Zatsiorsky VM. Muscle modes during shifts of the center of pressure by standing persons: effect of instability and additional support. *Experimental Brain Research* 157: 18-31, 2004.

Krishnamoorthy V, Latash ML, Scholz JP, and Zatsiorsky VM. Muscle synergies during shifts of the center of pressure by standing persons. *Experimental Brain Research* 152: 281-292, 2003.

Kumagai M, Shiba N, Higuchi F, Nishimura H, and Inoue A. Functional evaluation of hip abductor muscles with use of magnetic resonance imaging. *J Orthop Res* 15: 888-893, 1997.

Kuo AD. An optimal control model for analyzing human postural balance. *IEEE Trans Biomed Eng* 42: 87-101, 1995.

Kuo AD. An optimal state estimation model of sensory integration in human postural balance. *J Neural Eng* 2: S235-249, 2005.

Lacquaniti F, and Maioli C. Independent control of limb position and contact forces in cat posture. *J Neurophysiol* 72: 1476-1495, 1994.

Latash ML, Scholz JP, and Schoner G. Motor control strategies revealed in the structure of motor variability. *Exercise and Sport Sciences Reviews* 30: 26-31, 2002.

Lee DD, and Seung HS. Algorithms for non-negative matrix factorization. *Adv Neural Info Proc Syst* 13: 556-562, 2001.

Lemay MA, and Grill WM. Modularity of Motor Output Evoked By Intraspinal Microstimulation in Cats. *J Neurophysiol* 91: 502-514, 2004.

Macpherson JM. Changes in a postural strategy with inter-paw distance. *J Neurophysiol* 71: 931-940, 1994.

Macpherson JM. How flexible are muscle synergies? In: *Motor Control: Concepts and Issues*, edited by Humphrey DR, and Freund H-J. New York: Wiley Press, 1991, p. 33-47.

Macpherson JM. Strategies that simplify the control of quadrupedal stance. I. Forces at the ground. *J Neurophysiol* 60: 204-217, 1988a.

Macpherson JM. Strategies that simplify the control of quadrupedal stance. II. Electromyographic activity. *J Neurophysiol* 60: 218-231, 1988b.

Macpherson JM, and Fung J. Activity of thoracic and lumbar epaxial extensors during postural responses in the cat. *Experimental Brain Research* 119: 315-323, 1998.

Macpherson JM, and Fung J. Weight support and balance during perturbed stance in the chronic spinal cat. *Journal of Neurophysiology* 82: 3066-3081, 1999.

Macpherson JM, Lywood DW, and Van Eyken A. A system for the analysis of posture and stance in quadrupeds. *J Neurosci Methods* 20: 73-82, 1987.

Massion J, Alexandrov A, and Frolov A. Why and how are posture and movement coordinated? In: *Brain Mechanisms for the Integration of Posture and Movement* 2004, p. 13-27.

Matsuyama K, Mori F, Nakajima K, Drew T, Aoki M, and Mori S. Locomotor role of the corticoreticular-reticulospinal-spinal interneuronal system. *Prog Brain Res* 143: 239-249, 2004.

McIlroy WE, and Maki BE. Changes in early 'automatic' postural responses associated with the prior-planning and execution of a compensatory step. *Brain Res* 631: 203-211, 1993.

McIlroy WE, and Maki BE. The control of lateral stability during rapid stepping reactions evoked by antero-posterior perturbation: does anticipatory control play a role? *Gait Posture* 9: 190-198, 1999.

Minino AM, Arias E, Kochanek KD, Murphy SL, and Smith BL. Deaths: final data for 2000. *Natl Vital Stat Rep* 50: 1-119, 2002.

Misiaszek JE. Early activation of arm and leg muscles following pulls to the waist during walking. *Experimental Brain Research* 151: 318-329, 2003.

Misiaszek JE, Stephens MJ, Yang JF, and Pearson KG. Early corrective reactions of the leg to perturbations at the torso during walking in humans. *Exp Brain Res* 131: 511-523, 2000.

Mussa-Ivaldi FA, and Bizzi E. Motor learning through the combination of primitives. *Philosophical Transactions of the Royal Society of London Series B-Biological Sciences* 355: 1755-1769, 2000.

Nashner LM. Adapting reflexes controlling the human posture. *Exp Brain Res* 26: 59-72, 1976.

Nashner LM. Balance Adjustments of Humans Perturbed While Walking. *Journal of Neurophysiology* 44: 650-664, 1980.

Nashner LM. Fixed patterns of rapid postural responses among leg muscles during stance. *Exp Brain Res* 30: 13-24, 1977.

Nichols TR. A biomechanical perspective on spinal mechanisms of coordinated muscular action: an architecture principle. 151: 1-13, 1994.

Nichols TR. The organization of heterogenic reflexes among muscles crossing the ankle joint in the decerebrate cat. *J Physiol* 410: 463-477, 1989.

Nichols TR, Cope TC, and Abelew TA. Rapid spinal mechanisms of motor coordination. *Exerc Sport Sci Rev* 27: 255-284, 1999.

Park S, Horak FB, and Kuo AD. Postural feedback responses scale with biomechanical constraints in human standing. *Exp Brain Res* 154: 417-427, 2004.

Peterka RJ. Sensorimotor integration in human postural control. *J Neurophysiol* 88: 1097-1118, 2002.

Poggio T, and Bizzi E. Generalization in vision and motor control. *Nature* 431: 768-774, 2004.

Poppele R, and Bosco G. Sophisticated spinal contributions to motor control. *Trends Neurosci* 26: 269-276, 2003.

Poppele RE, Bosco G, and Rankin AM. Independent representations of limb axis length and orientation in spinocerebellar response components. *J Neurophysiol* 87: 409-422, 2002.

Raasch CC, and Zajac FE. Locomotor strategy for pedaling: Muscle groups and biomechanical functions. *Journal of Neurophysiology* 82: 515-525, 1999.

Raasch CC, Zajac FE, Ma B, and Levine WS. Muscle coordination of maximum-speed pedaling. *J Biomech* 30: 595-602, 1997.

Riemann BL, Myers JB, and Lephart SM. Comparison of the ankle, knee, hip, and trunk corrective action shown during single-leg stance on firm, foam, and multi-axial surfaces. *Archives of Physical Medicine and Rehabilitation* 84: 90-95, 2003.

Rocchi L, Chiari L, Cappello A, Gross A, and Horak FB. Comparison between subthalamic nucleus and globus pallidus internus stimulation for postural performance in Parkinson's disease. *Gait Posture* 19: 172-183, 2004.

Runge CF, Shupert CL, Horak FB, and Zajac FE. Role of vestibular information in initiation of rapid postural responses. *Exp Brain Res* 122: 403-412, 1998.

Sabatini AM. Identification of neuromuscular synergies in natural upper-arm movements. *Biol Cybern* 86: 253-262, 2002.

Saltiel P, Tresch MC, and Bizzi E. Spinal Cord Modular Organization and Rhythm Generation: An NMDA Iontophoretic Study in the Frog. *J Neurophysiol* 80: 2323-2339, 1998.

Saltiel P, Wyler-Duda K, d'Avella A, Ajemian RJ, and Bizzi E. Localization and connectivity in spinal interneuronal networks: the adduction-caudal extension-flexion rhythm in the frog. *J Neurophysiol* 94: 2120-2138, 2005.

Saltiel P, Wyler-Duda K, D'Avella A, Tresch MC, and Bizzi E. Muscle synergies encoded within the spinal cord: evidence from focal intraspinal NMDA iontophoresis in the frog. *J Neurophysiol* 85: 605-619, 2001.

Schmidt RA, and Lee TD. Retention and Transfer. In: *Motor control and learning: a behavioral emphasis*. Champaign: Human Kinetics, 2005.

Scholz JP, and Schoner G. The uncontrolled manifold concept: identifying control variables for a functional task. *Exp Brain Res* 126: 289-306, 1999.

Schwartz AB, Kettner RE, and Georgopoulos AP. Primate motor cortex and free arm movements to visual targets in three-dimensional space. I. Relations between single cell discharge and direction of movement. *J Neurosci* 8: 2913-2927, 1988.

Scott SH. Optimal feedback control and the neural basis of volitional motor control. *Nature Reviews Neuroscience* 5: 534-546, 2004.

Scott SH, and Kalaska JF. Reaching movements with similar hand paths but different arm orientations. I. Activity of individual cells in motor cortex. *J Neurophysiol* 77: 826-852, 1997.

Shadmehr R, and Mussa-Ivaldi FA. Adaptive representation of dynamics during learning of a motor task. *J Neurosci* 14: 3208-3224, 1994.

Stein P. Neuronal control of turtle hindlimb motor rhythms. *Journal of Comparative Physiology a-Neuroethology Sensory Neural and Behavioral Physiology* 191: 213-229, 2005.

Stein RB, and Kearney RE. Nonlinear behavior of muscle reflexes at the human ankle joint. *J Neurophysiol* 73: 65-72, 1995.

Thoroughman KA, and Shadmehr R. Electromyographic correlates of learning an internal model of reaching movements. *J Neurosci* 19: 8573-8588, 1999.

Thoroughman KA, and Shadmehr R. Learning of action through adaptive combination of motor primitives. *Nature* 407: 742-747, 2000.

Ting LH, Kautz SA, Brown DA, and Zajac FE. Contralateral movement and extensor force generation alter flexion phase muscle coordination in pedaling. *J Neurophysiol* 83: 3351-3365, 2000.

Ting LH, Kautz SA, Brown DA, and Zajac FE. Phase reversal of biomechanical functions and muscle activity in backward pedaling. *J Neurophysiol* 81: 544-551, 1999.

Ting LH, and Macpherson JM. A limited set of muscle synergies for force control during a postural task. *J Neurophysiol* 93: 609-613, 2005.

Ting LH, and Macpherson JM. Ratio of shear to load ground-reaction force may underlie the directional tuning of the automatic postural response to rotation and translation. *J Neurophysiol* 92: 808-823, 2004.

Ting LH, Raasch CC, Brown DA, Kautz SA, and Zajac FE. Sensorimotor state of the contralateral leg affects ipsilateral muscle coordination of pedaling. *J Neurophysiol* 80: 1341-1351, 1998.

Todorov E, and Ghahramani Z. Analysis of the synergies underlying complex hand manipulation. *Conf Proc IEEE Eng Med Biol Soc* 6: 4637-4640, 2004.

Torres-Oviedo G, Macpherson JM, and Ting LH. Muscle synergy organization is robust across a variety of postural perturbations. *J Neurophysiol* 96: 1530-1546, 2006.

Tresch MC, Cheung VC, and d'Avella A. Matrix factorization algorithms for the identification of muscle synergies: evaluation on simulated and experimental data sets. *J Neurophysiol* 95: 2199-2212, 2006.

Tresch MC, Saltiel P, and Bizzi E. The construction of movement by the spinal cord. *Nat Neurosci* 2: 162-167, 1999.

Tropp H, and Odenrick P. Postural control in single-limb stance. *J Orthop Res* 6: 833-839, 1988.

Valero-Cuevas FJ. Predictive modulation of muscle coordination pattern magnitude scales fingertip force magnitude over the voluntary range. *J Neurophysiol* 83: 1469-1479, 2000.

Valero-Cuevas FJ, Zajac FE, and Burgar CG. Large index-fingertip forces are produced by subject-independent patterns of muscle excitation. *J Biomech* 31: 693-703, 1998.

van Bolhuis BM, and Gielen CC. A comparison of models explaining muscle activation patterns for isometric contractions. *Biol Cybern* 81: 249-261, 1999.

Van Deun S, Staes FF, Stappaerts KH, Janssens L, Levin O, and Peers KKH. Relationship of chronic ankle instability to muscle activation patterns during the transition from double-leg to single-leg stance. *American Journal of Sports Medicine* 35: 274-281, 2007.

Weiss EJ, and Flanders M. Muscular and postural synergies of the human hand. *Journal of Neurophysiology* 92: 523-535, 2004.

Wilmink RJ, and Nichols TR. Distribution of heterogenic reflexes among the quadriceps and triceps surae muscles of the cat hind limb. 90: 2310-2324, 2003.

Winter DA, Patla AE, Prince F, Ishac M, and Gielo-Perczak K. Stiffness control of balance in quiet standing. *J Neurophysiol* 80: 1211-1221, 1998.

Wolpert DM, Miall RC, and Kawato M. Internal models in the cerebellum. *Trends Cogn Sci* 2: 338-347, 1998.

Woollacott MH, Burtner P, Jensen J, Jasiewicz J, Roncesvalles N, and Sveistrup H. Development of postural responses during standing in healthy children and children with spastic diplegia. *Neurosci Biobehav Rev* 22: 583-589, 1998.

Woollacott MH, and Shumway-Cook A. Attention and the control of posture and gait: a review of an emerging area of research. *Gait Posture* 16: 1-14, 2002.

Zajac FE. Understanding muscle coordination of the human leg with dynamical simulations. *J Biomech* 35: 1011-1018, 2002.

Zajac FE, and Gordon ME. Determining muscle's force and action in multi-articular movement. *Exerc Sport Sci Rev* 17: 187-230, 1989.

Zar JH. *Biostatistical Analysis* Upper Saddle River, NJ: Prentice-Hall, 1999.

VITA

GELSY TORRES-OVIEDO

Gelsy Torres-Oviedo was born in Mexico City, DF on February 5th 1977. In the fall of 1996 she started her studies of Engineering in Physics at the ITESM Campus Monterrey in Monterrey, NL. Mexico. In 1999, she transferred to The University of Texas at Austin TX, from which she received a B.S. in Physics in May 2001 before coming to Georgia Tech and Emory University in Atlanta GA to pursue a doctorate in Biomedical Engineering. She joined Prof. Ting Lab in the fall of 2002 as her first student and helped developed what the lab has become today.

When she is not working on her research, Gelsy enjoys dancing, traveling, and socializing. Her identity with her culture and country is strong and often times she could be found sharing this love with others. Gelsy is also passionate about doing sports. During her doctoral work she accomplished a black belt in Tae Kwon Do and ran two half marathons and one full marathon.